

Carnegie Mellon University

Gene Function of the Transcription Factors
Mig1, Mig2, and Zfu2 in *Candida albicans*

by

Katherine Lagree

A thesis submitted in partial fulfillment for the
degree of Doctor of Philosophy

in the

Lab of Dr. Aaron P. Mitchell
Department of Biological Sciences

August 21st, 2018

Declaration of Authorship

I, Katherine Lagree, declare that this thesis titled, ‘Gene Function of Transcription Factors in *Candida albicans* ’ and the work presented in it are my own. I confirm that:

- This work was done wholly or mainly while in candidature for a research degree at this University.
- Where any part of this thesis has previously been submitted for a degree or any other qualification at this University or any other institution, this has been clearly stated.
- Where I have consulted the published work of others, this is always clearly attributed.
- Where I have quoted from the work of others, the source is always given. With the exception of such quotations, this thesis is entirely my own work.
- I have acknowledged all main sources of help.
- Where the thesis is based on work done by myself jointly with others, I have made clear exactly what was done by others and what I have contributed myself.

Signed:

Date:

“All you really need to know for the moment is that the universe is a lot more complicated than you might think, even if you start from a position of thinking it’s pretty damn complicated in the first place.”

-Douglas Adams

Carnegie Mellon University

Abstract

Lab of Dr. Aaron P. Mitchell
Department of Biological Sciences

Doctor of Philosophy

by Katherine Lagree

Candida albicans is a commensal fungus that can cause life-threatening illnesses for those that are immunocompromised, have had major surgery, or have in-dwelling medical devices. *C. albicans* lives on most mucosal surfaces in the body where it employs drastically different transcriptional patterns depending on which body site it inhabits, or whether it acts as a commensal or a pathogenic organism. The ability of *C. albicans* to alter its transcriptional landscape to live in these diverse niches within the body is a testament to its genetic flexibility. This thesis will attempt to understand the functions of three distinct transcription factors Mig1, Mig2, and Zfu2 that enable *C. albicans* to coordinate proper gene expression *in vivo* and *in vitro*. These transcription factors play distinct roles in controlling proper gene expression in two different contexts. Zfu2 may control gene expression in the context of *in vivo* biofilm formation, while Mig1 and Mig2 are repressors of alternative carbon source utilization genes and control cell wall integrity. All three of these transcription factors play a role in virulence and therefore are of importance to study.

Acknowledgements

I would like to extend my sincerest gratitude to all of the people that have helped me with my scientific projects or with emotional support during my graduate career. Science is always a collaborative effort and nothing I have accomplished would be possible without the support of my current and former labmates, fellow graduate students, and scientific collaborators.

Specifically,

Thanks to my advisor, Dr. Aaron Mitchell for his wisdom and guidance

Thanks to my committee members, Dr. Fred Lanni, Dr. Luisa Hiller, and Dr. Sarah Gaffen

Thanks to Tatyana Aleynikova for technical support in the lab

Thanks to Dr. Carol Woolford for all of your help

Thanks to Dr. Askash Verma and Dr. Sarah Gaffen for their help with the OPC experiments

Thanks to Norma Solis and Dr. Scott Filler for their help with in vivo experiments

Thanks to Hiram Sanchez and Dr. David Andes for their help with in vivo experiments

Thanks to Gemma May and Dr. Joel McManus for help with the RNA-sequencing

Thanks to Manning Huang for research discussions

Contents

Declaration of Authorship	i
Abstract	iii
Acknowledgements	iv
List of Figures	vii
List of Tables	ix
Abbreviations	x
1 Introduction	1
1.1 Carbon Utilization	2
1.1.1 Carbon sources in the host	3
1.1.2 Metabolism and virulence	5
1.1.3 Macrophage Interactions	7
1.1.4 Glucose signaling through Snf1 and Mig1	8
1.1.5 Mig2	10
1.2 Antifungal drugs	10
1.3 Iron acquisition and Regulation	12
1.4 Biofilm formation	14
1.4.1 Biofilm gene expression	15
1.4.2 Biofilm gene regulation	18
1.4.3 Imaging biofilms	20
2 Methods	21
2.1 Strains and Media	21
2.2 Fungal Transformation	21
2.3 <i>mig1 mig2</i> Strain Construction	21
2.4 <i>zfu2</i> Strain Construction	23
2.5 Macrophage Killing Assay	23
2.6 Hyphal Growth Assay	24
2.7 Endothelial Cell Damage Assay	25
2.8 RNA Extraction	25

2.9	RT-PCR	25
2.10	NanoString Analysis	26
2.11	RNA Sequencing and Analysis	26
2.12	OPC Infections	27
2.13	Rat Venous Catheter Infections	28
2.14	Statistical Analysis	28
3	Results	29
3.1	Mig1 and Mig2 are redundant in function	31
3.2	Mig1 and Mig2 are repressors of alternative carbon utilization genes	34
3.2.1	RNA-sequencing results	34
3.3	The <i>mig1 mig2</i> mutant gene expression profile shows changes in cell wall genes	35
3.4	Profile of the <i>mig1 mig2</i> mutant strain in YPG media	38
3.5	Mig1 and Mig2 are not transcriptional regulators of the caspofungin response	41
3.6	The <i>mig1 mig2</i> double mutant is hypersensitive to caspofungin on the non-fermentable carbon source glycerol	41
3.7	The gene expression profile of the <i>mig1 mig2</i> strain in YPD shows similar changes in gene expression compared to the profile of <i>C. albicans</i> cells phagocytosed by bone-marrow-derived mouse macrophages	44
3.8	Mig1 and Mig2 control morphogenesis	44
3.9	Mig1 and Mig2 may function in the TOR signaling pathway	48
3.10	Sak1 regulates alternative carbon source utilization through inactivation of the repressors Mig1 and Mig2	50
3.11	<i>SNF1</i> is not essential in a <i>mig1 mig2</i> mutant background strain.	52
4	Discussion	55
5	Supplement	59
6	Zfu2	82
6.1	Zfu2 is required for <i>C. albicans</i> biofilm formation <i>in vivo</i> but not <i>in vitro</i>	85
6.2	The impact of Zfu2 on <i>in vitro</i> biofilm gene expression	85
6.3	The CFEM proteins are critical targets of Zfu2 <i>in vivo</i>	86
6.4	Addition of ferric chloride restores biofilm formation ability of the <i>zfu2</i> mutant <i>in vivo</i>	87
6.5	Zfu2 and Hap43 may be dispensable for virulence in an oral candidiasis model	88
6.6	Discussion	91
7	Supplement	94
8	Conclusion	98
	Bibliography	101

List of Figures

1.1	Simplified schematic of known regulatory pathway for Mig1 and Mig2 in <i>Saccharomyces cerevisiae</i>	9
3.1	Protein sequence alignment of <i>CaMig</i> , <i>CaMig2</i> , <i>ScMig1</i> and <i>ScMig2</i>	30
3.2	The <i>mig1 mig2</i> double mutant is hypersensitive to caspofungin	32
3.3	The <i>mig1 mig2</i> double mutant is hypersensitive to calcofluor white, but not fluconazole. Cell wall stress from caspofungin can be reversed with sorbitol	33
3.4	Venn Diagram summary of the distribution of differentially expressed genes between the <i>mig1</i> , <i>mig2</i> , and <i>mig1 mig2</i> double mutant strains compared to the wild-type strain in YPD media	36
3.5	Gene Ontology (GO)-term analysis of upregulated genes in the <i>mig1 mig2</i> double mutant strain compared to the wild-type strain in YPD media	37
3.6	Upregulated alternative carbon source utilization genes in the <i>mig1 mig2</i> double mutant show various types of genetic regulation	37
3.7	Dot plots showing log ₂ -fold change (p<0.05) for differential expression of all genes	39
3.8	Comparison of gene expression response of the <i>mig1 mig2</i> double mutant in YPD to the gene expression response of the <i>mig1 mig2</i> double mutant in YPD + caspofungin	40
3.9	The <i>mig1 mig2</i> double mutant is sensitive to caspofungin when grown on glycerol media	42
3.10	The <i>mig1 mig2</i> double mutant gene expression profile in YPD is similar to the gene expression profile of wild-type <i>C. albicans</i> cells interacting with bone-marrow-derived mouse macrophages from [23]	43
3.11	The <i>mig1 mig2</i> double mutant is less virulent in an <i>in vitro</i> model of macrophage cell damage	45
3.12	Mig1 and Mig2 control morphogenesis	46
3.13	The <i>mig1 mig2</i> double mutant is less virulent in an <i>in vitro</i> model of endothelial cell damage	47
3.14	The <i>mig1 mig2</i> double mutant is sensitive to the drug rapamycin	49
3.15	Deletion of <i>SAK1</i> in the <i>mig1 mig2</i> double mutant relieves growth defects and morphogenesis defects of the <i>sak1</i> mutant on alternative carbon sources	51
3.16	<i>SNF1</i> is not essential in a <i>mig1 mig2</i> mutant background strain	52
3.17	Mig1 and Mig2 network schematic	53
6.1	Zfu2 is required for <i>C. albicans</i> biofilm formation <i>in vivo</i>	83
6.2	The <i>zfu2</i> mutant strain is not defective in biofilm formation <i>in vitro</i>	84

6.3	Functional GO categories enriched in the <i>zfu2</i> mutant profile compared to the control strain	86
6.4	Overexpression of the CFEM protein genes in the <i>zfu2</i> mutant strain restores biofilm <i>in vivo</i>	87
6.5	Addition of FeCl ₃ restores biofilm formation of the <i>zfu2</i> mutant	88
6.6	Zfu2 and Hap43 may be dispensable for virulence in a mouse model of oral candidiasis	90
6.7	Hap43 may be dispensable for virulence in a mouse model of a 24 h oral candidiasis infection	91

List of Tables

5.1	<i>mig1 mig2</i> mutant vs. WT YPD gene expression compared to wild-type <i>C. albicans</i> interacting with mouse macrophages for 1hr vs. wild-type <i>C. albicans</i> alone gene expression	59
5.2	<i>mig1 mig2</i> Primer List	78
5.3	<i>mig1 mig2</i> Strain List	81
6.1	NanoString gene expression results from OPC infection	91
7.1	<i>zfu2</i> Strain List	94
7.2	<i>zfu2</i> Primer List	97

Abbreviations

MIG	M ulticopy I nhibitor of GAL
SNF	S ucrose N on F ermenting
TOR	T arget O f R apamycin
FBS	F etal B ovine S erum
OPC	O ro P haryngeal C andidiasis
YPD	Y east E xtract P eptone D extrose
YNB	Y east N itrogen B ase
CFEM	C ommon in F ungal E xtracellular M embrane
GO	G ene O ntology
PBS	P hosphate B uffer S aline
LDH	L actate D e H ydrogenase

Chapter 1

Introduction

Candida albicans is a commensal fungus found throughout the body on skin and mucosal surfaces. However, because it is ubiquitous and uniquely adapted to the human host, *C. albicans* is poised to become pathogenic when significant changes in the host occur such as antibiotic driven dysbiosis, immunodeficiency from HIV infections, or the presence of indwelling medical devices such as venous or urinary catheters [1]. These infections can become very dangerous for patients when *Candida albicans* enters the blood stream causing systemic candidiasis where mortality rates can reach up to 50% [2]. Diverse classes of antifungals to treat these infections are extremely limited, so the identification of new drug targets is a high priority for medical mycologists. To identify new drug targets, extensive research must be done to understand the molecular and biological function of the 70% of uncharacterized genes in the *C. albicans* genome and further characterize the 30% of genes that have some functional data [3]. Characterizing approximately 4,360 unknown genes is a daunting task to undertake for a field that is sometimes considered a lower priority compared with other infectious disease fields [4]. This thesis will seek to advance the molecular and genetic understanding of genes in the *C. albicans* genome through the investigation of three transcription factors of interest Zfu2, Mig1, and Mig2. Transcription factors were chosen to study because they often control the expression of many other genes in the genome, thus allowing some functional or at least correlative data to group large numbers of genes together. Specifically, this thesis will characterize genetic and molecular pathways in *C. albicans* that regulate its ability to control carbon source acquisition, cell wall integrity, and the ability to form biofilms in *in vivo* which

are all important virulence determinants for *C. albicans* to thrive in diverse niches of the human body.

1.1 Carbon Utilization

The fungus *Candida albicans* is a significant component of the human microbiome. It is commonly isolated from the skin, mouth, gastrointestinal tract, and vaginal tissue of both healthy and diseased hosts[5][6]. These different sites on the body have dramatically different environments. For example, the pH of those body sites vary from pH 5.5 to pH 8.5, so *C. albicans* has to persist in the acidic environment of vaginal tissue and the alkaline environment of the gastrointestinal tract[7]. Additionally, there are varying types of carbon sources available at each of these body sites ranging from lipids and amino acids to complex carbohydrates[8]. The ability of *C. albicans* to thrive at these diverse sites means that it must be able to adapt. The transcriptome and proteome of *C. albicans* must remain flexible to control which metabolic enzymes are turned on or off for each environment. Additionally, *C. albicans* must quickly adapt to changing host conditions during the progression of an infection. Much of the research on the metabolic flexibility of *C. albicans* has been investigated in reference to the model organism *Saccharomyces cerevisiae*, which last shared a common ancestor with *C. albicans* roughly 840 million years ago[9]. Despite this long period of time, *C. albicans* and *S. cerevisiae* share significant conservation in terms of homologous genes, proteins, and the structure of general metabolic pathways[10]. For one, glucose is the preferred carbon source for both yeasts. On the surface, this may not seem surprising, since glucose is a readily available nutrient source, but *C. albicans* is confined to the host niche where glucose may be limiting[11]. Therefore, one would expect significant reprogramming of the metabolic pathways between *S. cerevisiae* and *C. albicans* to adapt to these different niches.

Indeed, there are many ways in which *C. albicans* has diverged from its beer-making brethren, *S. cerevisiae*. For example, the transcription factor *ScAdr1* (Alcohol Dehydrogenase Regulator 1)[12] is aptly named because it was shown to be necessary for the expression of the gene *ScADH2* which encodes the enzyme alcohol dehydrogenase[13]. *ScAdr1* was shown to be necessary for expression of metabolic genes involved in the utilization of ethanol as a carbon source and was necessary for growth on nonfermentable carbon

sources such as glycerol, ethanol, citrate, pyruvate, and formate[14]. However in *C. albicans*, expression of *CaADR1* is not required for growth on these nonfermentable carbon sources or for expression of several alternative carbon utilization genes[15]. It is likely that *C. albicans* has a more adaptable regulatory network for carbon acquisition, since mutations in the network often fail to produce observable phenotypes[16].

Another surprising divergence from *S. cerevisiae* came from a *C. albicans* proteomics study that sought to identify proteins that were regulated in response to alternative carbon sources more likely than glucose to be found in the host, such as lactate, oleate, and amino acids[17]. In *S. cerevisiae*, transcription of alternative carbon utilization genes is repressed when glucose is present[18]. Additionally, to begin utilizing glucose, remaining alternative carbon source utilization proteins are degraded through ubiquitin-mediated proteolysis[19][20]. *C. albicans* similarly represses alternative carbon source utilization genes in response to glucose, but surprisingly, *C. albicans* does not degrade the remaining metabolic proteins. Even more surprising, *C. albicans* retains the ubiquitination machinery necessary to degrade the metabolic proteins Icl1 and Pck1 from *S. cerevisiae*, but the homologous proteins in *C. albicans* lack these ubiquitination sites. Therefore, in *C. albicans* proteins required for gluconeogenesis and the glyoxylate cycle remain present even in the presence of the preferred carbon source, glucose[17]. It is unclear why this rewiring of posttranslational modifications evolved, but it is hypothesized that it affords *C. albicans* the ability to remain metabolically flexible during infection[21][22][23][24]. Retention of these enzymes could allow *C. albicans* to adapt to new energy requirements more readily than *S. cerevisiae*.

1.1.1 Carbon sources in the host

Understanding how *C. albicans* interacts with the host environment has emerged as an important topic of research for understanding how it causes infections, but also for how it persists as a commensal. Microbiome research has exploded in the last few years resulting in fecal transplants being used in the clinic for recurrent *Clostridium difficile* infections[25]. In fact, fecal transplants can now be administered by a simple oral capsule[26]. It is not hard to imagine that many other medical treatments or preventative medicine strategies will be investigated by manipulating the patient's microbiome[27]. This leads mycobiologists to ask whether fungi will play a role in those treatments. Among fungi

isolated from the human gut, *Candida albicans* is one of the most common[6], but it is not clear what role it plays in a healthy human gut. Furthermore, it is clear that *Candida* species in the gut can lead to deadly intra-abdominal candidiasis (IAC) in susceptible patients, which accounts for almost 50% of all invasive *Candida* infections[28]. Despite its statistical frequency, IAC remains poorly studied compared to systemic candidiasis. Therefore, understanding how *C. albicans* survives and interacts with the environment of the gut, or how it promotes commensalism is an important research avenue that is just beginning to gain traction.

It is unclear which carbon sources *C. albicans* utilizes in the gastrointestinal tract or how competition with the other gut flora affects the availability of these carbon sources. However, it has been shown that mutations in glycolytic and galactose utilization regulators (Tye7, Rtg1, and Rtg3) can result in reduced fitness during gastrointestinal tract colonization[29]. Although not directly linked to carbon utilization, regulators of iron acquisition and utilization (Sef1, Sfu1) have also been shown to promote commensalism in mouse models[30]. To further complicate investigations of the metabolic requirements of fungi in the gut, several reports have shown that filamentous growth is negatively associated with gut colonization. Three transcription factor mutants that displayed hyperfilamentous growth *in vitro*, had defects in colonization of the mouse gut[31], indicating that the hyphal form of *C. albicans* is selected against in the gastrointestinal tract of mice. Several metabolic regulators such as Sak1, Gcn4, and Ace2 have been shown to regulate hyphal formation, and Sak1 was shown to be necessary for competitive fitness with a wild-type strain in the gastrointestinal tract[32]. Mutant strains of *ACE2* and *GCN4* have not been tested in a model of commensalism, but Ace2 inhibits hyphal formation under hypoxic conditions. The gastrointestinal tract is likely an oxygen-poor niche, so commensalism might be regulated by signaling through Ace2 to maintain the desired yeast form[33]. Clearly, metabolism, morphogenesis, and virulence are intimately intertwined and the interconnected signaling between these pathways will have to be deduced to understand fungal commensalism in the GI tract.

Research into *C. albicans* gut colonization has generally used germ-free, gnotobiotic, or antibiotic treated mice[31][30][27][34]. This is mainly due to technical reasons, since mice are not normally colonized by *C. albicans* when their normal flora is maintained, although one group found that this resistance to *Candida* gut colonization in mice was correlated with the amount of *Lactobacilli* the mice obtained from their diets[35]. Also,

studies that maintain the normal flora can be much more complex and harder to interpret[36]. Therefore, one group used an *ex vivo* approach to understand how *C. albicans* interacts with metabolites that would be found in a normal gut flora[37]. Cottier et al. found that the transcription factor Mig1 was necessary for the resistance to weak organic acids (WOAs). Weak organic acids or short chain fatty acids are a common metabolite stemming from the bacteria in normal human gut flora[38]. Confirmation that these metabolites are present was verified using high-performance liquid chromatography from healthy human stools[37]. Wild-type cells were more sensitive to WOAs when grown in media with maltose compared to cells grown in glucose, indicating that carbon source can impact cell stress phenotypes[39]. However, a *mig1* mutant strain was equally sensitive to WOAs when grown in maltose or glucose media[37]. This suggests that Mig1 may play a role in promoting commensalism in the gut in response to glucose availability.

1.1.2 Metabolism and virulence

Proper metabolic regulation is a key virulence trait in *C. albicans* [22][23][24]. This is likely due to the fact that the host contains diverse sources of carbon. Sites of infections can be dynamic and have complex ecosystems due to the influx of immune cells. For example, blood contains low levels of glucose, the phagosome of a macrophage contains alternative carbon sources, [24][23] and advanced infections in the kidney are hypoxic, which causes a shift from glycolysis to the glyoxylate cycle and gluconeogenesis pathways[40][21][41]. One study was able to deduce the metabolic gene expression profile of an oropharyngeal candidiasis (OPC) infection using microarray technology to capture a timecourse of gene expression patterns during the progression of infection[42][43]. However, this study used an *in vitro* system of reconstituted human oral epithelial cells to simulate a host infection. To validate this model, some of the gene response was consistent with profiles from human HIV-positive patient samples[43]. The gene expression timecourse showed metabolic shifts from glycolysis towards gluconeogenesis and the glyoxylate cycle, similar to an *in vivo*, mouse kidney infection[21]. Fanning et al. profiled an *in vivo* mouse model of an OPC infection using nanoString technology and found that two glucose transporters *HGT6* and *HGT12* and *PCK1*, a gluconeogenic gene, were highly expressed. However, minimal metabolic genes were included in the study[44]. Profiling gene expression in an *in vivo* infection is still a technical feat due to the large amount of host RNA that dwarfs the fungal RNA, so nanoString is sensitive enough for

in vivo infections, but only a few hundred genes can be profiled at a time. Hence there are concessions for most profiling technique choices depending on what questions you want to answer. Nevertheless, it seems clear from several studies that late-stage tissue infections of *C. albicans* are glucose poor environments[21][22][42].

Using reporter constructs and fusion proteins, glyoxylate genes *ICL1*, *PYK1*, *PFK2*, *PCK1* and short-chain carboxylic acid transporter genes *JEN1* and *JEN2* have been shown to be upregulated in response to *C. albicans* cells interacting with host immune cells[45][11]. This is consistent with the transcript profiling data from several bodies of work[23][24]. However, the ability of *C. albicans* to survive in the presence of immune cells and escape the phagosome was not dependent on the presence of *JEN1* or *JEN2*. As further proof, Vieira et al. showed that Jen1 and Jen2 GFP fusion constructs were expressed in *C. albicans* cells in an infected mouse kidney, but mutants of these two genes did not affect survival rate of mice in a model of systemic infection[45]. Conversely, loss of *ICL1* does result in a virulence defect in a mouse model of systemic infection[24]. The genes *JEN1*, *JEN2*, and *ICL1* are all upregulated in glucose poor niches, but *ICL1*, which encodes the enzyme isocitrate lyase, is specifically necessary for the glyoxylate cycle. The glyoxylate cycle bypasses certain steps in the TCA cycle and allows the conversion of acetyl-CoA to succinate in order to build carbohydrates when glucose is not available. Humans lack a glyoxylate cycle, so these enzymes have been noted as possible drug targets for treating fungal infections[24].

Something to note is that the other glyoxylate cycle gene *MLS1*, which encodes malate synthase has not been investigated for a role in pathogenesis. If the ability to utilize the anabolic processes of the glyoxylate cycle is necessary for virulence, then the *mls1* mutant should also be defective in virulence, similar to the *icl1* mutant[24]. The other intriguing possibility is the notion that several metabolic enzymes in yeast have been classified as “moonlighting” proteins[46]. The term "moonlighting" means these proteins have been found in non-canonical locations or serve functions other than their canonical biological processes. For example, several metabolic enzymes have been found in the cell wall of *C. albicans*[47], and other metabolic enzymes have been shown to regulate gene transcription[46]. Enzymes like Icl1 could be playing a role outside of the peroxisome and promoting virulence in a new, yet to be discovered way.

1.1.3 Macrophage Interactions

C. albicans is able to survive and escape macrophage-induced death in an *in vitro* co-culture model. What mechanisms drive this ability? One known mechanism involves the alkalization of the phagosome environment through the utilization of alternative carbon sources. The genetic determinants of this alkalization include 1) the catabolism of amino acids which is controlled by the transcription factor Stp2[48], 2) the utilization of N-acetylglucosamine (GlcNAc) through the transporter Ngt1[49], and 3) the utilization of carboxylic acids controlled by the transcription factors Cwt1[50]. Evidence suggests that *C. albicans* is able to escape the phagosome by utilization of these alternative carbon sources, resulting in excretion of ammonia as a byproduct. The excess ammonia alkalizes the environment, causing auto-induction of hyphal formation[48]. Hyphae grow within the macrophage eventually triggering pyroptosis and leading to death of the macrophage[51]. Although the yeast-hyphae transition is correlated with escape from the macrophage, evidence has shown that hyphae are not required for survival within the macrophage. A yeast-locked *efg1 cph1* double mutant strain was able to survive and replicate within the macrophage, but was unable to escape[52]. The phagosome environment is glucose-poor, but following escape from the macrophage, *C. albicans* is able to resume glycolysis through consumption of glucose from the surrounding culture medium in an *in vitro* culture. In a coinubation experiment with *C. albicans*, Tucey et al. showed compelling evidence that macrophage cells are stuck undergoing the glycolytic cycle since glycolysis fuels antimicrobial defenses[53]. However, as *C. albicans* emerges from the macrophage cells, it resumes the consumption of glucose and the fungal cells quickly out-compete the immune cells[23]. The ability to shift back to the glycolytic cycle was shown to rely on two transcription factors, Tye7 and Gal4. A double *tye7 gal4* mutant strain was able to form hyphae and escape the macrophage, but was not able to rapidly deplete glucose from the surrounding media in competition with the macrophages[23]. This indicates that there are multiple genetic pathways allowing evasion from the host immune system that require precise metabolic adaption and control.

1.1.4 Glucose signaling through Snf1 and Mig1

Signaling cascades in response to glucose have been extensively studied in *Saccharomyces cerevisiae*. One such pathway signals through the protein kinase *ScSnf1*, which is conserved in humans where it is known as the AMP kinase[54]. In response to glucose limitation, *ScSak1* (*Snf1* Activating Kinase) phosphorylates *ScSnf1* which then phosphorylates the cytoplasmic transcription factor *ScMig1* and causes *ScMig1* to leave the nucleus. *ScMig1* is a repressor of alternative carbon utilization genes and is constitutively expressed in the cells. (See schematic for reference 1.1). Therefore, nuclear export of *ScMig1* is the main regulatory mechanism for repression of alternative carbon source utilization genes[55][56][57]. Interestingly, *Snf1* has been shown to be essential in the canonical *C. albicans* strain, SC5314, while it is not essential in *S. cerevisiae*[58]. It has been hypothesized that this is because *CaSnf1* is constitutively phosphorylated [15][59]. In *S. cerevisiae*, *ScSnf1* is only phosphorylated in response to various forms of stress stimuli [60]. However, *CaSNF1* has not been investigated in other clinical isolates of *C. albicans* to test if the essentiality is conserved. Reports have shown that evolution can influence the extent of essentiality of certain genes[61]. On the other hand, the upstream kinase, *CaSak1*, is not essential in *C. albicans*. The *Casak1* mutant fails to grow on various alternative carbon sources such as glycerol, ethanol, citrate, lactate, mannitol and oleate and shows hypersensitivity to multiple cell wall stressors[32]. *CaSak1* was also shown to directly activate *CaSnf1* by phosphorylation, in line with its homolog from *S. cerevisiae*[32]. However, *CaSnf1* showed a level of phosphorylation even in a *Casak1* mutant strain, so kinases other than *CaSak1* must also phosphorylate *CaSnf1*[32].

MIG1 in *Candida albicans* was first isolated and characterized in 2000 and was heterologously expressed in *Saccharomyces cerevisiae* showing that it could complement a *Scmig1* mutant strain [64]. *CaSNF1* was also shown to functionally complement a *snf1* mutant strain in *S. cerevisiae*[58]. The fact that *CaSNF1* and *CaMIG1* can complement mutants in *S. cerevisiae* is intriguing because both genes have clearly diverged in function from their counterparts. *CaMIG1* was able to restore repression of *SUC2* (*SUC*rose hydrolyzing enzyme) expression in *S. cerevisiae*, even though the amount of α -glucosidase activity was unchanged in the *Camig1* mutant strain[64]. (*C. albicans* does not contain a direct homologue for *SUC2*). To investigate the role of *CaMig1* as a general repressor of alternative carbon source utilization gene expression, a *mig1* mutant strain was profiled

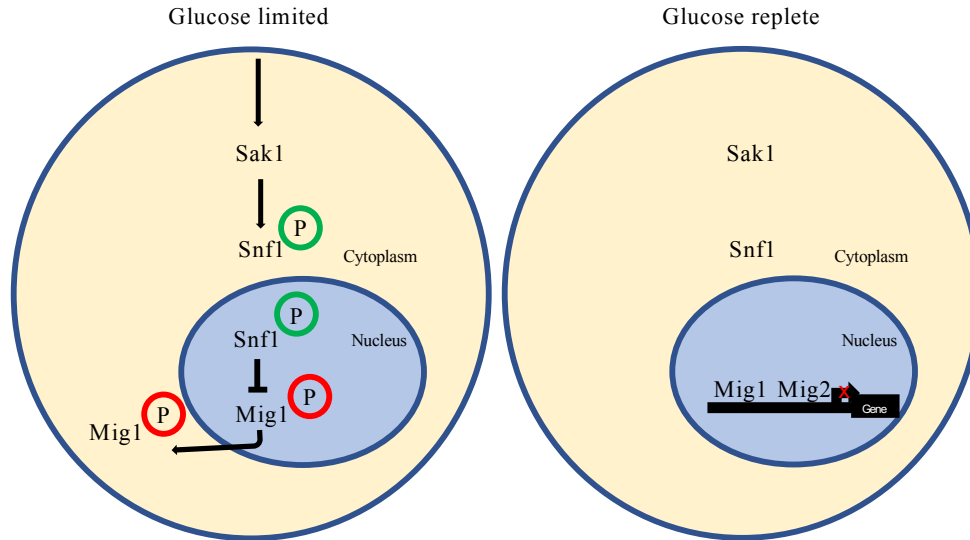
Saccharomyces cerevisiae

FIGURE 1.1: **Simplified schematic of known regulatory pathway for Mig1 and Mig2 in *Saccharomyces cerevisiae***

In glucose limiting conditions, the kinase Sak1 phosphorylates the kinase Snf1 which phosphorylates the transcription factor Mig1, causing it to move out of the nucleus. In glucose replete conditions Mig1 is not phosphorylated and remains in the nucleus to act as a repressor of alternative carbon utilization genes. Schematic is based on work from the following references [62][55][56][57][63].

using microarray technology. The mutant strain was profiled in YPD to induce glucose replete conditions at 30°C. Consistent with the hypothesis, there was some derepression of alternative carbon utilization genes in the *Camig1* mutant profile, but the effect was less pronounced than the *Scmig1* mutant profile[65]. *ScMig1* is known to form a complex with two other transcriptional repressors, *ScTup1* and *ScSsn6*(homologous with *CaNrg1*), so mutants of these strains in *C. albicans* were profiled as well to investigate the extent of overlap in transcriptional control. There was certainly overlap between genes regulated by all three of these repressors. However, there were many regulated genes that were unique to each mutant strain, indicating that these transcription factors have independent functions as well. This is in line with the fact that *CaNrg1* and *CaTup1* are known to be repressors of filamentation[66][67], whereas there is no data to suggest *CaMig1* plays a role in that function.

1.1.5 Mig2

In *Saccharomyces cerevisiae* *MIG1* has a paralog termed *MIG2*. In this species, Mig1 is the main repressor of alternative carbon utilization genes because Mig1 is sufficient to fully repress some genes. Mig2 is only necessary for repression of a subset of Mig1 regulated genes and has not been shown to regulate any carbon genes by itself[68]. There is no evidence to suggest that Snf1 phosphorylates or regulates Mig2 in response to glucose[62], so its regulatory mechanisms may be unrelated to the nuclear import/export form of regulation for Mig1 (3.1). Instead, there is some evidence to suggest that Mig2 exhibits mitochondrial localization in response to glucose limitation[69]. However, specific isoforms of Snf1 phosphorylate Mig2 and Mig1 in response to alkaline stress, so some Snf1 regulatory mechanisms may be conserved among the two paralogs in *S. cerevisiae*[70].

In *Candida albicans*, Mig2 has been mostly uncharacterized. A homozygous mutant strain of *mig2* is available as part of a homozygous transcription factor mutant library[71], and was phenotypically characterized in a large screen[72]. The only phenotypes that emerged for the *mig2* mutant strain were resistance to 5-fluorocytosine and a mild sensitivity to Fenpropimorph[72]. The *mig2* homozygous mutant has never been profiled prior to this thesis work, so the extent of conservation or functional redundancy between *CaMig1* and *CaMig2* was unknown.

It is interesting to note that *S. cerevisiae* contains a third paralog for *MIG1* and *MIG2* termed *MIG3*. *ScMig3* responds to glucose by binding the *SUC2* promoter, but it does not seem to functionally repress glucose related genes[68][62]. The transcription factor gene *MIG3* likely arose following the whole genome duplication event that occurred during the evolution of *S. cerevisiae*[73][74]. The whole genome duplication event that created *MIG3* occurred after the split in the evolutionary tree that led to the CUG clade of *Candida* species[75]. Therefore, *C. albicans* does not contain a homolog of *ScMIG3*.

1.2 Antifungal drugs

Investigating and developing new antifungal drugs is of the utmost importance due to the limited catalog of options. Caspofungin has emerged as an antifungal of choice in

the clinic[76], but how *C. albicans* responds to the drug is not fully understood. What we do understand is that caspofungin is an antifungal in the class of echinocandins and inhibits 1,3- β -glucan synthase in the cell wall of *C. albicans*. The gene *FKS1* encodes 1,3- β -glucan synthase[77] and mutations in *FKS1* have been shown to cause resistance to caspofungin in clinical isolates of *Candida* species[78]. However, the regulatory mechanisms of the transcriptional response of *C. albicans* to caspofungin have not been fully elucidated.

Cas5 is one transcription factor that has been investigated thoroughly and shown to regulate transcriptional responses to caspofungin[79][80]. However, a *cas5* mutant is also sensitive to the azole antifungal fluconazole[81] which effectively targets the fungal cell membrane by inhibiting the cytochrome P450 enzyme that is required for ergosterol synthesis. Since a *cas5* mutant is sensitive to both cell membrane and cell wall inhibitors, this suggests that Cas5 is not specific to the caspofungin response and may play a role in controlling general stress responses in the cell. Indeed, Xie et al. showed that Cas5 governs the cell cycle through the control of cell cycle, meiosis, and DNA replication genes, linking cell wall stress and cell cycle progression in *C. albicans*[80]. Similarly, many protein kinases control cell stress responses and mutants of these protein kinases exhibit hypersensitivity to caspofungin and other cell wall stresses such as oxidative or osmotic stress[82].

Sko1 is another transcription factor that has been shown to control caspofungin resistance in *C. albicans*[83]. Sko1 has a conserved homolog in *Saccharomyces cerevisiae* that forms a complex with *CaSsn6*/(homolog of *ScCyc8*) to regulate hyphal morphogenesis[84]. Sko1 is phosphorylated by the protein kinase Hog1 in response to osmotic stress, but surprisingly Sko1 was not phosphorylated in response to caspofungin. This results indicates that Sko1 may not be acting downstream of Hog1 in the MAP kinase pathway in response to cell damage. Instead, the protein kinase Psk1 may act upstream of Sko1, as *PSK1* expression was necessary for the induction of *SKO1* transcription in response to caspofungin treatment [83].

How is a transcriptional regulator of caspofungin responses identified and characterized? Bruno et al. attempted to define this question by identifying a set of 34 genes they called the "core caspofungin-responsive genes". This core set was based on genes that

were differentially regulated in their microarray dataset and in agreement with a previous dataset from Liu et al.[79][85]. Both of these studies performed their profiling using media containing 2% glucose and grew the cells in planktonic culture at 30°C. These conditions are convenient to handle *C. albicans* in the lab, but are not necessarily indicative of an *in vivo* infection where antifungals would be used. Xu et al. used nanoString technology to profile gene expression of an *in vivo* model of a systemic infection treated with caspofungin and found virtually no correlation between genes induced in *C. albicans* by caspofungin *in vitro* compared to *in vivo*[21]. This lack of correlation persisted even when the *in vivo* transcriptional profile was compared to cells grown at 37°C treated with caspofungin *in vitro*, indicating that the hyphal growth form was not sufficient to explain the lack of correlation[21]. These data suggests that the *in vivo* condition has unique properties for fungal drug response that we are currently unable to replicate *in vitro*.

1.3 Iron acquisition and Regulation

Iron is an essential nutrient for the host and virtually every microbe on earth[86]. Iron serves as an essential cofactor for metabolic reactions such as respiration. To obtain iron from the host, *C. albicans* has evolved multiple different strategies based on the complexities in which iron is stored in the host. These strategies include expression of the siderophore transporter Sit1, expression of multiple different ferric reductases, direct transport of reduced iron through Ftr1 and Fet34, and the acquisition of iron from hemoglobin through the expression of CFEM proteins[87][88][89]. Most of the iron content in the human body is stored in hemoglobin, so the ability to extract heme for use as an iron source is a necessary virulence trait for pathogens[90]. The CFEM Proteins (*Common in Fungal Extracellular Membrane*) are a family of related genes consisting of *CSA2*, *PGA7*, *RBT5*, *CSA1*, and *PGA10*. Currently, only Csa2, Pga7 and Rbt5 have been functionally linked to iron acquisition [88][91]. Csa2, Pga7, and Rbt5 function as receptors in a "relay network" to pass methemoglobin (Fe⁺³) to each subsequent protein based on localization. Csa2 is found extracellularly, Rbt5 is located at the cell periphery, and Pga7 is located at the cell membrane. Following this relay network, the iron is presumably endocytosed, but the receptor that functions at the endosome is currently unknown[92][93]. The CFEM proteins have been implicated in a number of roles in *C.*

albicans pathogenesis including biofilm integrity and virulence[94][92]. Although these proteins appear to function linearly in a network, the expression levels and phenotypic impact of each protein varies dramatically. *RBT5* is the most highly expressed gene of the three, but mutations in *PGA7* cause the most severe defect in growth on heme-containing media[92][93]. Clearly, there is more to uncover about the function of these proteins. Understanding the mechanisms of how these proteins promote virulence would be important to understand, since modulation of host nutritional immunity is an active field for translational research. There are several FDA approved iron chelators (deferoxamine and deferasirox), which have led to investigations into iron chelators as potential therapeutics for preventing infections[95] or used in combination with antifungals to clear infections[96][97].

Concentrations of iron in the human body can vary as widely as the carbon source. Iron in the gut can reach levels that are high enough to be toxic for *C. albicans*, but iron in blood and tissues is thought to be limiting[90]. How does *C. albicans* control the expression of iron uptake and utilization systems to survive in environments with different iron acquisition requirements? The iron regulatory network that maintains control of its iron requirements currently consists of three transcription factors: Sef1, Hap43, and Sfu1. The functions of these transcription factors were identified and characterized using a combination of phenotypic analysis[72], gene expression profiling[98], and whole-genome chromatin immunoprecipitation analysis[30]. These three transcription factors all regulate each other's expression and have unique roles depending on the iron requirement for *C. albicans*[30]. *SFU1* is highly expressed in the mouse gastrointestinal tract where it functions to repress iron uptake genes directly and through an indirect mechanism by repression of *SEF1*[30]. Sef1 directly activates iron uptake genes[72] and also activates Hap43, which controls expression of iron utilization genes necessary for respiration. Hap43 also represses *SFU1*, resulting in an indirect, mutual, regulatory relationship between Hap43 and Sef1[99][30]. Hap43 and Sef1 are essential for virulence in mouse models of systemic infections, while Sfu1 is dispensable[99][30]. However, Sfu1 and Sef1 are essential for persistence in the mouse gastrointestinal tract[30]. Therefore, this interweaving network allows *C. albicans* to precisely tune its regulation of iron acquisition and utilization to maintain its lifestyle as a commensal in the gut and a pathogen in the bloodstream.

1.4 Biofilm formation

(Edited from a review written by myself and Dr. Aaron Mitchell[100])

Biofilms are surface-associated microbial communities, encased in self-produced extracellular material, that exhibit phenotypes distinct from those of planktonic (free-living) cells. Microbes are thought to grow predominantly as biofilms in nature[101]. The surfaces with which biofilm cells are associated may be diverse, and include solid abiotic materials, tissues and cells, and air-water interfaces. In fact, a colony growing on an agar plate is a type of biofilm.

Biofilm cells are quite different from the mid-logarithmic phase planktonic cells that modern microbiologists were trained to study[102]. Biofilm populations are invariably heterogeneous. Cells at the periphery of the biofilm are bathed in the external medium; cells at the base of the biofilm may be limited for nutrients and oxygen, and surrounded by their neighbors' waste products. Cells at the periphery may be exposed to a rapidly fluctuating environment; cells at the base are buffered from many abrupt changes. Thus a mature biofilm may include cells exposed to a range of different nutrients, and the biofilm cell population may be growing at a range of different rates.

Our focus on biofilms stems from their central role in infection biology[103]. Biofilms are medically relevant in two major contexts: device-associated infection and *in vivo* growth. Device-associated infection is the phenomenon that presence of an implanted medical device is a significant risk factor for bloodstream or deep-tissue infection. The specific risk factor and the likely types of infecting organisms vary with the kind of device and its location. The connection to biofilm formation was first elucidated by Costerton and colleagues[103][101], who found biofilms of infecting organisms on the devices that were removed from infected patients. In the vast majority of cases, the devices are sterile when implanted, and later become colonized by microbes that enter the bloodstream. The biofilm on a device serves as a reservoir that continually seeds the infection. Unfortunately, as detailed later in this chapter, biofilm cells are generally resistant to antimicrobials; thus device removal may be the only therapeutic option. Because the usage of implanted devices continues to increase worldwide, the problem of device-associated infection will only grow in the future.

The second connection between biofilms and infection has to do with the nature of growth *in vivo*. Some infections are quite obviously surface-associated growth. Examples include mucosal infections such as thrush and vaginitis. Invasion of the surface may follow initial infection, and the surface itself may change over the course of infection due to inflammation and tissue damage. Other infections are not associated with host surfaces, but the infecting organisms grow as an aggregate encased in extracellular matrix material. The aggregates may be considered self-contained biofilms, analogous to the flocs that form at the end of industrial fermentations[104].

1.4.1 Biofilm gene expression

There has been long-standing interest in identification of genes that are induced during biofilm formation. Such genes have proven to be enriched for genes that contribute to biofilm formation, and can be informative in terms of broader biological processes that are biofilm-relevant. As such, biofilm-associated genes can reveal the identities of major regulatory systems and environmental signals that act during biofilm formation. Below we call these genes "biofilm-associated genes" because they have been defined through many different kinds of comparisons. Any one particular comparison may yield a distinctive set of genes that are up-regulated in biofilm cells.

Is there a fundamental biofilm-associated gene expression pattern? There have been a few different approaches to this problem. Garcia-Sanchez et al. profiled biofilm cells grown under diverse conditions in comparison to planktonic cells also grown under diverse conditions[105]. They arrived at a set of 325 genes (out of only 2002 represented on their microarrays) whose differential expression was characteristic of biofilm cells from multiple comparisons; 214 genes were up-regulated in biofilms. These 214 genes were enriched in transcription and translation genes as well as biosynthetic genes for amino acids, polyamines, nucleotides, and lipids. Up-regulation of numerous translation-associated genes in biofilm cells was also observed in a comparison that looked for shared gene expression features among two different wild-type strains, SC5314 and WO-1[106]. These findings argue that biofilm growth enables cellular biogenesis to occur over a prolonged period compared to planktonic growth in the same medium. A simple explanation is that a biofilm may capture excreted metabolites, thus facilitating their utilization when preferred metabolites are exhausted.

Many studies have reported that hyphal genes are up-regulated in biofilms compared to planktonic cells [107][108][109]). Garcia-Sanchez et al. had filtered those genes out by design through inclusion of the nonfilamentous *efg1 cph1* double mutant grown under biofilm and planktonic conditions [105]; it was discovered that the mutant had the novel ability to form a biofilm on a glass surface. However, in the RNA-Seq biofilm-planktonic comparison of both SC5314 and WO-1, down-regulation of hyphal genes was consistently observed in biofilm cells [106]. The biofilm time-course analysis of Fox et al.[110] may explain these disparate results: at early times, hyphal genes were up-regulated in biofilm cells, but at later times, they were down-regulated, relative to planktonic hyphae. Perhaps sufficiently high concentrations of quorum sensing molecules such as farnesol accumulate in mature biofilms [111][112], inhibiting hyphal growth and hyphal gene expression at late times.

How do gene expression features compare between biofilms grown *in vitro* and *in vivo*? Profiling of *C. albicans* catheter biofilms by Nett et al. [113] reveals some consistent responses. Specifically, amino acid biosynthetic genes and transcription/translation genes were up-regulated in biofilm cells *in vivo*. In addition, numerous transporters were up-regulated, thus suggesting that biofilm cells may be limited for nutrients. The study compared biofilm cells to planktonic hyphae, a likely basis for the failure to detect up-regulation of hyphal-associated genes in biofilm cells. Overall, then, the correlations among broad trends in gene expression indicate that *in vitro*-grown biofilms serve as a useful model for catheter biofilms that form *in vivo*.

Have biofilm-associated genes been validated functionally? In other words, is gene regulation a predictor of gene function? One approach is to use biofilm-associated gene properties to deduce biofilm-relevant regulatory pathways. This approach was implemented by the d'Enfert lab in their initial study of biofilm gene expression[105]. Because many amino acid biosynthetic genes were up-regulated in biofilm cells, they inferred that the general amino acid control regulator, Gcn4, may be critical for biofilm formation. Indeed, they observed that a *gcn4* mutant produced a defective biofilm, one with reduced biomass compared to the wild-type strain [105]. Another illustration of this kind of rationale comes from the observation that biofilm-associated gene expression resembles the response to hypoxia [114], an observation first reported for *Candida parapsilosis*. That observation suggests that a mutant defective in hypoxic regulation may be defective in biofilm formation. Indeed, Bonhomme et al. found that Tye7, a

transcription factor required for the hypoxic response [114], is required for many features of *C. albicans* biofilms[115]. A third example comes from the point raised above that hyphal-associated genes have often been observed to be up-regulated in biofilms (depending on the specific biofilm-planktonic comparison). That observation makes sense because hyphae are a prominent feature of *C. albicans* biofilms grown under almost any condition, and suggests that mutants defective in expression of hyphal-associated genes will be defective in biofilm formation. That prediction has turned out to be correct time and again ([116][117][108][112]). Therefore, inferences from biofilm profiling data about biofilm-relevant regulatory pathways has proven successful in terms of functional validation.

The second approach to functional validation is to determine whether each specific biofilm-associated gene has a measurable function in biofilm formation. Here the results have been mixed, though there may be some useful lessons for the future. The initial study of this kind, from the d'Enfert group, examined deletion mutants of 38 biofilm-associated genes for defects in biofilm biomass or hyphal morphogenesis [115]. The genes had been chosen based on the magnitude of their up-regulation in biofilms after elimination of likely essential genes and members of gene families. Eight of the 38 mutants produced biofilms with moderately reduced biomass but had no planktonic growth defect; one mutant had severely reduced biofilm biomass and a severe planktonic growth defect. On its face, the results were slightly disappointing because the yield of biofilm-defective mutants was low, and because the biofilm-defective mutants identified had mild defects. In a related approach, Desai et al. focused on genes that were up-regulated in biofilms of two different clinical *C. albicans* isolates [106]. Of 62 most highly up-regulated genes, viable insertion mutants could be isolated for 25 genes. The mutants were screened for a panel of biofilm-related phenotypes, including biofilm formation, drug tolerance, quorum-sensing signaling, and others. Most of these mutants, 20 of 25, had significant defects in at least one biofilm-related phenotype. The high yield of biofilm-relevant phenotypes in this study may have reflected both the gene selection criteria as well as the range and sensitivity of the phenotypic assays.

The validation approaches and results presented above apply to *in vitro*-grown biofilms. However, the specific *in vitro* conditions used can have dramatic effects on biofilm properties [118][119], and some mutations cause a biofilm defect only under a subset of *in vitro*

conditions. In fact, one theme that has emerged repeatedly in all aspects of infection biology is that *in vitro* conditions can be poor mimics of *in vivo* conditions. Hence the key validation approach in our view is to determine whether a biofilm-associated gene can be shown to function in an animal model of biofilm infection. The most frequently used model is a rat venous catheter biofilm model [120]. Several mutant strains have similar biofilm defects *in vitro* and *in vivo* [106][121][122][123][108][124][125]. However, there are examples in which the severity of a mutant defect is much greater *in vitro* than in a catheter model *in vivo*, and vice versa [106][121][108][123]). It would accelerate biofilm research considerably if there existed an *in vitro* model that could accurately predict *in vivo* outcomes.

1.4.2 Biofilm gene regulation

It has proven useful to identify biofilm regulators for three main reasons. First, because a single transcription factor often controls many functionally related target genes, a single biofilm-defective transcription factor mutant can lead to discovery of many biofilm-relevant genes among the target genes that it regulates. One of the initial illustrations of this principle came from studies of the *S. cerevisiae* mating type locus, which specifies master regulators whose target genes confer individual cell type-specific properties[126]. Second, there are many examples in which a transcription factor mutant has a more prominent phenotype than mutants defective in individual target genes of the transcription factor. A simple illustration comes again from studies of *S. cerevisiae*, this time of meiosis and spore formation: many mutations that caused a prominent sporulation defect affected meiotic regulators rather than the machinery that mediated specific meiotic events [127]. This outcome could reasonably be considered a result of the first principle. Third, some biofilm regulators identified in *C. albicans* have orthologs in other *Candida* species that also govern biofilm formation (discussed below). Hence a biofilm regulator can provide an entry point for definition of biofilm-relevant genes and biological processes in many organisms.

The transcription factors that control biofilm formation have been identified through several approaches. One approach is deductive logic based upon expression profiling or other biofilm features, as discussed above [115][116][117][128]. A second approach is to screen a set of transcription factor mutants for defects in biofilm formation or

related phenotypes. For example, panels of both insertion and deletion mutants have been screened for failure to form biofilms [110][108][129]. An elegant variation on this approach was to assay mutants at several time points in biofilm formation [110]. Another related screen was for mutants that were defective in adherence to a silicone substrate [121]. Overall, 51 transcription factor genes have been shown to affect biofilm-related properties in these large-scale screens as well as more focused studies [116][130].

These studies have revealed that there is a major biofilm regulatory network, sometimes called the "core network"[130], comprising transcriptional regulators of hyphal morphogenesis and hyphal genes. These transcription factors include Flo8, Rfx2, Gal4 [110], Brg1, Bcr1, Rob1, Efg1, Ndt80, and Tec1 [108] [129][128]. These transcription factors are functionally interconnected, in that each binds to at least one other network regulator's upstream region and regulates its expression [110][108]. Rfx2 and Gal4 are negative regulators of biofilm formation; the respective null mutations cause increased biofilm formation and, for Rfx2, an increase in expression of many hyphal genes [131]. The other transcription factors in this network are positive regulators of biofilm formation; null mutations cause reduced biofilm formation and reduced expression of hyphal genes [110][108][129][128]. For many of the positive regulators in this network, current evidence indicates that adhesin genes ALS1, ALS3, and HWP1 are critical downstream target genes, because overexpression of one of these genes can restore considerable biofilm formation [123][108][132]. However, there are likely to be additional network target genes that contribute to biofilm formation, because phenotypic rescue by adhesin overexpression is only partial in some cases [108]. In fact, there are 21 transcription factor genes whose 5' regions are bound by one or more network regulators, and that govern biofilm-relevant phenotypes (AHR1, BPR1, CAS5, CRZ2, CZF1, FCR3, GCN4, GRF10, GZF3, MSS11, NRG1, RFG1, RIM101, TRY4, TRY5, TRY6, TYE7, UME6, ZAP1, ZCF31, and ZCF8) [116][130]. Hence this regulatory network controls adhesins and, potentially, many additional diverse biofilm properties.

Are all biofilm properties under control of this core network? It is not clear as of yet. There are 21 transcriptional regulatory genes that control biofilm formation or biofilm-relevant properties, including ACE2, ADA2, ARG81, DAL81, FGR27, LEU3, MET4, NOT3, RLM1, SNF5, SUC1, TAF14, TRY2, TRY3, UGA33, WAR1, ZCF28, ZCF34, ZCF39, ZFU2, and ZNC1 [130]. These regulators govern such properties as the level of extracellular matrix [133] or the adherence of yeast-form cells [121]. These features could

conceivably be regulated independently of hyphal adhesins. Whether they are controlled through the core network is an interesting question for future studies.

Have we found all of the biofilm regulators? One could reasonably argue that 51 regulators are plenty! We suspect that there are others, though, and that they are worth studying. We think that there are others worth studying because of the *in vitro-in vivo* differences mentioned earlier in this chapter. Specifically, our lab has identified transcription factors that are required for biofilm formation *in vivo*, but not *in vitro* [121] (and this work). Thus we hypothesize that the systematic screens used thus far may have overlooked other transcription factors with these properties. Perhaps they could be identified through application of the elegant mutant pool screens used by Noble [71] to assay *in vivo* biofilm formation assays.

1.4.3 Imaging biofilms

Please see my co-authored method paper [134]

Using confocal microscopy to observe and characterize *Candida albicans* biofilms is a technical challenge that has been a key part of this thesis. Biofilms of *C. albicans* are often dense and can reach upwards of 600 μ M in height. This density blocks almost all light penetration through the biofilm, making fluorescence imaging impossible. I worked with Dr. Fred Lanni to devise and improve a new protocol to clarify biofilms using methyl salicylate allowing light penetration through the biofilm and vastly speeding-up our imaging protocol. We published a method/review article discussing this protocol in depth. This work was presented in concert with work done by previous members of the lab, Dr. Jigar Desai, and Dr. Jonathan S Finkel. My contributions to the paper include helping with the methyl salicylate protocol and imaging biofilms using different culture mediums to show the heterogeneity and phenotypic plasticity of *C. albicans* biofilms. The full text of paper is included at the end of this thesis.

Chapter 2

Methods

2.1 Strains and Media

Strains were maintained in 15% glycerol frozen stocks at -80°C. Overnight cultures were grown in 15mL culture tubes, rotating at 75rpm, at 30°C in liquid YPD medium (2% dextrose, 2% peptone, 1% yeast extract). Transformants were selected on synthetic complete medium (0.67% yeast nitrogen base with ammonium sulfate without amino acids, 2% dextrose, 2% bacto agar and supplemented with synthetic amino acids supplements as needed). Spider media (1%mannitol 1%nutrient broth 0.2% K₂HPO₂, pH 7.2) or RPMI 1640 media plus 10% FBS was used where indicated to induce hyphal formation in liquid culture and on agar plates (2% agar).

2.2 Fungal Transformation

PCR products or linearized plasmids were transformed into *C. albicans* cells using the lithium acetate transformation method [135].

2.3 *mig1 mig2* Strain Construction

(See Table 5.3 for complete strain genotypes) Homozygous mutants were constructed in the SN152 background[71] using the pSN69 or pNAT[136] cassette. Both alleles were

deleted using a guide RNA targeting the gene of interest and a transient CRISPR-Cas9 system [136]. Strain KL742 was created by deleting *MIG2* in the *mig1Δ/Δ* parent strain from the Homann Deletion Collection[72] by PCR amplifying the pSN69 cassette containing the *Candida dubliniensis ARG4* gene using primers KL376 and KL377 which contain 80 basepairs of homology upstream of the coding region 80 basepairs of homology downstream of the *MIG2* coding region. Transformants were selected on arginine dropout media, restreaked onto a fresh plate, and verified as homozygous deletions using colony PCR.

Strains KL807 and KL829 were made by complementation of the parents strain KL742 using vector pAG6, a derivative of CIP10 marked with *SAT1* [137][50]. The vector pAG6 was a kind gift from the lab of Dr. Michael Lorenz. The vector was cut using restriction enzymes Xho1 and Apa1. The *MIG1* coding region plus 1941 basepairs upstream and 633 basepairs downstream and the *MIG2* coding regions plus 255 basepairs upstream 536 basepairs downstream were amplified from genomic DNA from strain SC5314. The PCR amplified region was cut using Xho1 and Apa1 and ligated to the vector backbone. The resulting vectors were transformed into XL1-Blue competent *E. coli* cells. The complementing vectors were linearized using enzyme Stu1 and transformed individually, into strain KL742 at the RPS10 locus selecting for *NAT* resistant colonies.

Strain KL794 was created by deleting *MIG1* in the *mig2Δ/Δ* parent strain from the Homann Deletion Collection[72] by PCR amplifying the pSN69 cassette containing the *Candida dubliniensis ARG4* gene using primers KL401 and KL402 containing 80 basepairs of homology upstream of the coding region and 80 basepairs of homology downstream of the *MIG1* coding region. Transformants were selected on arginine dropout media, restreaked onto a fresh plate, and verified as homozygous deletions using colony PCR.

Strains KL924 (*sak1Δ/Δ mig2Δ/Δ mig2Δ/Δ* mutant and KL926 (*snf1Δ/Δ mig2Δ/Δ mig2Δ/Δ*) were constructed using the parent strain KL794 by PCR amplifying the pNAT cassette[136] using deletion primers verified from [138] containing 80 basepairs of homology upstream of the coding region and 80 basepairs of homology downstream of the *SAK1* coding region. *NAT* resistant colonies were selected, restreaked, and verified using colony PCR.

2.4 *zfu2* Strain Construction

(See Table 7.1 for complete strain genotypes) *C. albicans* mutants were derived from the parent strain background, BWP17[139]. The mutant strain TA114 (*zfu2* Δ/Δ) was designed through gene disruption by PCR amplifying pRS-*URA3* and pRS-*ARG4* with homology to directly upstream and downstream of the *ZFU2* coding region. The *URA+* and *ARG+* transformants were verified as homozygous deletions using colony PCR and made *His+* using plasmid pDDB78[140] by integration of the Nru1-digested plasmid at the *HIS1* locus. For construction of the complemented strain KL124 plasmid pDDB78 was digested with Sac1 and Not1 and combined with PCR amplified product from genomic DNA 1.2Kb upstream and 500 downstream of the *ZFU2* coding region. CFEM protein gene overexpression strains KL269, KL271, and KL273 were constructed with PCR primers designed to amplify the *NAT1*-p*TDH3* cassette from plasmid pCJN542 [141] and contained homology to the region directly upstream of the start codon of *CSA2*, *RBT5*, and *PGA7*. The PCR products were then transformed into the *zfu2* mutant strain TA114. Strains were checked with colony PCR to confirm replacement of the promoter of one allele of *CSA2*, *RBT5*, or *PGA7* with the *TDH3* promoter. DAY185 was used as the prototrophic wild-type strain in all cases[142].

2.5 Macrophage Killing Assay

This macrophage killing assay protocol was graciously provided by Elisa Vesely from the lab of Dr. Michael Lorenz [49]. The J774A.1 murine macrophage cell line was obtained from Sai Gopalakrishna Yerneni from the lab of Dr. Phil Campbell. Cells were maintained in RPMI media without phenol red, with 10% Serum, and 5% penicillin streptomycin at 37°C in 5% CO₂. Cells were used from passages 8-16. 100 μ L of macrophages were plated at a concentration of 2.5x10⁵ cells/mL overnight in a 96 well tissue culture treated polystyrene plate. The following day, overnight cultures of *C. albicans* were subcultured in YPD media for 5 hours. Subcultured cells were washed twice in PBS and diluted to a concentration of 3x10⁶ in pre-warmed RPMI media without FBS, without phenol red, with 5% penicillin streptomycin at 37°C. Macrophages that were incubated overnight, should have doubled to a concentration of 5x10⁵ cells/mL. Media was removed and replaced with 150 μ L of RPMI without FBS (FBS interferes with the LDH release

quantification). 50 μ L of *C. albicans* cells were added to each well for a MOI of 3. (3 *C. albicans* cells:1 macrophage). 6 wells of macrophages were not incubated with *C. albicans* cells for 3 spontaneous release control wells and 3 max release control wells. Cells were incubated for 5 hours. To achieve max LDH (Lactate Dehydrogenase) release, 10 μ L lysis solution from the Pierce LDH Cytotoxicity Assay Kit was added to each max release control well. For positive control wells, 200 μ L of a 10mL PBS + 1%BSA freshly made stock was added to 3 blank wells and 2 μ L of positive control mix from the kit was added. Supernatant from all wells was diluted 1:5 in PBS and 100 μ L was pipetted into a new 96 well plate. 50 μ L of substrate mix from Pierce LDH Cytotoxicity Assay Kit was added to each well, protected from light, and incubated for 30min. at RT. Following incubation, 50 μ L of Stop Solution from the kit was added to each well. Absorbance was read on a Tecan at 490nm and background absorbance was read at 680nm which was subtracted from the 490nm reading. Percent cytotoxicity was calculated according to the manufacturers guidelines: For each well % cytotoxicity was calculated by subtracting the LDH activity of the spontaneous LDH release wells from the wells containing *C. albicans* cells and then divided by the total LDH activity [(Maximum LDH Release Control activity) – (Spontaneous LDH Release Control activity)], and multiplied by 100. The assay was performed in triplicate with three biological replicates to calculate percent cytotoxicity. Significance was calculated using the GraphPad PRISM one-way ANOVA test $p < 0.05$ significance.

2.6 Hyphal Growth Assay

Hyphal morphology was accessed as previously described[138]. Overnight cultures were washed in sterile water and inoculated at an OD of 0.2 into 5mLs of pre-warmed media as indicated. Cells were grown in glass culture tubes for 4 hours rotating at 75 rpm. Cells were fixed in 4% formaldehyde for 20 minutes, washed in PBS, and stained with calcofluor white at a final concentration of 30 μ g/mL for 10 minutes. Cells were washed in PBS and kept in the dark at 4°C until imaged. Cells adhered to slides by coating with concanavalin A and visualized with a Zeiss Axio Observer Z.1 fluorescence microscope and a 60x objective.

2.7 Endothelial Cell Damage Assay

Endothelial cell damage by *C. albicans* was assessed as previously described using a ^{51}Cr release assay[143][144]. Briefly, human endothelial cells were cultured in RPMI 1640 medium and loaded with 5 $\mu\text{Ci}/\text{ml}$ Na_2 $^{51}\text{CrO}_4$ overnight. Cells were washed, and inoculated with *C. albicans* cells at a concentration of 410^4 organisms per well. Cells were incubated for 3 hours and the perfect ^{51}Cr release was quantified using the formula: (experimental release - spontaneous release)/(total incorporation - spontaneous release). The assay was performed in triplicate using three biological replicates. Statistical significance was calculated using GraphPad PRISM one-way ANOVA test $p < 0.05$ significance.

2.8 RNA Extraction

RNA samples were prepared as follows. Wild-type, KL742, KL820, and KL738 5.3 were inoculated at an OD of 0.2 and grown in 50mL of YPD or YPG media for 4 hours, shaking at 220rpm, at 37°C. RNA preparations were prepared as previously described [138]. Briefly, cells were harvested by filtration and frozen at -80°C. RNA was then extracted using a Qiagen RNeasy Kit (cat#74104) following the protocol with a few modifications. Frozen cells were thawed, washed, and pelleted in microfuge tubes. 600 μL of RLT buffer with 1%BME and 300 μL of zirconia beads, and 600 μL of phenol-chloroform were added to the cells. This mixture was vortexed with a bead-beater at 4°C for 3 minutes. The supernatant was mixed 50:50 with 70% ethanol and then RNA isolation was performed following the manufacturer's instructions.

2.9 RT-PCR

RNA used for RT-PCR was extracted from strains following 4 hours growth in YPD at 37°C. DNase (Turbo-DNase Ambion) was added to 10 μg of total RNA to remove all DNA from the RNA. cDNA was then synthesized from the RNA, including a control sample where no reverse transcriptase was added to ensure that the RNA was not contaminated with DNA. 2X iQ SYBR Green Supermix (Bio-Rad), 1 μl of the cDNA reaction mixture, and 0.2 μM of primers were mixed in a total volume of 25 μl per reaction. Real-time PCR

was performed in triplicate using a CFX Connect Real-Time System (Bio-Rad) using the following cycle: 95°C for 5 min, 40 cycles of 95°C for 45s, 58°C for 30s. Gene expression was determined using Bio-Rad iQ5 software ($\Delta\Delta\text{CT}$ method)[145], with primers for *TDH3* used for normalization. A standard curve for the efficiency of each primer pair was determined and factored into the final normalization.

2.10 NanoString Analysis

Nanostring analysis was performed on tissue samples from a mouse model of oral candidiasis as previously described [21][138][121]. For this analysis, 73 target genes associated with iron acquisition and utilization and 3 normalization genes were selected. For each assay, 125–300 ng of *Candida* RNA extracted from mouse tongue tissue was added to the nanoString codeset mix and incubated at 65°C overnight (16–18 hours). Reaction mixes were loaded on the nanoString nCounter Prep Station for binding and washing, and the resultant cartridge was transferred to the nanoString nCounter digital analyzer for scanning and data collection. 600 fields were captured per sample. To analyze ratio differences in gene expression among samples, negative counts were subtracted from all samples, and the average of the geometric mean of target genes *arp3*, *dst1*, and *yra1* was used for normalization among all samples. Three samples for each mutant or wild-type strain were analyzed.

2.11 RNA Sequencing and Analysis

The RNA was run on a TapeStation to check integrity of the RNA and then treated with DNase: 5 to 6 μgrams of total RNA was incubated with 2 units of TurboDNase (Invitrogen) in a 50 μl reaction for 15 minutes at 37°C. To inactivate the DNase, NaCl, Tris-HCl pH7.5, and EDTA, were added to a final concentration of 500mM, 200mM, and 10mM respectively. The RNA was extracted with PCI (acidic) and the supernatant containing the RNA was purified over a Zymo research RNA clean up column, and eluted into 15 μl of nuclease free water. The RNA integrity was again checked on the TapeStation (RNA tape). The concentration of RNA was quantified using the Nanodrop. 2 micrograms of total RNA was used as input for the Lexogen mRNA sense kit v2. The kit was used according to the manufacturer’s instructions for shorter amplicons. Eleven cycles of

PCR were performed (the kit has varying instructions for the PCR). The libraries were run on a D1000 DNA tape (Tapestation) to assess the size and quality of the library. The concentrations of the libraries were measuring using the High sensitivity DNA assay for the Qubit (Invitrogen). The libraries were diluted and pooled at 8nM and run on the Miseq, clustered at 8pM, 2x75, 13 million reads. Samples were then sent to Novogene to run on the HiSeq. Reads were aligned to the reference genome (SC5314 assembly 22) using TopHat and statistical analysis was performed using the DESeq package.

2.12 OPC Infections

OPC infections were performed as previously described[146]. Five immunosuppressed wild-type, female BALB/c mice (6 weeks old) were used for each strain of *C. albicans*. Mice were immunocompromised using cortisone acetate treatment. A suspension of cortisone acetate at a concentration of 225 mg/kg cortisone in 0.05% Tween and sterile PBS was prepared. A 26-gauge needle was used to inject 10uL of cortisone stock per 1 gram of mouse subcutaneously on the posterior neck. This treatment was administered for three days prior to infection. On the day of infection, primary anesthetic was prepared using ketamine(15mg/mL) and xylazine(1.5mg/mL) at a dose of 6.7x the weight of the mouse. Anesthetic was administered using an intraperitoneal injection. Prototrophic strains CW542, KL475, KL522, KL478, and KL506 were grown in YPD overnight and diluted to a cell density of 2×10^7 cells/mL in sterile YPD media. A sterile cotton ball weighing between 0.0023-0.0027g was soaked in the diluted *C. albicans* yeast culture or sterile PBS for the Sham control and was placed sub-lingually for 75 minutes. During the 75 minute infection, 1mL of saline was injected subcutaneously in two locations on the back of the mice and the mice were kept warm with a heat lamp. Following the infection, the cotton balls were removed and the animals were allowed to recover from the anesthetic. The infection was carried out for a total of 5 days, and the mice were monitored daily. Cortisone acetate treatment was administered during the 5 day infection on days 1 and 3. On the 5th day, mice were sacrificed and the tongues were excised, weighed, and dissected lengthwise into 2 halves. One half was used for fungal burden quantification and the other half was used for Nanostring gene expression analysis. Tongue tissue for fungal burden analysis was homogenized using a GentleMACS(Miltenyi Biotec) dissociator and serially diluted onto YPD plates containing 50g/mL of ampicillin. Fungal burden was

calculated by averaging the colony forming units per gram tissue. The CFU/gram of tissue was averaged among the five mice for the final fungal burden calculation. All efforts were made to minimize suffering, in accordance with recommendations in the Guide for the Care and Use of Laboratory Animals of the NIH.

2.13 Rat Venous Catheter Infections

In vivo analysis of biofilm formation in the rat central venous catheter model was performed as described previously[120]. Female Sprague-Dawley rats weighing 400 g (Harlan Sprague-Dawley, Indianapolis, Ind.) were used for all biofilm assays. Catheters were inoculated with the strain as indicated. 24 hours post inoculation, the catheters were removed, sliced to reveal the lumen of the catheter, and the biofilms were imaged via scanning electron microscopy. For the ferric chloride iron rescue biofilm assay, 200 μ g per liter of FeCl₃ (the concentration of iron in synthetic defined culture medium) was added to the inoculum and the biofilm assay was carried out normally.

2.14 Statistical Analysis

Data for (3.13) (3.11) and (6.6) were analysed using Graph Pad Prism (v.6). Statistical significance was determined by one-way ANOVA test with a *post hoc* Dunnett comparison test. All tests were performed with a confidence level of 95%.

Chapter 3

Results

3.1 Mig1 and Mig2 are redundant in function

We screened a panel of transcription factor mutant strains of *Candida albicans* in an attempt to identify mutants that exhibited hypersensitivity to the echinocandin caspofungin. We chose to focus on transcription factor mutants due to the gap in knowledge of transcriptional regulators that control the response to caspofungin. The transcription factors Cas5 and Sko1 have been characterized previously and shown to control the cell wall damage response [79][80][142], but other transcription factors have not been extensively characterized. We found that the *mig1* mutant and the *mig2* mutant strains showed mild sensitivity to caspofungin. Mig1 and Mig2 are named for their homologs in *Saccharomyces cerevisiae*, *ScMig1* and *ScMig2*. An alignment of the protein sequences shows good conservation within the DNA binding domain of all four transcription factors, but little conservation among the remaining regions of the proteins (See Fig. 3.1). Since Mig1 and Mig2 have largely overlapping functions in *S. cerevisiae* [68], we decided to construct a double *mig1 mig2* mutant strain and tested it for caspofungin sensitivity. We found that the double mutant strain was drastically more sensitive to caspofungin compared to either single mutant, (See Fig. 3.2) indicating that Mig1 and Mig2 have overlapping or redundant functions in *C. albicans*. Complementation of the double mutant strain with one copy of *MIG1* or *MIG2* restored growth comparable to the wild-type strain.

We wanted to determine whether Mig1 and Mig2 show redundancy in response to other cell stress-inducing agents, so we tested the double mutant and complemented strains for sensitivity to calcofluor white and the azole antifungal, fluconazole. The *mig1 mig2* double mutant strain showed sensitivity to calcofluor white, but not fluconazole (See Fig. 3.3). Calcofluor white and caspofungin both target components of the cell wall, while fluconazole affects ergosterol synthesis. This suggests that the *mig1 mig2* double mutant cells exhibits cell wall defects but not cell membrane defects. Complementation of the double mutant strain with one copy of *MIG1* or *MIG2* restored growth comparable to the wild-type strain, adding further evidence that Mig1 and Mig2 redundantly control cell wall integrity. The hypersensitivity of the double mutant to caspofungin could be reversed by the addition of an osmoprotectant (1.5mM sorbitol) (See Fig. 3.3). This phenotype is consistent with a defect in cell wall biogenesis or cell wall integrity[148].

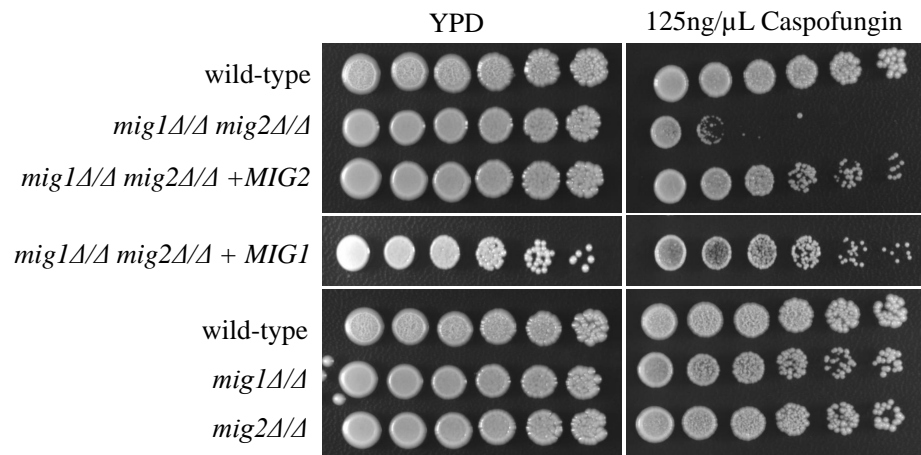


FIGURE 3.2: **The *mig1 mig2* double mutant strain is sensitive to the drug caspofungin.**

Strains CW542(wild-type), KL742(*mig1* Δ/Δ / *mig2* Δ/Δ), KL829(*mig1* Δ/Δ *mig2* Δ/Δ + *MIG1*), KL807(*mig1* Δ/Δ / *mig2* Δ/Δ + *MIG2*), KL820(*mig1* Δ/Δ), and KL738(*mig2* Δ/Δ) were serially diluted 5-fold on YPD and YPD plates containing 125ng/mL of caspofungin. Plates were incubated for 2 days at 37°C. Complementation of one allele of *MIG2* or *MIG1* restored growth of the double mutant on caspofungin plates.

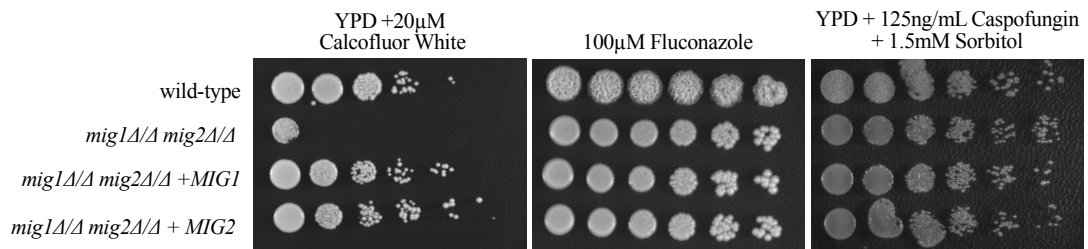


FIGURE 3.3: The *mig1 mig2* double mutant strain is sensitive to calcofluor white but not fluconazole. Addition of sorbitol can restore cell wall integrity defects in the double mutant strain.

Strains CW542(wild-type), KL742(*mig1*Δ/Δ/ *mig2*Δ/Δ), KL829(*mig1*Δ/Δ*mig2*Δ/Δ+ *MIG1*), and KL807(*mig1*Δ/Δ/ *mig2*Δ/Δ+ *MIG2*), were serially diluted 5-fold on YPD plates and YPD plates containing 20μM calcofluor white, 100μM fluconazole, or 125ng/mL of caspofungin + 1.5mM sorbitol. Plates were incubated for 2 days at 37°C.

3.2 Mig1 and Mig2 are repressors of alternative carbon utilization genes

To determine the function of the transcription factors Mig1 and Mig2, we used RNA-sequencing to profile the wild-type, *mig1*, *mig2*, and *mig1 mig2* double mutant strains. We chose to profile these mutants under three different conditions of interest: 1. YPD (2% glucose) 2. YPG (2%glycerol) 3. YPD + 125ng/mL caspofungin. All four strains were profiled in YPD media at 37°C for a high glucose condition. This condition would tell us whether *CaMig1* and *CaMig2* have conserved roles as repressors of alternative carbon utilization sources, similar to their homologs in *Saccharomyces cerevisiae*. We chose to profile the single mutant strains because we wanted to determine the extent of redundancy of the single homozygous mutant strains compared to the double mutant strain. Two previous studies have profiled the *mig1* mutant strain [65][149], but the gene expression profile of the double mutant strain or a *mig2* mutant strain have never been investigated. The second condition we chose was YPG (*Yeast Peptone Glycerol*) media at 37°C. We chose this condition because in *S. cerevisiae*, glycerol relieves repression by Mig1 and Mig2. In *S. cerevisiae*, the presence of glycerol results in phosphorylation of Mig1, causing it to relocate to the cytoplasm where it can no longer act as a repressor in the nucleus [55][62][57]. This derepression allows expression of alternative carbon source utilization genes and utilization of glycerol as a carbon source. Finally, we chose to profile the *mig1 mig2* double mutant and wild-type strains in YPD + 125ng/mL of caspofungin at 37°C. This condition would allow us to determine how the transcription factors, Mig1 and Mig2, control the cell wall integrity response.

3.2.1 RNA-sequencing results

To avoid false positives, three independent replicates were performed and only genes that were at differentially regulated at least 2-fold with a statistical confidence of $p < 0.05$ were included. Deletion of both *MIG1* and *MIG2* had a dramatic impact on global gene expression; a total of 617 genes or $\sim 10\%$ of open reading frames in the genome were differentially regulated in the double mutant strain in YPD media (See Fig. 3.4). 245 genes were uniquely upregulated in the double *mig1 mig2* mutant strain compared to only 90 genes that were uniquely downregulated. 42 upregulated genes were in common

among all three mutant strains. Several of the 42 of transcripts are upregulated by a greater fold change in the double mutant strain indicating that for these genes, the repressors work in a synergistic manner. There were several genes whose expression were differentially regulated only in the single *mig1* and *mig2* mutants but not in the double mutant. It is unclear how these genes might be controlled in this manner. Of the upregulated genes in the double mutant strain, many are obvious alternative carbon utilization genes including glucose transport scavengers, *HGT17*, the carboxylic acid transporter genes *JEN1*, *JEN2*, glyoxylate cycle genes *ICL1*, and the gluconeogenic gene *PCK1* (See Fig. 3.5 See Fig. 3.6). These genes exhibited various forms of redundant control by Mig1 and Mig2 including complete redundancy for *JEN1*. Other genes showed partial dependency on Mig1 (*JEN2*) or partial dependency on Mig2 (*ICL1*). Overall, our results indicate that Mig1 and Mig2 function as repressors of alternative carbon source utilization genes in a largely, but not completely, overlapping fashion.

3.3 The *mig1 mig2* mutant gene expression profile shows changes in cell wall genes

Several cell wall remodeling genes were upregulated in the *mig1 mig2* mutant strain when grown in YPD media. The mutant strain show increased expression of chitanase genes *CHT1* and *CHT2*, a chitin deacetylase *CDA2*, general cell wall protein genes *PGA17*, *PGA25*, *RBR2*, *PGA32*, *PGA15*, *PGA45*, *IFF4*, and several hyphal-associated cell wall protein genes *RBT1*, *ALS1*, and *CSP37*.

Conversely, β -glucan remodeling and cell wall glycosylation genes were downregulated in the double mutant, including *XOG1* which encodes a 1,3- β -glucanase, *PIR1* which encodes a 1,3- β -glucan-linked structural cell wall protein, and three mannosyltransferase genes *MNN1*, *MNN12*, and *MNN22*.

These changes in cell wall protein genes accompany the vast number of carbon related transporters that are upregulated in the *mig1 mig2* mutant strain (See Fig. 3.5). These gene expression changes lead us to suggest that the drug sensitivity in the mutant may be due to wide-ranging structural and functional differences between the mutant and wild-type strains. This might be similar to a conclusion from Cottier et al. where they found that Mig1 controls the resistance of *C. albicans* to weak organic acids through

the repression of membrane transporters [149]. However, it is unclear how overexpression of these membrane transporters affects stress responses, cell wall integrity, or drug transport.

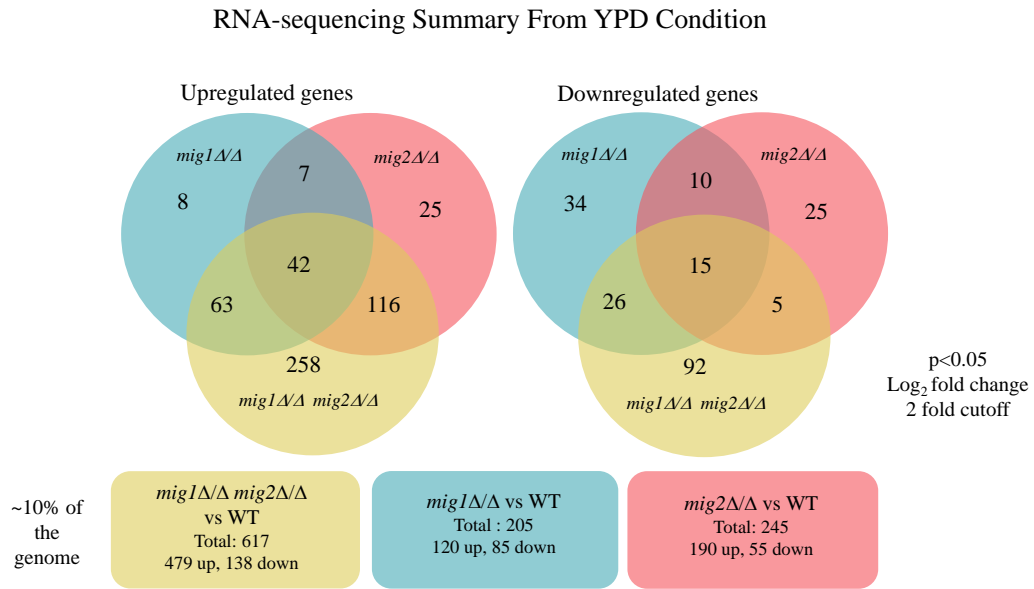


FIGURE 3.4: **Venn Diagram** summary of the distribution of significant differentially expressed genes between the *mig1*, *mig2*, and *mig1 mig2* double mutant strains compared to the wild-type strain in YPD media. Included in the diagram are strains CW542(wild-type), KL742(*mig1* Δ/Δ /*mig2* Δ/Δ), KL820(*mig1* Δ/Δ), and KL738(*mig2* Δ/Δ).

Gene Ontology categories of upregulated genes in the *mig1 mig2* double mutant in YPD

GO name	Adjusted p-value	# genes / category	# genes / input
oxidation-reduction process	4.0806e-10	56 / 264	56 / 479
glyoxysome	4.0806e-10	17 / 28	17 / 479
fatty acid beta-oxidation	1.774e-9	11 / 12	11 / 479
peroxisomal membrane	9.0306e-8	10 / 12	10 / 479
sugar transmembrane transporter activity	1.1691e-7	13 / 22	13 / 479
glucose transport	1.1691e-7	13 / 22	13 / 479
carbohydrate transport	2.1446e-7	13 / 23	13 / 479
fatty acid catabolic process	1.8108E-06	7 / 7	7 / 479
glucose transmembrane transporter activity	2.2584E-06	11 / 19	11 / 479

FIGURE 3.5: Gene Ontology (GO)-term analysis of significant upregulated genes in the *mig1 mig2* double mutant strain compared to the wild-type strain in YPD media

Included in the diagram are strains CW542(wild-type), and KL742(*mig1* Δ/Δ *mig2* Δ/Δ) from the RNA-sequencing results in YPD media at 37°C.

		Log ₂ Fold Change			
		<i>mig1</i> Δ/Δ	<i>mig2</i> Δ/Δ	<i>mig1</i> Δ/Δ <i>mig2</i> Δ/Δ	
HGT17	Glucose transporter	4.12	n.s.	8.97	Mig1 dependent partial redundancy
JEN1	Lactate transporter	n.s.	n.s.	5.7	Complete redundancy
JEN2	Dicarboxylic acid transporter	6.17	n.s.	8.28	Mig1 dependent partial redundancy
ICL1	Isocitrate lyase	n.s.	1.34	6.48	Mig2 dependent partial redundancy
PCK1	Phosphoenolpyruvate carboxykinase	2.76	1.13	4.77	Possible additive interaction
ADH2	Alcohol dehydrogenase	1.96	n.s.	7.73	Mig1 dependent partial redundancy

n.s. = Not Significant

FIGURE 3.6: Upregulated alternative carbon source utilization genes in the *mig1 mig2* double mutant show various types of genetic regulation

Included in the chart are strains KL820(*mig1* Δ/Δ), KL738(*mig2* Δ/Δ), and KL742(*mig1* Δ/Δ *mig2* Δ/Δ) compared to the wild-type strain CW542 from the RNA-sequencing results in YPD media at 37°C.

3.4 Profile of the *mig1 mig2* mutant strain in YPG media

We profiled the *mig1 mig2* mutant strain in media containing glycerol as the carbon source because nonfermentable carbon sources have to shown to alleviate repression of genes by Mig1 [55][62]. 322 genes were upregulated and 140 genes were downregulated in the double mutant strain compared to wild-type indicating that Mig1 and Mig2 may still function as repressors in the presence of glycerol as a carbon source. Although a significant number of genes were derepressed, the extent of fold change increase was dampened overall compared to the YPD condition, as shown in the dot plots (See Fig. 3.7).

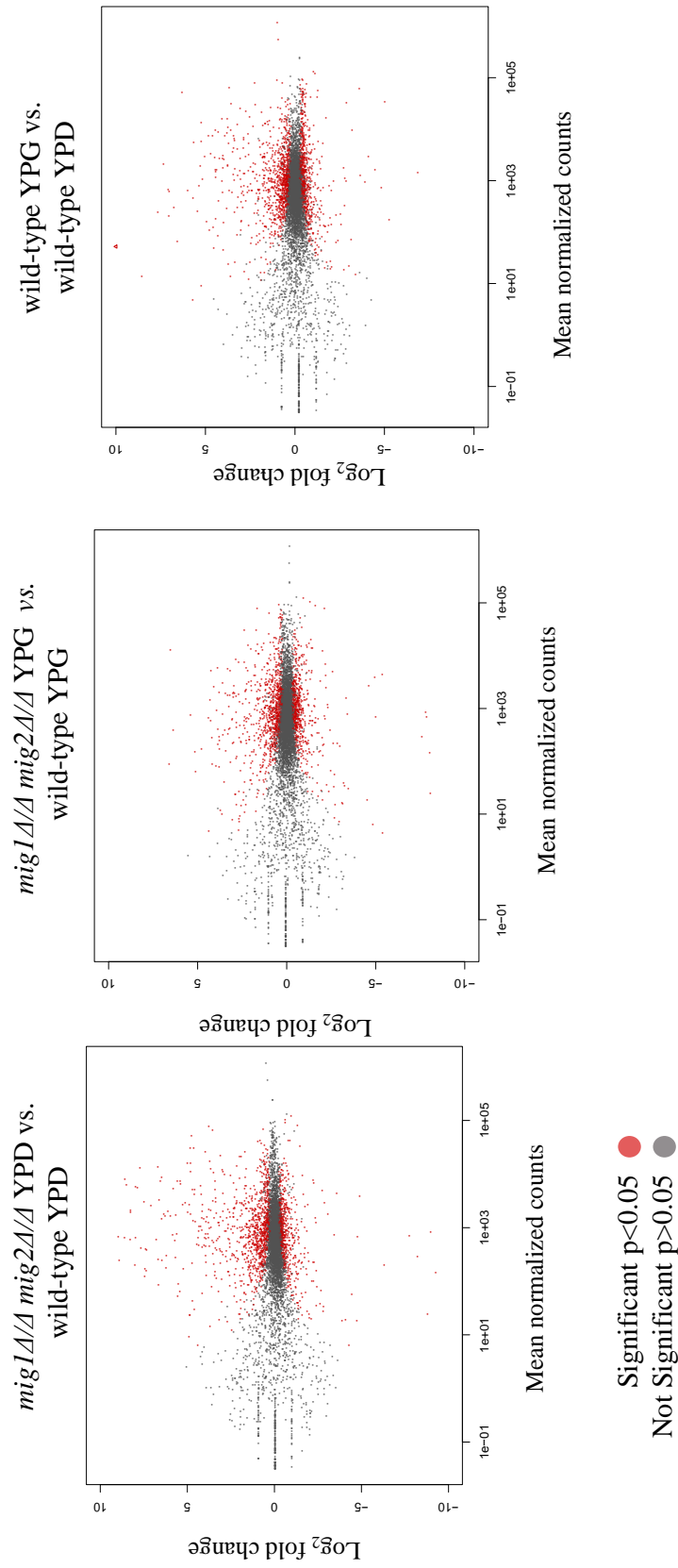


FIGURE 3.7: **Dot plots showing log₂fold change ($p < 0.05$) for differential expression of all genes** The differential gene expression of the strain KL742 (*mig1Δ/Δ/mig2Δ/Δ*) compared to strain CW542 (wild-type) in YPD and YPG media show that Mig1 and Mig2 function as repressors. The YPG condition shows a decrease in the extent to which genes were derepressed in the *mig1 mig2* double mutant. The wild-type strain shows significant upregulation of gene expression in response to YPG compared to YPD.

mig1 Δ/Δ *mig2* Δ/Δ YPD vs. WT YPD (x axis) compared to
mig1 Δ/Δ *mig2* Δ/Δ + Caspofungin vs. WT + Caspofungin (y axis)

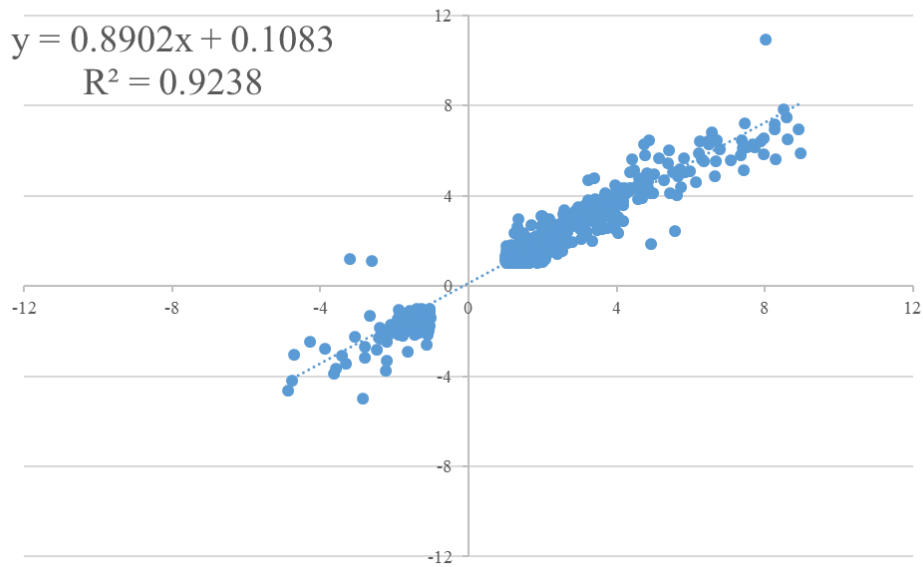


FIGURE 3.8: Comparison of gene expression response of the *mig1 mig2* double mutant in YPD to the gene expression response of the *mig1 mig2* double mutant in YPD + caspofungin

Differential gene expression of strain KL742(*mig1* Δ/Δ /*mig2* Δ/Δ) compared to CW542(wild-type) in YPD (x-axis) versus KL742(*mig1* Δ/Δ /*mig2* Δ/Δ) in YPD + 125ng/mL caspofungin compared to CW542(wild-type) in YPD + 125ng/mL caspofungin (y-axis) A blue dot indicates a single gene that was significantly regulated in both conditions ($p < 0.05$).

3.5 Mig1 and Mig2 are not transcriptional regulators of the caspofungin response

Despite some changes in expression of cell wall-related genes in the *mig1 mig2* mutant strain, these transcription factors do not appear to control transcriptional changes in response to caspofungin. We profiled the double mutant and wild-type strain in YPD containing 125ng/mL of casofungin, but the gene expression response of the double mutant strain with drug compared to without drug was highly correlated, represented by an R^2 value of 0.9238 (See Fig. 3.8). Therefore, Mig1 and Mig2 are more responsive to the high glucose condition than they are responsive to caspofungin. The cell wall integrity defect of the double mutant strain (See Fig. 3.2) does not appear to be due to a failure of the mutant to transcriptionally respond to cell wall stress. Instead, derepression of alternative carbon source utilization genes may predispose the cells to cell wall integrity defects.

3.6 The *mig1 mig2* double mutant is hypersensitive to caspofungin on the non-fermentable carbon source glycerol

Since Mig1 and Mig2 are regulated by glucose, we wanted to know whether their control of cell wall stress was dependent on the carbon source. To check this hypothesis, we tested growth of the *mig1 mig2* double mutant on agar plates containing caspofungin and 2% glycerol as the sole carbon source. We found that the *mig1 mig2* double mutant was still hypersensitive to caspofungin under these conditions (See Fig. 3.9). Interestingly, the cells showed markedly decreased resistance to caspofungin in YNB glycerol media compared to YPD media (60ng/mL vs. 125ng/mL) and decreased resistance to caspofungin at 37°C compared to 30°C.

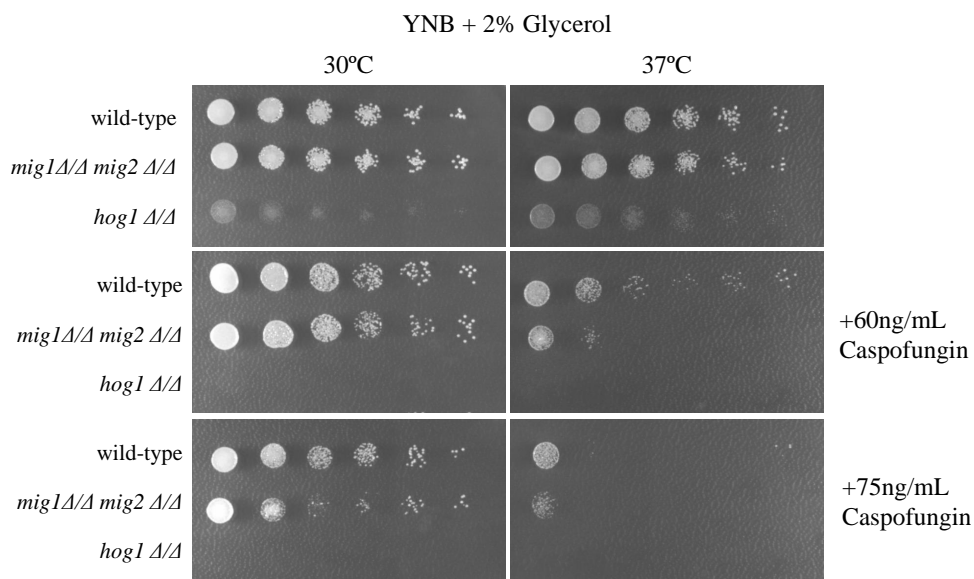


FIGURE 3.9: **The *mig1 mig2* double mutant is sensitive to Caspofungin when grown on glycerol media**

Strains CW542(wild-type), KL742(*mig1Δ/Δ/mig2Δ/Δ*) and JMR121 (*hog1Δ/Δ*)[83] were serially diluted 5-fold onto YNB media containing 2% glycerol as a carbon source. Plates were incubated for 5 days at 30°C and 37°C. The *hog1* mutant strain was used as a caspofungin sensitive control strain, but it unexpectedly grew poorly on glycerol media.

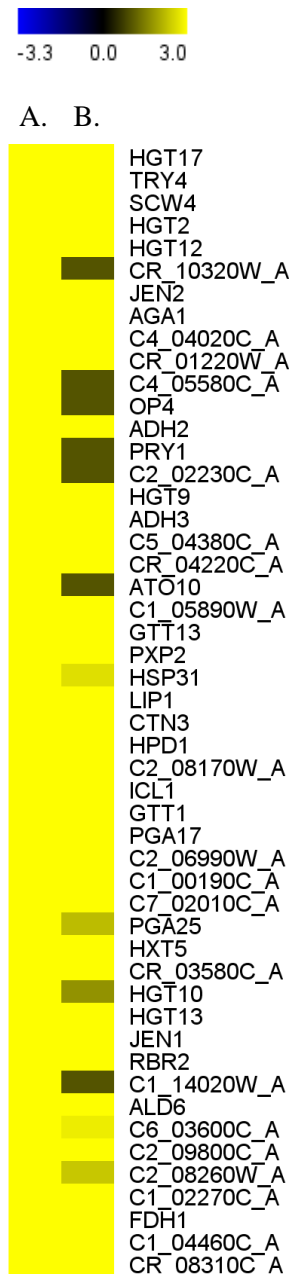


FIGURE 3.10: The *mig1 mig2* double mutant gene expression profile in YPD is similar to the gene expression profile of wild-type *C. albicans* cells interacting with bone-marrow-derived mouse macrophages.

Dataset A: *mig1 mig2* mutant strain compared to wild-type in YPD media.

Dataset B: wild-type *C. albicans* strains interacting with bone-marrow-derived mouse macrophages in culture for 1 hr from Tucey et al. [23]. The top 50 upregulated genes that showed that greatest fold change in the *mig1 mig2* mutant in YPD were chosen for comparison. The full list of gene comparisons is listed in a supplemental table 5.1. Yellow indicates upregulated genes, blue indicates downregulated genes (\log_2 fold change), and grey indicates no significant change (<2 fold change $p < 0.05$). Heatmap was generated using MultiExperimentViewer(MeVv4.6.2).

3.7 The gene expression profile of the *mig1 mig2* strain in YPD shows similar changes in gene expression compared to the profile of *C. albicans* cells phagocytosed by bone-marrow-derived mouse macrophages

In response to phagocytosis by macrophages, *C. albicans* upregulates genes involved in the utilization of alternative carbon sources and downregulates genes involved in glycolytic processes[24][23]. Remarkably, we found that the gene expression profile of the *mig1 mig2* mutant *in vitro*, in YPD media, was very similar to from *C. albicans* cells engulfed by macrophages from the Tucey et al. 2018 dataset (See Table 5.1). Of the top 50 upregulated genes that showed that greatest fold change in the *mig1 mig2* mutant in YPD, 43 out of 50 genes were similarly upregulated in a wild-type *C. albicans* strain interacting with bone-marrow-derived mouse macrophage (See Fig 3.10). Therefore, we wondered whether the *mig1 mig2* mutant might be transcriptionally predisposed to phagocytosis and would survive better than wild-type in the phagosome by more quickly utilizing alternative carbon sources. However, we found that the *mig1 mig2* double mutant strain was less virulent in the macrophage cell damage assay (See Fig. 3.11). This result was surprising, given the prevailing research that utilization of alternative carbon sources is necessary to excrete ammonia and auto-induce hyphal formation[48]. However, this result again reinforces the notion that Mig1 and Mig2 are redundant in function, as the single homozygous *mig1* and *mig2* mutant strains were not defective in cell damage.

3.8 Mig1 and Mig2 control morphogenesis

Since the *mig1 mig2* mutant strain was defective in an *in vitro* model of macrophage cell damage, we were curious whether the mutant might be defective in other phenotypes that are correlated with virulence. Hyphal formation is an important virulence trait in *C. albicans*, so we tested the *mig1 mig2* double mutant strain for its ability to form hyphae in several hyphae-inducing conditions. The double mutant strain showed reduced ability to form hyphae in RPMI media. The cells exhibited abnormal morphology compared to the wild-type, with constrictions at the septae, indicative of pseudohyphal growth[150]. In contrast to the RPMI condition, the double mutant strain formed normal hyphal

cells in RPMI containing 10% FBS and in spider media (See Fig. 3.12). The ability to properly regulate morphogenesis has long been correlated with the ability of *C. albicans* to promote infection[151][152], so the wild-type, *mig1* mutant, *mig2* mutant, *mig1 mig2* double mutant, and the coresponding complemented strains were tested for the ability to invade and damage human endothelial cells by the lab of Dr. Scott Filler. The double mutant strain exhibited reduced virulence in this assay (See Fig. 3.13). This result indicates that the *mig1 mig2* double mutant strain is defective in virulence in *in vitro* models.

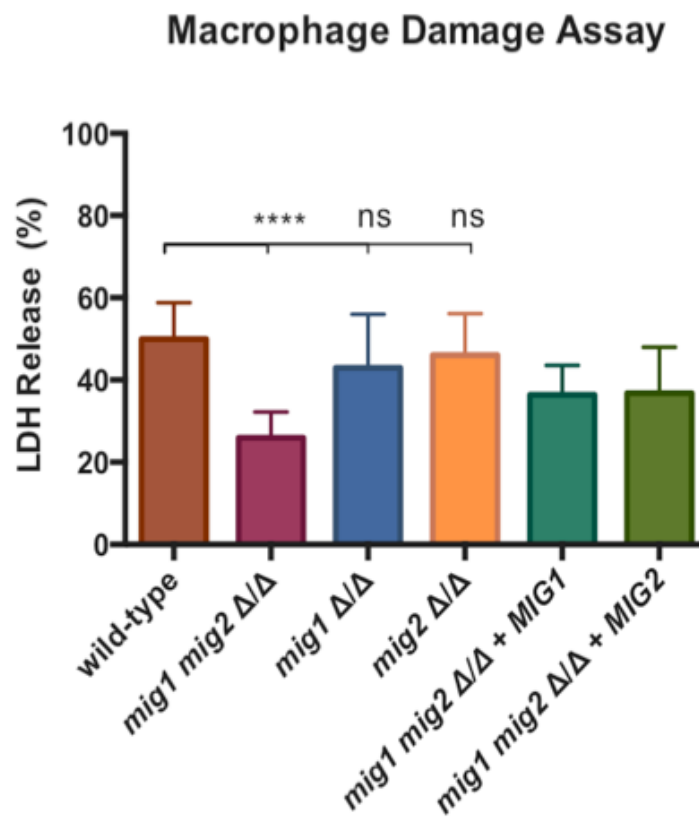


FIGURE 3.11: The *mig1 mig2* double mutant strain is less virulent in an *in vitro* model of macrophage cell damage.

Strains CW542(wild-type), KL742(*mig1* Δ/Δ / *mig2* Δ/Δ), KL829(*mig1* Δ/Δ / *mig2* Δ/Δ + *MIG1*), KL807(*mig1* Δ/Δ / *mig2* Δ/Δ + *MIG2*) were incubated with J774A.1 macrophage cells for 4h. Cell damage was measured by a LDH release assay

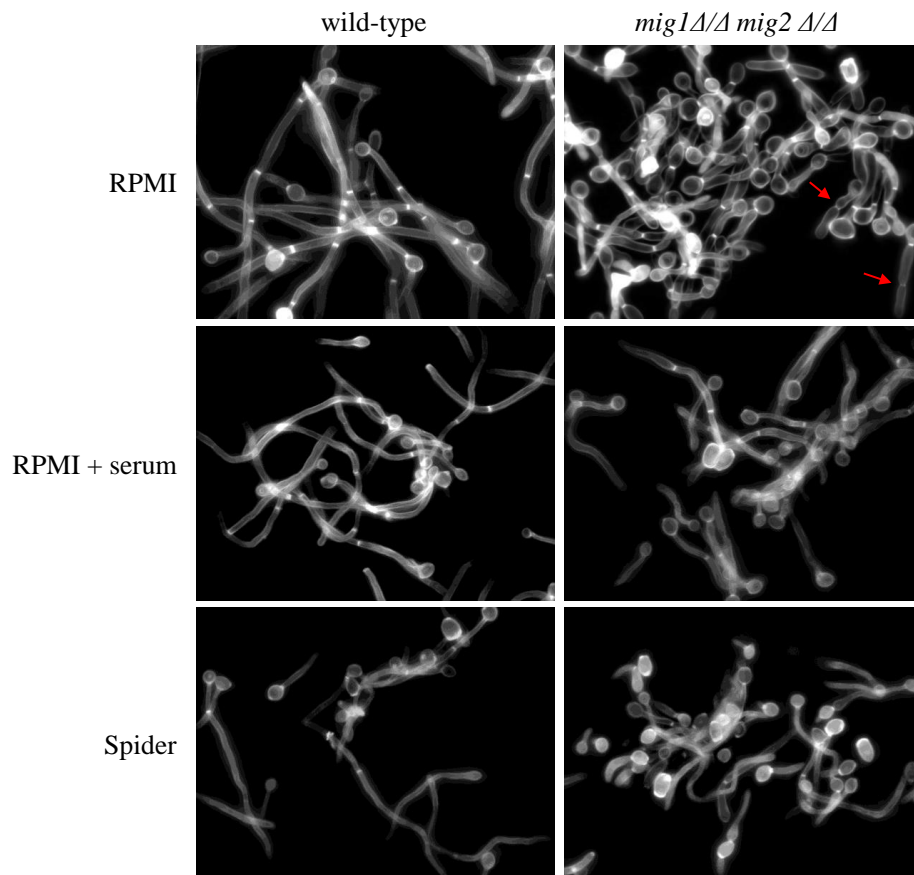


FIGURE 3.12: Mig1 and Mig2 control morphogenesis.

Overnight cultures were inoculated into liquid hypha-inducing media at an OD of 0.2 and incubated at 37°C for 4 hours. Cells were stained with calcofluor white and imaged. Red arrows show constrictions at the septae indicating pseudohyphal growth.

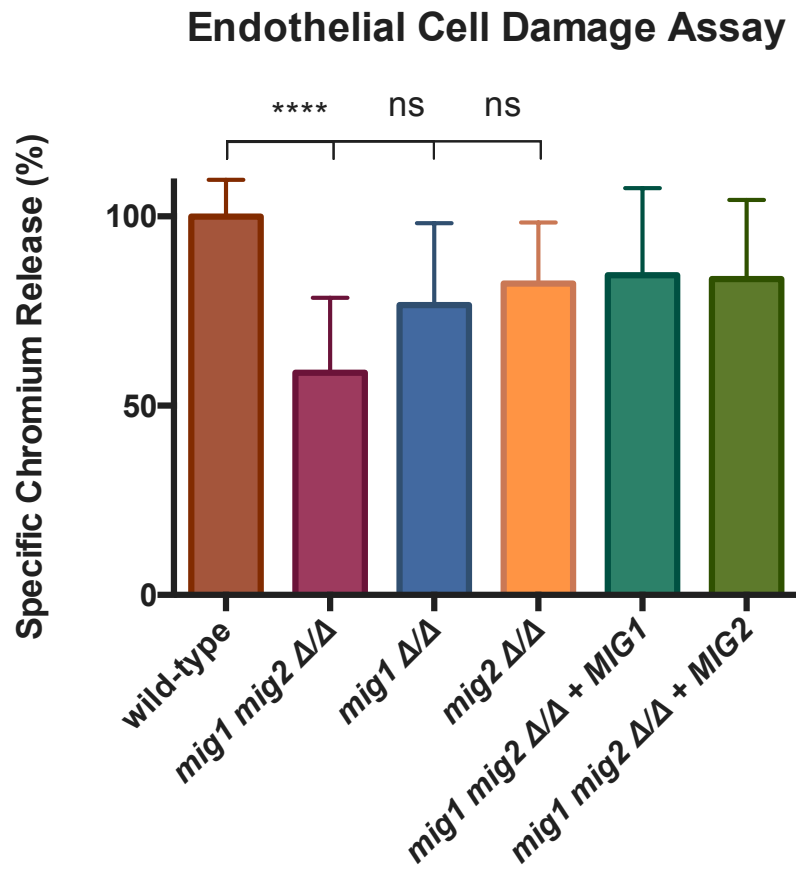


FIGURE 3.13: The *mig1 mig2* double mutant strain is less virulent in an *in vitro* model of endothelial cell damage.

Strains CW542(wild-type), KL742(*mig1*Δ/Δ/ *mig2*Δ/Δ), KL829(*mig1*Δ/Δ*mig2*Δ/Δ+ *MIG1*), KL807(*mig1*Δ/Δ/ *mig2*Δ/Δ+ *MIG2*) were incubated with human umbilical vein endothelial cells for 3h. Cell Damage was measured using a chromium release assay.

3.9 Mig1 and Mig2 may function in the TOR signaling pathway

The TOR (*Target Of Rapamycin*) pathway is known to respond to three main signals in *C. albicans*: nitrogen source, filamentation, and phosphate acquisition[153][154]. In *Saccharomyces cerevisiae*, Snf1 coordinates a wide range of nutrient and stress signals in the cell[60], but evidence has shown that there is also significant cross-talk between *ScSnf1* and TOR signaling pathways[155]. Because *CaSnf1* is possibly an upstream regulator of *CaMig1* and *CaMig2*, we asked whether these two transcription factors might function downstream of the TOR signaling pathway. To answer this question, we tested the *mig1 mig2* double mutant strain for hypersensitivity to the drug rapamycin, which directly inhibits the Tor1 kinase by binding to the FKBP12 domain[156]. We found that the *mig1 mig2* double mutant strain was more sensitive to Rapamycin compared to the wild-type strain or either single homozygous mutants (See Fig. 3.14). Bolstering this hypothesis, several amino acid permease genes (*CAN1*, *CAN2*, *GAP2*, *CAR2*, *DIP5*, and *AAP1*) are derepressed in the *mig1 mig2* double mutant strain. Changes in expression of amino acid permeases can be indicative of a nitrogen limitation response coordinated by TOR signaling[157], though *C. albicans* can also utilize amino acids as a carbon source[48]. Mig1 and Mig2 may serve as a link between nitrogen and carbon acquisition signaling.

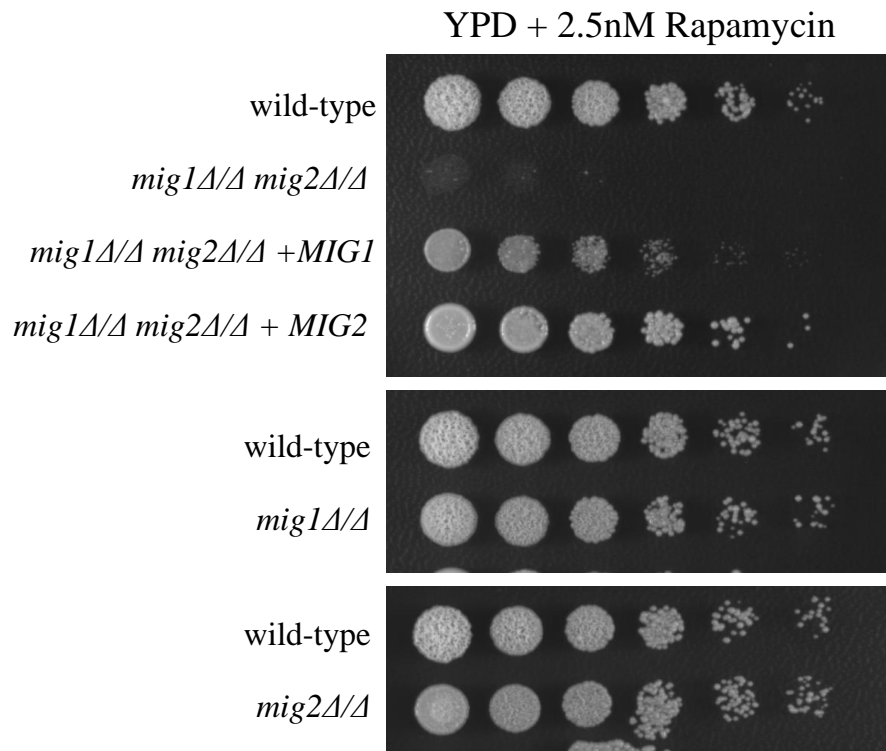


FIGURE 3.14: The *mig1 mig2* double mutant strain is sensitive to rapamycin
 Strains CW542(wild-type), KL742(*mig1* Δ/Δ / *mig2* Δ/Δ),
 KL829(*mig1* Δ/Δ /*mig2* Δ/Δ + *MIG1*), KL807(*mig1* Δ/Δ / *mig2* Δ/Δ + *MIG2*), were
 5-fold serially diluted onto YPD plates and YPD plates containing 2.5ng/ μ L
 rapamycin for 2 days at 37°C.

3.10 Sak1 regulates alternative carbon source utilization through inactivation of the repressors Mig1 and Mig2

In *C. albicans*, the protein kinase Sak1 has been shown to phosphorylate and activate the protein kinase Snf1 . Deletion of *SAK1* leads to morphological defects and the inability to utilize alternative carbon sources. These defects can be overcome by a hyperactive Snf1 strain, showing that Snf1 is downstream of Sak1. In *Saccharomyces cerevisiae*, phosphorylated *ScSnf1* in turn phosphorylates *ScMig1*, which inactivates the transcription factor by moving it out of the nucleus where it can no longer act as a repressor of alternative carbon source gene expression (See Fig. 1.1) [55][62][57]. Therefore in a *sak1* or *snf1* mutant, Mig1 and Mig2 might remain in the nucleus since they cannot be phosphorylated and hence move out of the nucleus. Based on this precedence and the fact that the *mig1 mig2* double mutant strain shows derepression of alternative carbon source genes, we hypothesized that a *sak1 mig1 mig2* triple mutant strain would be able to utilize alternative carbon sources by removing the Mig1 and Mig2 repressors. In agreement with our hypothesis, the triple mutant strain grew markedly better than the *sak1* mutant strain(See Fig 7A 3.15). This phenotype was observed using the non-fermentable carbon source glycerol, and spider media which contains mannitol as a carbon source. The triple mutant strain relieved the growth defect of the *sak1* mutant strain at both 30°C and 37°C. However, we noticed a temperature dependent growth defect for the *sak1* mutant. The mutant grew slightly better at 30°C, but growth was completely absent at 37°C on alternative carbon sources indicating that the control of alternative carbon acquisition genes by Sak1 may be temperature dependent. As a control, the *sak1* mutant grew as well as wild-type on rich YPD media at both temperatures. In *C. albicans*, Sak1 controls morphogenesis. The *sak1* mutant shows increased filamentation on solid YPD, but decreased filamentation in liquid spider media[32]. We found that the triple *sak1 mig1 mig2* mutant had increased filamentation in liquid spider media at 37°C, but it did not fully restore filamentation to wild-type levels(See Fig 7 B.3.15). These data suggests that the *sak1* mutants inability to properly form hyphae in response to mannitol is at least in part due to the repression of certain genes by Mig1 and Mig2.

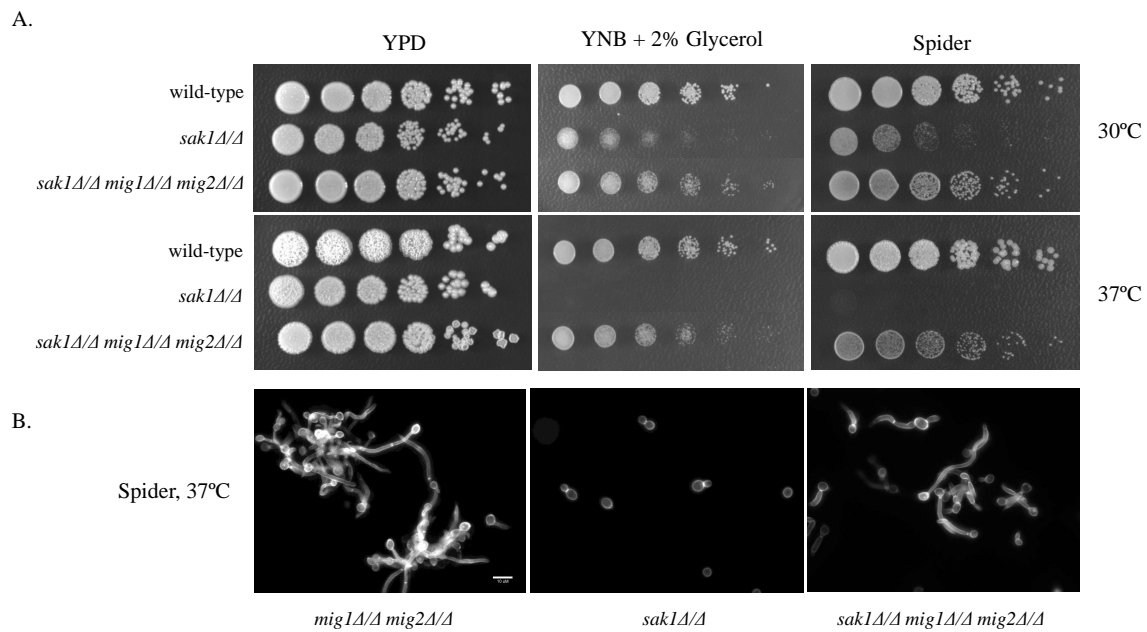


FIGURE 3.15: **A triple *mig1 mig2 sak1* mutant relieves growth and morphogenesis defects of the *sak1* mutant on alternative carbon sources**
 A. Strains CW542(wild-type), KL924(*sak1*Δ/Δ), KL926(*sak1*Δ/Δ*mig1*Δ/Δ*mig2*Δ/Δ), were 5 fold serially diluted onto YPD, 2% glycerol, and spider plates, and incubated for 2 days at 30°C and 37°C. B. Strains KL794 (*mig1*Δ/Δ*mig2*Δ/Δ), KL924, and KL926 were diluted to an OD of 0.2 and inoculated into pre-warmed Spider media at 37°C for 4 hours, rotating at 60rpm. Cells were stained with calcofluor white and imaged.

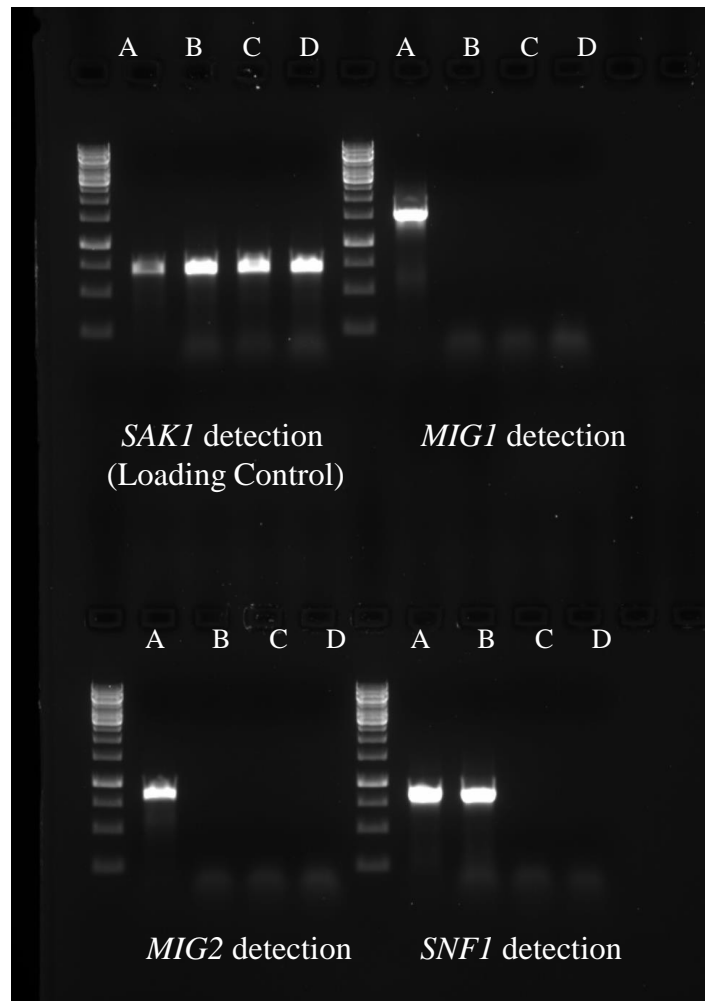


FIGURE 3.16: **PCR genotype validation of the *snf1 mig1 mig2* triple mutant strain** Primer pairs for detection of *SAK1* *MIG1* *MIG2* *SNF1* were used to validate the genotypes from genomic DNA extracted from the following strains: wild-type(A) KL794(B) KL929(C) KL930(D). Detection of *SAK1* was used as a loading control for the genomic DNA since the gene should be present in all strains

3.11 *SNF1* is not essential in a *mig1 mig2* mutant background strain.

Previous reports have shown that *SNF1* is essential in *C. albicans* inferred from a failure to obtain homozygous mutants[82][158]. Since these data suggest that Mig1 and Mig2 might function downstream of Snf1, we reasoned that deletion of *MIG1* and *MIG2* in a *snf1* mutant strain might relieve repression of alternative carbon source utilization

genes and possibly reverse the essentiality of *SNF1*. To verify that *SNF1* is essential, 16 transformants were tested using colony PCR in a wild-type (CW542) background strain, but no homozygous mutants were discovered. (Data not shown) However, in the *mig1 mig2* double mutant strain background (KL794) 3 out of 14 transformants were homozygous mutants. Genomic DNA was extracted from 2/3 of those isolates and PCR was performed to verify the genotype (See Fig. 3.16). This surprising results suggests that the essentiality of *SNF1* is due to the function of Mig1 and Mig2. Therefore, Mig1 and Mig2 likely function downstream of the Snf1 kinase. All together, these results suggest that Mig1 and Mig2 function downstream of Sak1 and Snf1 in a regulatory network in *C. albicans*. (See summary schematic 3.17)

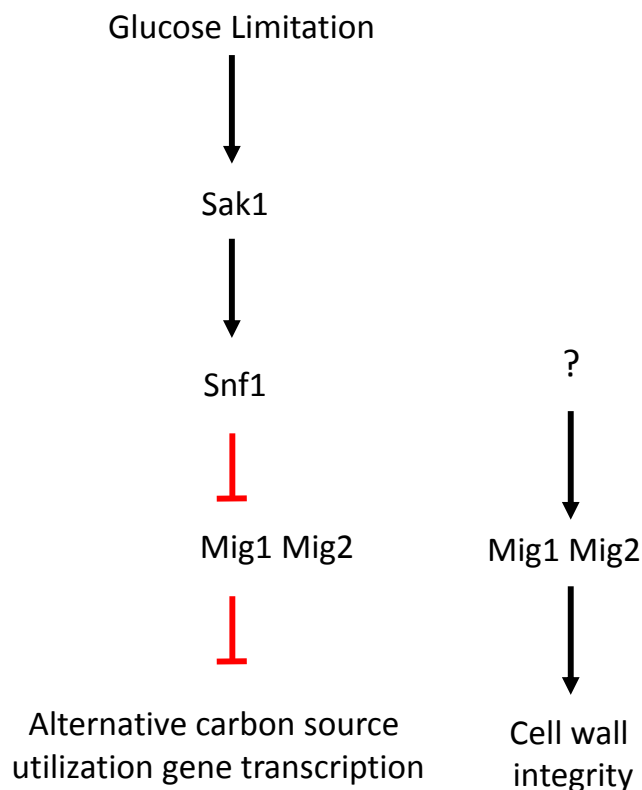


FIGURE 3.17: Simplified schematic showing the predicted Mig1 and Mig2 regulatory network based on this work and work from Ramirez et al.[32]

Chapter 4

Discussion

Here we have investigated the genetic and regulatory functions of two transcription factors, Mig1 and Mig2. We have shown that Mig1 and Mig2 have generally conserved roles as repressors of alternative carbon utilization genes across evolution between *Saccharomyces cerevisiae* and *Candida albicans*. We have also shown promising results that Mig1 and Mig2 may be required for virulence. This claim is based on the fact that the *mig1 mig2* mutant strain is defective in two models of virulence *in vitro* (See Fig. 3.11 and Fig. 3.14) An *in vitro* model of endothelial damage has been shown to correlate with defects in virulence in mouse models of systemic candidiasis infections[159][160]. To verify this claim, the *mig1 mig2* mutant should be tested using an *in vivo* mouse model of systemic candidiasis. Testing the *mig1 mig2* mutant in a mouse model of gut commensalism would also be interesting. As discussed in the introduction, Mig1 and Mig2 may positively regulate commensalism and competition with bacteria in the human gastrointestinal tract due to its role in regulating resistance to weak organic acids [37][149].

One important difference that emerged between *CaMig1/2* and *ScMig1/2*, is the increased redundancy in function of the two transcription factors in *C. albicans*. Most genes regulated by Mig1 and Mig2 show synergistic epistasis such as *TRY4*, which shows 4.12, not significant, and 8.99 log₂ fold upregulation in the *mig1*, *mig2*, and *mig1 mig2* double mutant respectively. Other genes show complete redundancy such as *SCW4*, which is significantly upregulated 8.6 log₂ fold only in the double mutant (See excel spreadsheet for full gene expression table). Similar to *TRY4*, several genes show some

derepression in one or both of the single homozygous mutant strains, but in many cases, the genes show further derepression in the double mutant. Therefore, Mig1 and Mig2 usually exhibit synergistic regulation of gene targets. This is in contrast to *ScMig1* and *ScMig2* where *ScMig1* is sufficient to fully repress some genes, while *ScMig2* is only necessary for repression of a subset of *ScMig1* regulated genes, and *ScMig2* has not been shown to regulate any carbon genes by itself[68]. Also, there is no evidence that Snf1 phosphorylates or regulates Mig2 in response to glucose[62]. However, Snf1 does phosphorylate *ScMig2* and *ScMig1* in response to alkaline stress[70], but Mig2 plays its own role in regulating the gene *PHO89* under alkaline stress[70]. *CaMig1* does not contain the phosphorylation sites that *ScSnf1* has been shown to phosphorylate in *ScMig1* (See Fig 3.1), suggesting that reprogramming of the network between *Saccharomyces cerevisiae* and *Candida albicans* has occurred.

This work has also provided evidence that Mig1 and Mig2 function downstream of Sak1 and Snf1. We have shown the surprising result that *SNF1* is not essential in a *mig1 mig2* mutant background strain. To confirm that Sak1 and Snf1 function upstream of both Mig1 and Mig2 in response to glucose limitation, *sak1 mig1* and *sak1 mig2* mutant strains will have to be constructed. Currently, this work has only shown that a double *mig1 mig2* mutant can reverse the *sak1* mutant phenotypes and reverse the lethality of *SNF1*. Given the redundancy in all of the other assays presented in this work, I would hypothesize that the double mutant would be necessary to relieve the growth defects of the *sak1* mutant and lethality of *SNF1*. However, if the molecular precedent in *S. cerevisiae* remains true, where Snf1 only phosphorylates Mig1, then a *sak1 mig1* mutant strain might be sufficient to improve growth on alternative carbon sources. The result of this assay would be extremely interesting to show if Snf1 has been reprogrammed to regulate both Mig1 and Mig2 in *C. albicans*.

Since *SNF1* is constitutively phosphorylated at low levels in *C. albicans*[32], it is possible that Mig1 or Mig2 are also constitutively phosphorylated at low levels. If *CaMig1* is regulated by nuclear localization similar to *ScMig1*, then a pool of Mig1 protein might always be located in the cytoplasm. Therefore, in a *snf1* mutant strain, Mig1 would never be phosphorylated and would remain in the nucleus at all times. The metabolic constriction from constant repression of alternative carbon source utilization genes might be essential for *C. albicans* viability. Construction of fluorescent fusion proteins for Mig1

and Mig2 would be informative to test whether these transcription factors are regulated by nuclear localization.

Another open question is what downstream genes mediate the lethality of a *snf1* mutation? The data presented here suggests that the deletion of *MIG1* and *MIG2* results in derepression of some alternative carbon source utilization genes that are necessary for viability. To answer this question, gene expression profiling could be used to determine which genes are derepressed in the *snf1 mig1 mig2* triple mutant strain. It is likely that derepression of multiple genes would be necessary to reverse the lethality of the *SNF1* since no obvious genes appear to be essential that are derepressed in the *mig1 mig2* double mutant expression profile presented in this work.

Another avenue to pursue is the mechanism for how *CaMig1* and *CaMig2* control cell wall stress. *ScMig1* and *ScMig2* have never been shown to regulate cell wall stress. The only previously known connection is the fact that Snf1 mediates crosstalk signaling to the TOR pathway[161], and the TOR signaling pathway has been shown to control cell wall stress[148]. Mig1 has been linked to the TOR pathway in the fungal pathogen *Cryptococcus neoformans*[162], but the *Cnmig1* mutant was resistant to rapamycin, so Mig1 is probably playing a different role in *Cryptococcus neoformans* than we are investigating here. Currently, the TOR pathway has been relatively understudied in *C. albicans*[154][153][163], compared to the vast body of work in *Saccharomyces cerevisiae*[164] and mammalian cells[54]. It would be interesting to know if Mig1 or Mig2 directly affect TOR signaling cascades. This question could be answered by using immunoblots to detect phosphorylation levels of TOR signaling targets such as Sch9[153] or ribosomal protein S6 [165] in the *mig1*, *mig2*, and double mutant strains. Confirming the role of Mig1 and Mig2 in the TOR pathway signaling network would be interesting because rapamycin was first developed as a possible antifungal[22][166]. If connections between rapamycin and glucose signaling can be made, then it is possible that the nutrient environment of the host could be modulated to make rapamycin more effective at lower concentrations. Rapamycin normally causes deleterious immunosuppressive effects through inhibition of the host mTOR signaling[167] and therefore is currently not promising as an antifungal drug.

It is unclear how Mig1 and Mig2 regulate cell wall stress, if not through reduced TOR

signaling. The upstream kinases, Snf1 and Sak1 negatively regulate Mig1 and Mig2 function, yet both the *snf1* mutant strain and a viable, non-phosphorylatable, *snf1* mutant strain are sensitive to cell wall stress[32]. Therefore, you would imagine that a *mig1 mig2* mutant strain might be resistant to cell wall stress. However, as this work has shown, the double mutant strain is hypersensitive to cell wall stress. This leads to the hypothesis that Mig1 and Mig2 regulate cell wall stress in a parallel pathway to Sak1 and Snf1 (3.17). Since the *mig1 mig2* mutant strain is still sensitive to caspofungin on media containing glycerol as the carbon source, this would suggest that their function is independent of glucose signaling.

Finally, several uncharacterized transcription factors emerged from our transcript profiling of the *mig1 mig2* mutant strain. Although it is still useful and arguably easier to study genes with direct homologs in *S. cerevisiae*, it is imperative to begin dissecting the 70% of uncharacterized genes in the *C. albicans* genome[3]. Genes *TRY4*, *ZCF5*, *C4_05870C*, *TRY5*, *ZCF16*, *ZCF16*, *ZCF6*, *C1_13880C* and *ZCF20* are all verified or putative transcription factor genes that are derepressed in the *mig1 mig2* mutant strain. If *C. albicans* maintains a more integrated and overlapping regulatory network for carbon source acquisition than *S. cerevisiae*, then these uncharacterized transcription factor genes may play redundant roles in positively regulating transcription of alternative carbon source utilization genes. A combination of constructing multiple mutant strains among these genes and transcriptional profiling could determine what role they may play in the carbon regulatory network.

Chapter 5

Supplement

TABLE 5.1: *mig1 mig2* mutant vs. WT YPD gene expression compared to wild-type *C. albicans* interacting with mouse macrophages for 1hr vs. wild-type *C. albicans* alone gene expression

	mig1 Δ/Δ mig2 Δ/Δ vs. WT YPD	WT + macrophages 1h vs. WT alone
HGT17	8.979149738	5.579713331
TRY4	8.922152091	6.206574386
SCW4	8.618033829	7.329122777
HGT2	8.590772458	7.4025916
HGT12	8.507871983	8.252587587
CR_10320W_A	8.292766371	0
JEN2	8.27721963	7.121625365
AGA1	8.269265593	7.734132813
C4_04020C_A	8.029586044	6.558001575
CR_01220W_A	7.983444751	8.688421215
C4_05580C_A	7.982317943	0
OP4	7.882344069	0
ADH2	7.725631259	8.102082126
PRY1	7.682121291	0
C2_02230C_A	7.501237254	0
HGT9	7.463941471	3.494622369
ADH3	7.444911726	8.22539714

C5_04380C_A	7.403725645	10.71242393
CR_04220C_A	7.36748795	5.664538601
ATO10	7.357137839	0
C1_05890W_A	7.091564287	7.413811622
GTT13	6.798947572	7.338469022
PXP2	6.700031286	6.102947655
HSP31	6.680985372	2.640568999
LIP1	6.664530629	8.347311504
CTN3	6.627064036	7.071332482
HPD1	6.562983813	7.02229438
C2_08170W_A	6.484491509	6.472378165
ICL1	6.480679093	7.640708594
GTT1	6.463427895	6.626010012
PGA17	6.359627129	6.61666811
C2_06990W_A	6.2900034	4.887716527
C1_00190C_A	6.24316262	4.561355476
C7_02010C_A	6.211511122	4.409613508
PGA25	6.128668808	2.223840615
HXT5	5.976845023	6.234437227
CR_03580C_A	5.852853596	5.80008634
HGT10	5.818207569	1.73262535
HGT13	5.727159803	3.828169624
JEN1	5.70020669	3.441607669
RBR2	5.66822215	3.89135783
C1_14020W_A	5.62557037	0
ALD6	5.59411759	5.584176549
C6_03600C_A	5.562018547	2.803845185
C2_09800C_A	5.529488664	5.464030311
C2_08260W_A	5.434483146	2.354754524
C1_02270C_A	5.41306438	6.494193613
FDH1	5.395952695	7.879153924
C1_04460C_A	5.279298884	5.759519436
CR_08310C_A	5.233957272	9.092178189

SFC1	5.139588578	6.018463339
SAP2	5.051495062	0
MLS1	5.014233905	6.497835072
GCA2	4.991184874	2.552911894
C6_00810C_A	4.916066961	0
CAN2	4.90426573	2.228384753
C4_02230C_A	4.872692468	0
C1_06860W_A	4.855872641	0
RBT5	4.851977504	-0.919320898
FOX2	4.835706152	4.568012725
POT1	4.820549693	3.4988513
CR_07700W_A	4.818865101	2.783253149
PCK1	4.773974452	3.941415384
NAG4	4.734579394	0
FAA2	4.712297141	2.450283372
INO1	4.711432885	4.972009243
C2_05990C_A	4.68340165	4.187014669
POX1-3	4.645410543	3.383614271
ANT1	4.616302513	2.479747932
C1_10170W_A	4.610831089	0
CR_08920W_A	4.589328979	3.945942592
ECI1	4.546415229	4.630559712
CTN1	4.464414274	7.687371463
TNA1	4.383803619	10.88311006
C2_04480W_A	4.362228912	0
C6_03240W_A	4.359592178	4.150707749
ZCF5	4.34130682	0
MAL31	4.245317052	4.224487483
CSA2	4.244668936	0
FBP1	4.241983709	2.43982305
FOX3	4.2158722	3.155362506
HGT19	4.180853123	4.439823312
PGA32	4.171517951	0

C3_03570C_A	4.16876792	8.5447406
C4_04400C_A	4.165304864	8.276536451
C2_09280C_A	4.164025743	5.164342342
C4_05870C_A	4.163745728	2.723742046
PGA7	4.154297991	0.051908487
C4_02930W_A	4.149183346	3.502214087
CR_08670C_A	4.075523898	3.730239693
C4_00080C_A	4.053347604	3.379253706
CR_07260C_A	4.048398858	0
TES15	4.013227542	3.858679014
CAT1	3.98447439	4.836240997
C5_04940W_A	3.962450098	2.403848636
C1_11950W_A	3.956496747	4.431493726
BLP1	3.951616258	3.701526691
GAP2	3.94929438	7.648270385
PEX4	3.94676285	2.945903442
IFD3	3.944457885	2.036473242
FMO1	3.932434512	7.763961586
GCA1	3.877016009	0
C3_03470W_A	3.840719321	0
CR_07250C_A	3.799158869	3.939718369
CYB2	3.791066609	4.555083661
ALD5	3.785855932	3.646155089
FAA2-3	3.780944317	1.488276514
C7_02920W_A	3.749044362	5.07541419
C1_10240C_A	3.748082331	4.067314166
CAT2	3.718065096	3.798045085
CR_07140C_A	3.70934335	3.80591168
HGT1	3.679967185	-0.211732609
C5_02690W_A	3.678791407	3.322582132
MAL2	3.654738081	2.860217589
C2_10150W_A	3.6219214	0
CR_08830W_A	3.583044272	7.386608567

GDH2	3.561200709	2.251285385
C2_01450C_A	3.552608851	3.016610569
EHD3	3.537910648	4.266038296
ACS1	3.507301458	5.227126909
TRY5	3.506962329	0
C3_07590W_A	3.499734892	0
OSM2	3.4640422	4.809175432
C2_05130W_A	3.433164266	3.89819317
C1_07220W_A	3.426374181	1.880156843
POX18	3.41933388	3.533631884
C3_01420C_A	3.412202619	1.951833655
FRP1	3.394548527	-0.554170392
CSA1	3.372820501	-0.725525377
CR_09920W_A	3.372492167	1.285323916
C6_00080C_A	3.348599345	2.226530738
ALK6	3.337113704	0
FMO2	3.328545421	4.041016651
C3_06730W_A	3.323038299	0
C5_03710C_A	3.249126618	8.201575127
FAA2-1	3.227457458	2.276309112
C5_03730W_A	3.227274057	7.795154933
CFL4	3.222282345	7.645175453
C1_11850W_A	3.209396367	2.13330882
GAL1	3.189143583	1.746596487
DAL52	3.180223851	0
SPS20	3.166087108	0
C1_12140W_A	3.146486916	2.838401831
C1_09240C_A	3.121316722	0
HGT16	3.116364568	3.551493086
UCF1	3.112700271	3.395480665
PUT2	3.110426788	0
C6_01490C_A	3.046165668	3.747995311
C2_08520C_A	3.041069477	0

GCY1	3.026966615	3.933782577
FUM12	2.999098564	0.639023259
HRQ2	2.977664171	0
GAL10	2.976469995	0.439856371
C1_08770W_A	2.971555694	0
GST3	2.962239209	5.269521046
IDP2	2.956700566	3.321859904
MDH1	2.882772543	4.132258533
FAA21	2.868078975	1.835334521
C7_03280C_A	2.858259337	4.507612897
OPT7	2.825403984	0
C3_07760C_A	2.803982101	0
C1_09440W_A	2.792716072	1.353481135
ECM38	2.766875837	3.789662193
PEX6	2.757914053	1.621132039
CAN1	2.729543319	0
AOX2	2.704394424	8.714230366
CRG1	2.677094486	1.931581603
PDK2	2.677082939	3.549972197
CDR3	2.664019863	1.785548295
C3_00210C_A	2.65986238	0
C1_01220C_A	2.634542978	1.549665687
SUT1	2.602202102	1.152649413
FET31	2.598615857	4.841638488
GAL102	2.586618054	2.794578507
C5_02220C_A	2.576183521	2.73868415
C2_08330W_A	2.562664403	1.980226753
C3_05750C_A	2.561309811	0.700565295
C3_04630W_A	2.544760593	0
STF2	2.539575054	3.817321824
C3_04840C_A	2.536149623	1.992855798
ZCF16	2.507451024	4.182227816
ALK8	2.458362611	0

C1_11320C_A	2.447817141	4.022246875
CFL2	2.427378988	0.017883858
C7_00060C_A	2.403225562	1.639559008
UGA11	2.389355858	1.751720768
ATO1	2.365347306	3.926396869
IFE2	2.365083448	3.650331304
ADR1	2.356118831	3.035393396
SPO75	2.346153287	0
CR_04870C_A	2.345865429	1.737455677
PUT1	2.345383009	-1.054895932
PEX1	2.343551012	0
C2_03290W_A	2.307267079	1.894293537
UGA1	2.301521582	2.029472293
C1_11890W_A	2.301048749	2.762214535
CRC1	2.298891007	1.080214868
DLD1	2.29070389	0.57839637
C1_12910W_A	2.290137638	3.923806695
C4_02660W_A	2.266260049	0
NGT1	2.238030857	5.278605128
GIT1	2.235034169	8.278927066
C1_12880C_A	2.232509995	2.256987605
C5_02110W_A	2.216786863	3.763342797
GRE3	2.194264184	1.989184738
C2_09070C_A	2.173340632	1.366957555
HSP12	2.17326272	1.396015029
CR_10200W_A	2.168507837	0
C4_00950C_A	2.168330927	2.169810435
CAR2	2.165370026	1.559061319
PEX11	2.160391084	3.245127293
PGA34	2.143865836	0.725618848
C3_06490W_A	2.143043142	0.941452118
OPT4	2.12957587	6.238320729
PGA15	2.125462373	0

C5_05510C_A	2.115024162	0
C4_04140W_A	2.111689741	3.144711353
C1_04350C_A	2.072567349	0
C7_04320W_A	2.051786279	0
STD1	2.020757481	0.448156251
YHB1	2.018727616	6.605706267
CIT1	2.007580831	2.966074801
C6_04190C_A	1.998359168	0
C4_06620C_A	1.997744544	1.791102538
OYE22	1.994770311	0
CR_05480W_A	1.987391363	1.479205841
ZCF15	1.984119694	1.882333722
WH11	1.965874691	3.848683985
C3_05360C_A	1.954753184	2.36382806
BIO32	1.94912196	3.604308125
LAP3	1.944569362	3.662596031
CR_06030C_A	1.931791415	0
PST2	1.921688485	2.026114895
GAL7	1.919928894	0.764881464
CHT2	1.917381973	1.243073593
C6_02660C_A	1.915654429	3.401758672
ATO2	1.904887191	1.903171905
C1_09060C_A	1.885966287	2.240863037
C2_08390W_A	1.884813902	2.422383895
NAG3	1.872087613	-3.354256625
C7_04310C_A	1.871861409	1.365360534
PXA1	1.87047293	0.471624002
C3_01060W_A	1.861666318	4.265139086
C6_01450C_A	1.860731377	2.134585005
IFF4	1.83971095	2.799641218
C3_00400C_A	1.836597783	2.928147028
C2_06710W_A	1.828658504	2.07977311
C1_01840C_A	1.820896141	2.15426851

CSO99	1.803233226	1.330412942
CR_04610C_A	1.801599299	0
MDH1-3	1.798117191	1.439621459
FRP2	1.791528325	-1.301660177
LIP4	1.777031726	0
FGR22	1.772685013	0
ZCF20	1.768342881	0.732846946
C4_02110W_A	1.761282855	0
C5_01260W_A	1.760162082	2.995472322
PEX2	1.758040235	1.494424381
C6_02560W_A	1.754384601	0
FUS1	1.743099293	0
C2_07580W_A	1.740912808	4.133294484
C2_06930C_A	1.735068419	0
ALT1	1.727932146	1.991407575
C1_07160C_A	1.716261722	3.755203471
C3_07570C_A	1.714232034	-0.286530622
PHO112	1.710992789	5.419998706
ACH1	1.709130286	0.863210805
HGT14	1.688380583	1.183782204
RGS2	1.686346255	3.26475579
CDR4	1.682966037	1.467191159
CR_02570C_A	1.680954064	0
RBT1	1.679405737	-1.824492099
ALS1	1.679180584	-0.315565701
C1_07080W_A	1.677154206	0.922638835
CHT1	1.668106462	0
C1_13880C_A	1.66684032	2.336974608
PEX5	1.656800874	0.749773929
OFI1	1.653749572	6.056198
SUL2	1.645387774	8.505100035
PRO3	1.638505513	-1.473454112
DIP5	1.636062844	1.643908347

MET15	1.635853479	4.808515994
C3_05290C_A	1.632927496	2.62659432
MRR2	1.631782775	0
C6_01420C_A	1.629063151	0.498668932
MET3	1.613405316	6.664528174
PTR22	1.607331016	1.754150962
AMS1	1.605463895	3.73411467
FRP3	1.596635151	3.14908056
C7_00430W_A	1.595219908	6.553626035
CSP37	1.592089357	3.770320215
C1_07980C_A	1.590640935	2.467869028
C1_07840W_A	1.589129575	0
C3_07580W_A	1.576167766	0
OPT1	1.574551203	2.221803688
RGT1	1.573189989	1.473171978
PEX12	1.572960415	1.701468602
AFP99	1.533961918	0
RSN1	1.522922552	1.263977756
C5_04180W_A	1.517337343	4.921470567
LYS144	1.509389492	0.103104321
ADH5	1.505943586	0.581858772
PEX13	1.505396559	1.01337965
C2_00510W_A	1.504905141	2.605233333
SOD4	1.501895465	4.187632226
C4_00320C_A	1.501708338	1.242680497
C2_09590C_A	1.500565718	2.082983761
C2_08510W_A	1.496587627	1.801698515
DAL4	1.49012258	0
C1_09650W_A	1.48991421	1.04825383
C3_07120W_A	1.489352111	0
C2_07430C_A	1.485775841	0.204077276
PEX8	1.481808445	0.923880632
C1_10810W_A	1.477816657	0

GLG2	1.473497323	2.504147126
C4_02150C_A	1.472815628	2.239421041
CAR1	1.469878883	0.754057094
BMT1	1.465791849	0.951220668
CR_07820W_A	1.462890306	3.299370398
ETR1	1.461505133	0
C4_01090C_A	1.457280521	2.968033249
C5_05360C_A	1.453233268	0.827428258
ZCF6	1.449780847	3.515591875
C7_02090C_A	1.449388278	0
POX1	1.448795963	0.748741439
C5_03870C_A	1.447350888	2.391656672
C1_01490W_A	1.440774192	1.687972497
PHO86	1.436485597	0
C2_02750C_A	1.43114324	0
PXA2	1.429867301	0.926878225
C6_02420W_A	1.429360355	-0.529859825
LYP1	1.426958252	0
UGA2	1.424537132	1.771260362
C4_00050W_A	1.407492555	0.837383526
C3_07460W_A	1.404669531	0
C3_04800C_A	1.400514224	1.413210627
DAO1	1.396010339	2.017493082
C1_10140C_A	1.392628809	3.51855032
GUT1	1.391601494	0
C7_01170C_A	1.38010798	5.167804764
C7_03260C_A	1.378761406	1.435454187
KEL1	1.376925627	0
C7_02290W_A	1.37603941	0.571301172
C6_03530C_A	1.374862695	0.622061057
C7_02520W_A	1.370994324	0
C3_07880C_A	1.370911192	-0.695530457
C6_02020C_A	1.361955918	0.465945617

CR_06930W_A	1.359305712	0
C1_02040C_A	1.349909749	0
SEO1	1.349050326	2.93963953
C1_00880W_A	1.348249282	0
ZCF25	1.34719539	5.412248701
SAP99	1.343343628	0
C4_02200C_A	1.343025233	0
INO4	1.3426192	0
C2_01870C_A	1.333619596	0
HBR2	1.330638772	1.59643098
C3_01130C_A	1.32512409	3.526293298
C2_00880W_A	1.314203922	1.563948961
GLK4	1.308227216	0
C6_00930C_A	1.30221188	2.64337544
C3_07540C_A	1.298389198	1.68063925
AGC1	1.297913469	0
LEU42	1.293861234	1.145464401
C6_03470W_A	1.293551756	0
AAP1	1.292747951	0
C1_05990C_A	1.289086743	1.074909851
CR_02780W_A	1.289034997	4.633220338
POT1-2	1.284727646	1.793487368
C6_03050C_A	1.279606723	2.386913821
GLK1	1.279164641	0.892980074
C2_00890W_A	1.272489276	0
CR_04760C_A	1.263922186	0
C2_02580W_A	1.255809413	0
CR_10420W_A	1.255034092	1.576829231
PGA45	1.251384102	-0.584859535
C3_07170C_A	1.250680103	0.62432163
HIP1	1.250057523	0
LEU5	1.247596804	1.193136549
C1_09110W_A	1.247076241	1.799671789

IFM3	1.245605359	0
C1_10520W_A	1.24366337	1.01714295
C1_00200C_A	1.242374215	0
WAR1	1.235246672	0
C7_00870W_A	1.234659673	3.46205746
ECM29	1.23043117	0
ATC1	1.229303778	1.310102012
C2_07630C_A	1.224591161	0.394299676
ZCF23	1.224070928	-1.312806528
PLB4.5	1.223199873	1.255974349
C2_03500W_A	1.21993875	1.16256163
NUP159	1.219335122	0
C2_04180C_A	1.21188504	0
C2_03110W_A	1.211774964	1.326140892
CR_06510W_A	1.204392276	3.384042281
C3_04650W_A	1.202059317	0
CR_04280C_A	1.187241422	0.378547978
CTF1	1.182527636	0
C3_03760W_A	1.181942451	1.453637135
AYR2	1.180521459	1.834736135
DOT5	1.180128331	1.16372923
C2_07070W_A	1.177298091	2.255397544
TFS1	1.173572185	1.591233214
HNM1	1.166448934	0.889374027
C2_09710C_A	1.16245192	1.638686668
C2_09960W_A	1.15146613	1.169854373
C2_08660C_A	1.150882833	1.029943987
C3_02360C_A	1.141393241	5.506037752
C3_07290W_A	1.139247939	0
C2_04110W_A	1.138670251	0
SIP5	1.138445773	1.515734369
CR_09500C_A	1.137234126	0
C1_09980C_A	1.131861292	0

C3_07490W_A	1.131186949	0
C3_07940W_A	1.12892094	0
IFG3	1.12333989	1.471223676
PEX19	1.122718079	0
FGR13	1.122105376	0
IFR2	1.118684996	-0.488250955
C3_06520C_A	1.115595545	0
HMX1	1.115261031	-0.559354758
C1_11690W_A	1.114157978	1.9840155
C4_04250W_A	1.114052603	1.182951513
XUT1	1.112787352	0
C4_00100C_A	1.109761377	0
PEX3	1.104717419	0
C2_01660C_A	1.102752352	1.838580427
MDS3	1.101154249	0.687243469
SLK19	1.097664783	1.06613944
HAP41	1.095924235	1.84577556
PHO87	1.095436763	3.745029966
C3_07430W_A	1.09437619	1.04044466
C3_07400W_A	1.092669758	0
C4_01930C_A	1.09234536	0
C3_07920W_A	1.090619426	0
SAC7	1.087323209	0.776111751
C7_03780C_A	1.085795048	2.613586078
IFE1	1.082217683	0
C2_02390W_A	1.081992554	2.216290181
BPH1	1.081450919	1.516642203
UTP9	1.079152342	-1.176887926
C3_07230W_A	1.075859401	0
C2_06600W_A	1.066759153	1.979562676
IME2	1.064163963	0
MET14	1.06237188	6.037196001
SHE9	1.062129121	0

C3_07900C_A	1.06137671	0
FMP45	1.057949895	0
HAP31	1.056849928	0.586132059
NTG1	1.056682263	0.429546025
C3_03110W_A	1.053489468	0
DOG1	1.053287314	-0.269782932
CR_09750C_A	1.051100908	0.540631709
TIP120	1.043870573	0
C1_00830W_A	1.043401652	0.948985198
C1_00410C_A	1.043318339	1.093962238
C3_07450C_A	1.039995339	0
C3_07030C_A	1.03773893	0.894490983
C3_07680W_A	1.037225487	0
CDR11	1.037002678	0.700632202
MNN13	1.036277553	0.62441758
HGT4	1.03379686	1.033520217
C5_04140W_A	1.030488437	0
CR_03710C_A	1.023145016	0
C3_07910W_A	1.022972315	0
C3_07650C_A	1.020922112	0
ZFU2	1.020890465	0.629385778
C1_07640C_A	1.019896561	2.289025539
FAD1	1.019399887	0
GDB1	1.018237869	0.910561415
PCD1	1.016523134	0
C3_07740W_A	1.01532876	0
C2_00420W_A	1.013720827	0.663941237
SOD2	1.013463438	1.412135703
PEX14	1.009900089	0
GLY1	1.008984689	-0.329874455
C3_07820W_A	1.007815078	-1.429021954
XKS1	1.003247751	0.661297994
CDA2	1.002397857	0

RTA4	-1.011294146	3.884361337
C3_01150C_A	-1.013632211	0.039942839
BAT21	-1.015906701	-0.507004744
CR_07160C_A	-1.032288251	0
PIR1	-1.035105831	2.923434058
GAL4	-1.04293024	-1.353504434
ARO3	-1.045450377	-0.552072724
URA3	-1.049552538	-0.623816174
PGA44	-1.052832586	0
C2_05860C_A	-1.054550894	-0.629195703
C6_00230W_A	-1.055410002	0
C2_02200W_A	-1.059346824	-1.083488891
C7_03580C_A	-1.060471481	0
C3_01940C_A	-1.064570268	-1.167808361
CTA2	-1.066555496	-1.387857242
MEP1	-1.070291176	3.212592842
CEK2	-1.078771536	1.209375327
FGR23	-1.081029617	-3.165991151
C2_07790C_A	-1.099113758	0
XOG1	-1.104511701	-1.776927361
DAG7	-1.10606743	0
FCY24	-1.106352266	0.567308722
DEF1	-1.107345538	0.510453775
PGA31	-1.114110772	-0.376902435
CR_07480W_A	-1.119429427	0
PDC11	-1.12610273	-0.549636654
C2_06570C_A	-1.151459843	1.861193882
ROA1	-1.156252381	0
STE4	-1.159260278	0
C4_05250W_A	-1.159675432	-1.726722362
AGP2	-1.16242393	-1.714537966
C1_01930W_A	-1.162452718	0
EHT1	-1.166083182	-0.387193923

C1_01610C_A	-1.171609143	3.711648631
CR_03840C_A	-1.171963773	-2.137675906
CUP1	-1.179350434	1.26524716
C3_01280W_A	-1.180316441	-0.861131247
TLO16	-1.19515559	-1.169440634
ECM331	-1.200593598	0.177486496
YVH1	-1.201015164	-1.038136459
PSO2	-1.218276943	0
C1_11080W_A	-1.228568112	0.126399358
C1_05520W_A	-1.236102313	0.955843713
C2_02960C_A	-1.238024585	0
ARG1	-1.239871161	4.762485252
C1_03870C_A	-1.248088355	3.507624594
NAT4	-1.259562019	0
C3_05320W_A	-1.269256094	0
C2_06430C_A	-1.270693709	0
C1_01360C_A	-1.282624466	0
CAG1	-1.302183779	0.938982077
ALS3	-1.304833362	-1.065135176
AAH1	-1.312184013	-0.482280378
C2_07720C_A	-1.313046944	0
OYE23	-1.339569918	0.571241221
CSP2	-1.339595186	1.73729912
HWP2	-1.349975535	0
MNN14	-1.352264984	0
C1_02730W_A	-1.354066414	2.403235793
BMT4	-1.356213958	0
CTA26	-1.360060852	-1.556525915
CCC1	-1.365387201	0.177271614
CR_06550C_A	-1.366692875	3.114146199
C4_03500C_A	-1.392479578	4.356790353
CR_07220C_A	-1.399557722	0
C7_02080W_A	-1.403056338	-0.482155694

TEF4	-1.40332972	0
CWH8	-1.411222766	0
AOX1	-1.428441901	4.811434268
CDC19	-1.461610365	-1.413399547
CR_04710W_A	-1.464004103	-2.13048655
RAS2	-1.49161189	0.98677098
CR_09930W_A	-1.509097914	0.329630834
C6_04320C_A	-1.512242591	0
C6_00730W_A	-1.521989745	0
FAV1	-1.54332704	0.149461557
CR_00010C_A	-1.545832535	0
HGT8	-1.547499949	-2.135757124
ZRT1	-1.586328725	4.588199968
ABP2	-1.590572663	1.016772892
C1_10710C_A	-1.593508702	0
PYC2	-1.596044009	0
RBT4	-1.647720853	-0.535476365
C1_06870C_A	-1.654860148	2.532786641
C5_03770C_A	-1.689545933	10.07029834
CR_06230W_A	-1.716680973	0
FAV2	-1.729265669	0
C7_00630C_A	-1.733798462	4.054468667
CRD2	-1.742798013	1.244567853
IRO1	-1.744521887	0
C7_03140W_A	-1.748740906	0
CR_09350C_A	-1.778594342	0
FAR1	-1.782039094	0
QDR1	-1.812400271	0
C1_08900W_A	-1.854925851	1.175437375
CPA1	-1.855196637	2.63306548
C2_07910C_A	-1.874262306	-0.953963793
PLB1	-1.88163019	0
FUM11	-1.901091482	-0.975231884

TYE7	-1.927704038	-0.395793846
ARG5,6	-1.957796448	3.663543742
C3_03690W_A	-1.977142087	1.671890363
C6_01810W_A	-2.096743808	0
MNN1	-2.132351114	0.025740191
GPX2	-2.209313961	1.003445485
WOR2	-2.210323872	1.119647448
MNN22	-2.231475578	0
FET34	-2.245266594	-0.804841871
PGA46	-2.24590562	0
CPA2	-2.263010243	2.525726944
MNN12	-2.336953869	0.008689869
RHR2	-2.368949152	-2.149673409
C6_02100W_A	-2.401223587	7.524675699
MDR1	-2.401450125	-0.021427729
C7_00770W_A	-2.435958892	2.197506401
PGA26	-2.488635838	-1.48980508
C3_06660C_A	-2.61512734	6.14640933
C2_08890W_A	-2.667641325	0
SOD5	-2.730138	-0.998538104
C4_00640W_A	-2.751491688	0
WOR1	-2.795445152	0
C1_07040C_A	-2.800255096	-3.521025943
C2_10730W_A	-2.851365111	0
YWP1	-2.860843163	0
PGA13	-3.065221891	1.38978179
MRV8	-3.19211285	0
C2_08580W_A	-3.312163593	0
PGA10	-3.414181278	0
SAP6	-3.573403334	-1.864312018
C3_02660W_A	-3.628439534	1.242539101
PBR1	-3.871375742	0
C5_05180W_A	-4.065004928	0

MFALPHA	-4.268621808	0
IFA14	-4.426724291	0
C3_03460C_A	-4.714398136	0
SAP4	-4.76722993	0
SAP5	-4.880984338	-0.626954928
C5_04480C_A	-6.295508089	0

TABLE 5.2: *mig1 mig2* Primer List

KL409	Mig1_CompCIP10_F2	GTC GAC CTC GAG GGT GGT GGT GGC TCA ATT CAA AGA TTA AG
KL410	Mig1_CompCIP10_R	GGT ACC GGG CCC GGA AGG TTA ATC CGA GAC CCA CCC A
KL379	Mig2 CIP10 Comp F	TTC ACA CAG GAA ACA GCT ATG ACC ATG ATT ACG CCA AGC CAC TGG GGG AAA GAA AAA GAT
KL381	Mig2 CIP10 Comp R2	CGC GTG AAT TCG ATA TCA AGC TTA TCG ATA GTT GTG GGG TGT GCC AAT TCC GAC AAT GC
KL399	sgRNA_Mig1_F	GTT TGA GCC GAT GCC ATA GTG TTT TAG AGC TAG AAA TAG CAA GTT AAA
KL400	SNR/52_Mig1_R	ACT ATG GCA TCG GCT CAA ACC AAA TTA AAA ATA GTT TAC GCA AGT C
KL401	Mig1_Del_F	CTT TTT TGA ATT TAC TTA TTC TAC TTC TGT TTA TTT CAT TTT CAT TTT CAC TAT ACA AAA CTA GAC TTA TTA ATC AAG TTA ATC AAC GTC GCA GTG GAA TTG TGA GCG GAT A

Table 5.2 continued from previous page

KL402	Mig1_Del_R	GCT TCT ATT AAA AGA AAA AAG AAC CTA TAC TAC CCA AAA AAT CTA TCT AAA CCG TAT TGT AAA TCT ATC TAT AAA TTA AAA CAC CAG TAA TTA TAA ATC TTT CCC AGT CAC GAC GTT
KL382	Mig1_Int_F	AAT GCC ACC AAA GGA GAA AA
KL383	Mig1_Int_R	CGA TGC CAT AGT TGG TGA TG
KL384	Mig1_Up_F	GAG GCC CAG CAT TTG TAA AGC
KL366	sgRNA_Mig2_F	TAC ACA CCA ACC CCA ATA GCG TTT TAG AGC TAG AAA TAG CAA GTT AAA
KL367	SNR/52_Mig2_R	GCT ATT GGG GTT GGT GTG TAC AAA TTA AAA ATA GTT TAC GCA AGT C
KL376	Mig2_Del_F	GTT TTC TCC ATA TAA AAA AAA ATT TTT TCT CTC CCC ACG AAA AAC AAG CTT TCC CAA AAC CAT CAC CAT ACC ACT CCT TGT GGA ATT GTG AGC GGA TA
KL377	Mig2_Del_R	CGA AGC TGG TGG AGA CGA AGA GAC GTT GTT CAG TGA TAG AAT CGA AGA TGA AAA TGA AAT TTG GCA AGT AGG TAT ATA AGG TAT TTT CCC AGT CAC GAC GTT
KL378	Mig2_Up_F	CCC CTC CAG CTC CTT CTT TT
KL364	Mig2_Int_F	ACA AGA CAT ATC CGG ACC CA
KL365	Mig2_Int_R	AGG TTT GAA GGA GGC GAT CA
KL459	sgRNA_Sak1_F	TAG TGA TAG TCA GCA GAT AAG TTT TAG AGC TAG AAA TAG CAA GTT AAA
KL460	SNR/52_Sak1_R	TTA TCT GCT GAC TAT CAC TAC AAA TTA AAA ATA GTT TAC GCA AGT C

Table 5.2 continued from previous page

KL438	sgRNA_try4_F	TGA AAG AGG AGT TGT AGT TGG TTT TAG AGC TAG AAA TAG CAA GTT AAA
KL439	SNR/52_try4_R	CAA CTA CAA CTC CTC TTT CAC AAA TTA AAA ATA GTT TAC GCA AGT C
KL440	Try4_Int_F	TAC CTC AAG CAC CAC CAC AA
KL441	Try4_Int_R	TCC GGG GTA TCA TAA TCT TCG A
KL442	Try4_Del_F	CAC CCC ATA CTT AAT ATT AAT TAT TCA TAA CCT ATT TAT TCA TTG ATT ATA CAA CTA AAA ATT AAA ATA CCG AAT TAC ACC GTG GAA TTG TGA GCG GAT A
KL443	Try4_Del_R	CAC CCC ATG AAA ATA TAA ATC AAT CAC AAA TCA TAT TAA GAT TAA AAA TAA ATA TTA GTT TTG CCA AAA GAT TAA GTT ATT GTT TCC CAG TCA CGA CGT T

TABLE 5.3: *mig1 mig2* Strain List

Strain Name	Genotype	Parent	Condensed Genotype	Phenotype
CW542	<i>C.d.ARG4::leu2Δ ura3Δ-iro1Δ::imm434/URA3-IRO1 his1Δ/his1Δ arg4Δ/arg4Δ leu2Δ ::C.m.LEU2/leu2Δ ::C.d.HIS1</i>	SN250	wild-type	Prototrophic
KL738	<i>mig2Δ::C.d.ARG4/mig2Δ::C.d.ARG4 ura3Δ-iro1Δ::imm434/URA3-IRO1 his1Δ/his1Δ arg4Δ/arg4Δ leu2Δ::C.m.LEU2/leu2Δ::C.d.HIS1</i>	SN250	<i>mig2Δ/Δ</i>	Prototrophic
KL820	<i>mig1Δ::C.m.LEU2 mig1Δ::C.d.HIS1 C.a.ARG4::arg4Δ ura3Δ-iro1Δ::imm434/URA3-IRO1 his1Δ/his1Δ arg4Δ/arg4Δ leu2Δ/leu2Δ</i>	SN152 (Homann X2 A11)	<i>mig1Δ/Δ</i>	Prototrophic
KL742	<i>mig2Δ::C.d.ARG4/mig2Δ::C.d.ARG4 mig1Δ::C.m.LEU2 mig1Δ::C.d.HIS1 ura3Δ-iro1Δ::imm434/URA3-IRO1 his1Δ/his1Δ arg4Δ/arg4Δ leu2Δ/leu2Δ</i>	SN152 (Homann X2 A11)	<i>mig1Δ/Δ mig2Δ/Δ</i>	Prototrophic
KL794	<i>mig1Δ::C.d.ARG4/mig1Δ::C.d.ARG4 mig2Δ::C.m.LEU2 mig2Δ::C.d.HIS1 ura3Δ-iro1Δ::imm434/URA3-IRO1 his1Δ/his1Δ arg4Δ/arg4Δ leu2Δ/leu2Δ</i>	SN152 (Homann X1 D8)	<i>mig2Δ/Δ mig1Δ/Δ</i>	Prototrophic
KL807	<i>RPS10::pMIG2::NAT1 mig2Δ::C.d.ARG4/mig2Δ::C.d.ARG4 mig1Δ::C.m.LEU2 mig1Δ::C.d.HIS1 ura3Δ-iro1Δ::imm434/URA3-IRO1 his1Δ/his1Δ arg4Δ/arg4Δ leu2Δ/leu2Δ</i>	KL742	<i>mig2Δ/Δ mig1Δ/Δ + MIG2</i>	Prototrophic NAT ^R
KL829	<i>RPS10::pMIG1::NAT1 mig2Δ::C.d.ARG4/mig2Δ::C.d.ARG4 mig1Δ::C.m.LEU2 mig1Δ::C.d.HIS1 ura3Δ-iro1Δ::imm434/URA3-IRO1 his1Δ/his1Δ arg4Δ/arg4Δ leu2Δ/leu2Δ</i>	KL742	<i>mig2Δ/Δ mig1Δ/Δ + MIG1</i>	Prototrophic NAT ^R
KL924	<i>mig2Δ::C.d.ARG4/mig2Δ::C.d.ARG4 mig1Δ::C.m.LEU2 mig1Δ::C.d.HIS1 ura3Δ-iro1Δ::imm434/URA3-IRO1 his1Δ/his1Δ arg4Δ/arg4Δ leu2Δ/leu2Δ</i>	CW542	<i>sak1Δ/Δ</i>	Prototrophic NAT ^R
KL925	<i>mig2Δ::C.d.ARG4/mig2Δ::C.d.ARG4 mig1Δ::C.m.LEU2 mig1Δ::C.d.HIS1 ura3Δ-iro1Δ::imm434/URA3-IRO1 his1Δ/his1Δ arg4Δ/arg4Δ leu2Δ/leu2Δ</i>	CW542	<i>sak1Δ/Δ</i>	Prototrophic NAT ^R
KL926	<i>mig2Δ::C.d.ARG4/mig2Δ::C.d.ARG4 mig1Δ::C.m.LEU2 mig1Δ::C.d.HIS1 ura3Δ-iro1Δ::imm434/URA3-IRO1 his1Δ/his1Δ arg4Δ/arg4Δ leu2Δ/leu2Δ</i>	KL742	<i>sak1Δ/Δ mig1Δ/Δ mig2Δ/Δ</i>	Prototrophic NAT ^R
KL927	<i>mig2Δ::C.d.ARG4/mig2Δ::C.d.ARG4 mig1Δ::C.m.LEU2 mig1Δ::C.d.HIS1 ura3Δ-iro1Δ::imm434/URA3-IRO1 his1Δ/his1Δ arg4Δ/arg4Δ leu2Δ/leu2Δ</i>	KL742	<i>sak1Δ/Δ mig1Δ/Δ mig2Δ/Δ</i>	Prototrophic NAT ^R
KL929	<i>mig1Δ::C.d.ARG4/mig1Δ::C.d.ARG4 mig2Δ::C.m.LEU2 mig2Δ::C.d.HIS1 ura3Δ-iro1Δ::imm434/URA3-IRO1 his1Δ/his1Δ arg4Δ/arg4Δ leu2Δ/leu2Δ</i>	KL7942	<i>snf1Δ/Δ mig1Δ/Δ mig2Δ/Δ</i>	Prototrophic NAT ^R
KL930	<i>mig1Δ::C.d.ARG4/mig1Δ::C.d.ARG4 mig2Δ::C.m.LEU2 mig2Δ::C.d.HIS1 ura3Δ-iro1Δ::imm434/URA3-IRO1 his1Δ/his1Δ arg4Δ/arg4Δ leu2Δ/leu2Δ</i>	KL7942	<i>snf1Δ/Δ mig1Δ/Δ mig2Δ/Δ</i>	Prototrophic NAT ^R

Chapter 6

Zfu2

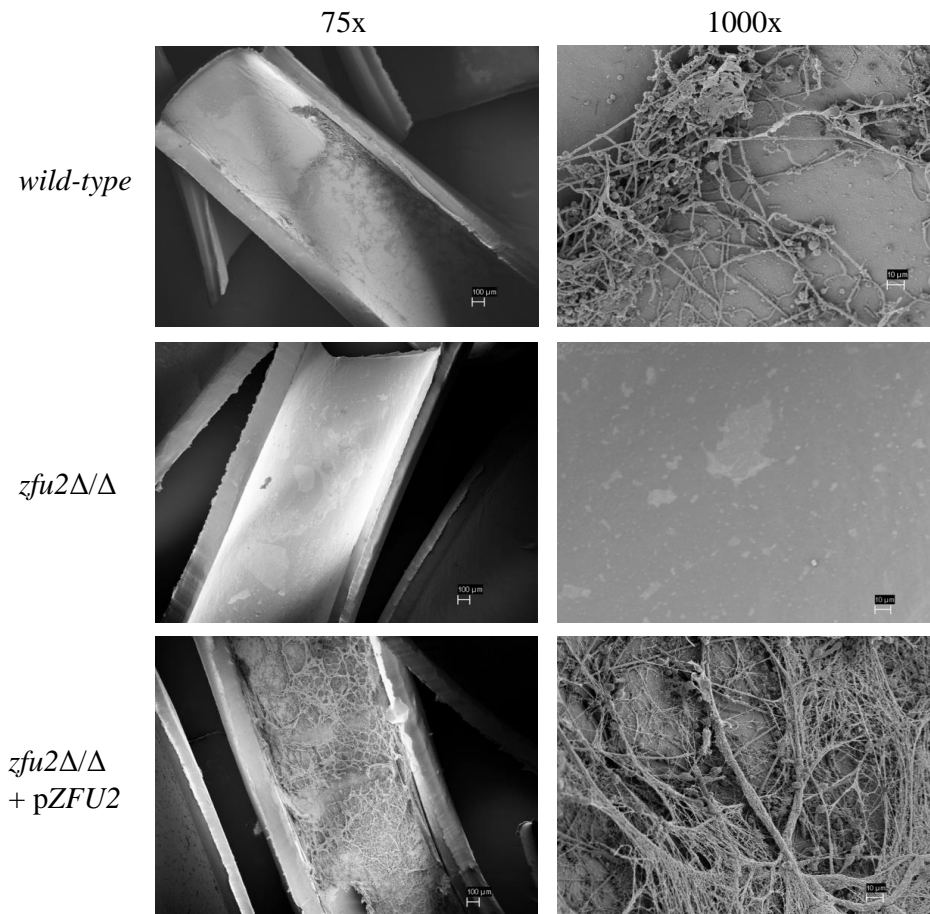


FIGURE 6.1: **Zfu2 is required for *C. albicans* biofilm formation *in vivo***
A. Strains DAY185 (wild-type) TA114 (*zfu2*Δ/Δ), KL124 (*zfu2*Δ/Δ pZFU2) were inoculated in rat venous catheters for 24 hours. Catheters were removed and the luminal surfaces were visualized using scanning electron microscopy at 75x and 1000x magnification.

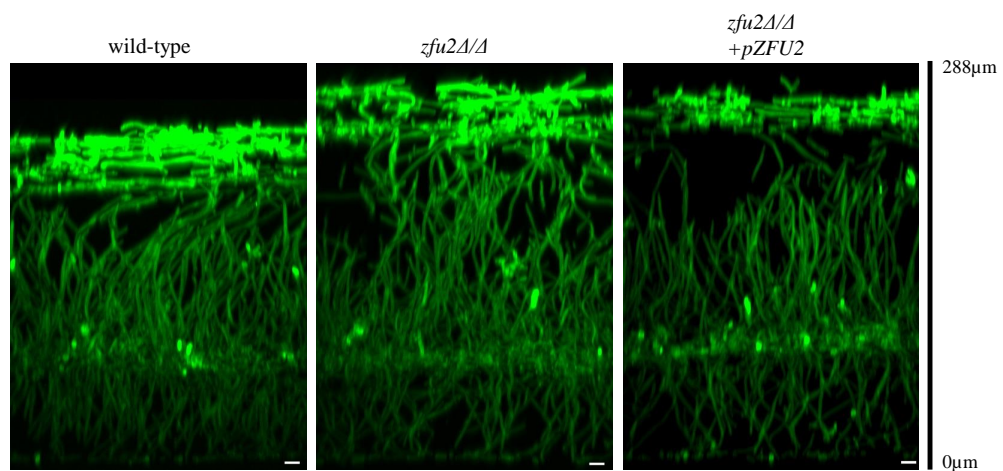


FIGURE 6.2: **The *zfu2* mutant strain is not defective in biofilm formation *in vitro*.**

Strains DAY185 (wild-type) TA114 (*zfu2*Δ/Δ), KL124 (*zfu2*Δ/Δ pZFU2) were grown in RPMI plus 10% serum for 24 hours. Biofilms were then fixed, stained with Alexa594 conA and imaged using confocal microscopy. Side-view projections were obtained by reslicing the image from bottom to top, max projected, and pseudo-colored. The scale bar corresponds to 10 μm.

6.1 Zfu2 is required for *C. albicans* biofilm formation *in vivo* but not *in vitro*

Zfu2 is a Zn₂Cys₆ transcription factor with homologs in closely related fungal species such as *Candida dubliniensis*, but no known homolog in *Saccharomyces cerevisiae*. Our interest in this transcription factor emerged from a screen of transcription factor mutants using a microfluidic flow channel to identify mutants that were defective in adherence[121]. We found that the *zfu2* Δ/Δ mutant was not defective in biofilm formation in our *in vitro* model (See Fig. 6.2). However, the *zfu2* Δ/Δ mutant was defective in an *in vivo* rat venous catheter model of biofilm formation performed by the lab of Dr. David Andes (See Fig. 6.1) indicating that the *in vitro* model of biofilm formation is not always predictive of outcomes *in vivo*.

6.2 The impact of Zfu2 on *in vitro* biofilm gene expression

Since Zfu2 is a transcription factor, we reasoned that its role in regulating gene expression during biofilm formation might be significant. Although the *zfu2* mutant showed no defect in our *in vitro* biofilm assay, we chose to profile the mutant strain compared to the complemented strain using RNA-sequencing during *in vitro* biofilm growth conditions. We could not study the gene expression of the cells during *in vivo* biofilm growth due to the lack of any cells that remained adhered to the catheter *in vivo*. Therefore, we hoped that there would still be some overlap of critically regulated genes in the *in vitro* profile that could inform us of functional consequences *in vivo*. We compared the transcriptome profiles of the *zfu2* mutant and the complemented strain using whole-genome expression profiling through RNA-Seq. Analysis of the expression profile showed that 296 transcripts were differentially regulated more than 2-fold $p < 0.05$. Using GO term enrichment analysis through the program FungiFun2[168], we found a few broad categories that were enriched for the upregulated and the downregulated genes (See Fig. 6.3). Specifically, genes encoding different types of transporters were upregulated in the mutant strain while the top categories of downregulated genes were cell surface or extracellular region. From the downregulated genes we focused on three genes, *CSA2*, *RBT5*, and *PGA7*. These genes are in a family of five related genes due to a shared CFEM (Common in Fungal Extracellular Membrane) motif that contains 8 cysteines[169].

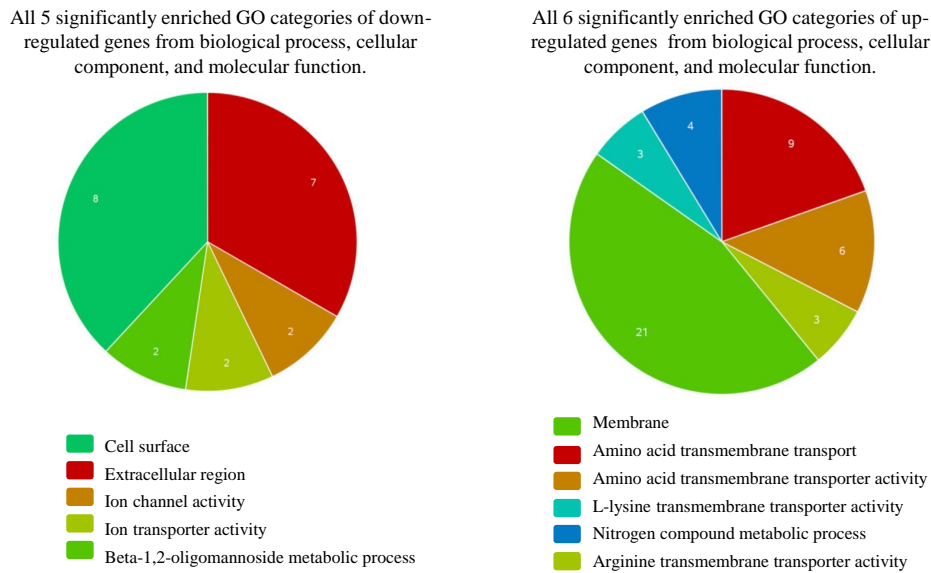


FIGURE 6.3: **Functional GO categories enriched in the *zfu2* mutant profile compared to the control strain using software FungiFun2**

The CFEM proteins have been shown to coordinate together in the shuttling of iron from heme extracted from hemoglobin due to their differential localization[92][88][91]. These proteins are also of interest because in the *in vivo* rat venous catheter model for biofilm formation, hemoglobin may be a main source of iron from whole blood.

6.3 The CFEM proteins are critical targets of Zfu2 *in vivo*

To determine if these CFEM protein genes are critical targets of Zfu2, we employed an overexpression system for each CFEM gene in the *zfu2* mutant. The *TDH3* promoter was exchanged in one allele for each gene's endogenous promoter. The overexpression of each CFEM gene was verified using RT-PCR (See Fig. 6.4). Overexpression of *CSA2* was the most significant, while *RBT5* was only overexpressed 2 fold. This may be because *RBT5* is already one of the most highly expressed genes in *C. albicans* hyphal cells and therefore the *TDH3* promoter may not be expressed higher than *RBT5* [21](6.1). Then, we tested whether these overexpression strains could restore biofilm formation in the *zfu2* mutant using an *in vivo* rat venous catheter model. The expression of *CSA2*, *RBT5*, and *PGA7* in the *zfu2* mutant strain all restored biofilm formation, albeit to differing degrees

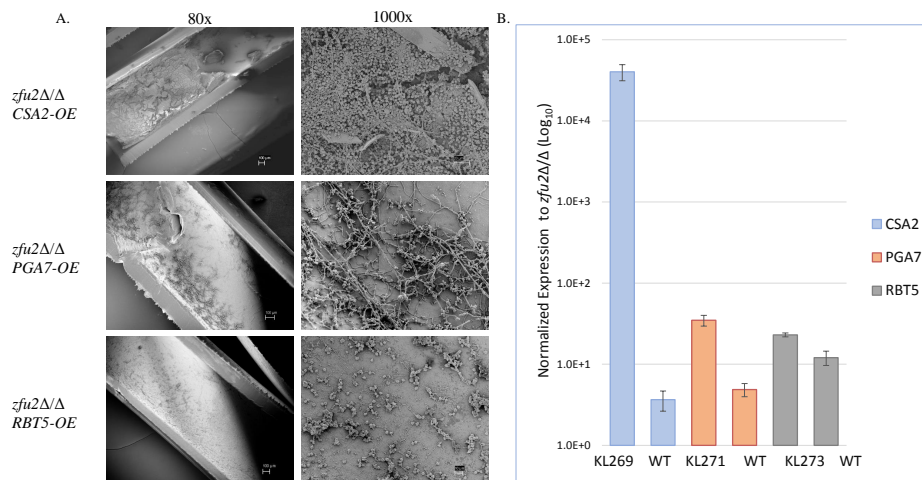


FIGURE 6.4: **The CFEM proteins are critical targets of ZFU2 in vivo.**
 A. Strains KL269 (*zfu2*Δ/Δ *CSA2*-OE), KL271 (*zfu2*Δ/Δ *PGA7*-OE), and KL273 (*zfu2*Δ/Δ *RBT5*-OE) were inoculated in rat venous catheters for 24 hours. Catheters were removed and the luminal surfaces were visualized using scanning electron microscopy at 80x and 1000x magnification. B. The over-expression of each CFEM gene compared to the *zfu2*Δ/Δ parent strain was confirmed using RT-PCR.

(See Fig. 6.4). This leads to the hypothesis that the *zfu2* mutant may be defective in utilizing heme as an iron source.

6.4 Addition of ferric chloride restores biofilm formation ability of the *zfu2* mutant *in vivo*

Since the CFEM proteins bind methemoglobin and overexpression of the CFEM protein genes restored biofilm growth, we asked whether we could bypass the need for these genes through the addition of an alternative iron source that expression of CFEM proteins would not used to acquire. To test this hypothesis, we added 200μg per liter of FeCl₃ (the concentration of iron in synthetic defined culture medium) to the inoculum in the rat venous catheter model. Addition of this iron source fully restored biofilm formation of the *zfu2* mutant strain *in vivo* (See Fig. 6.5).

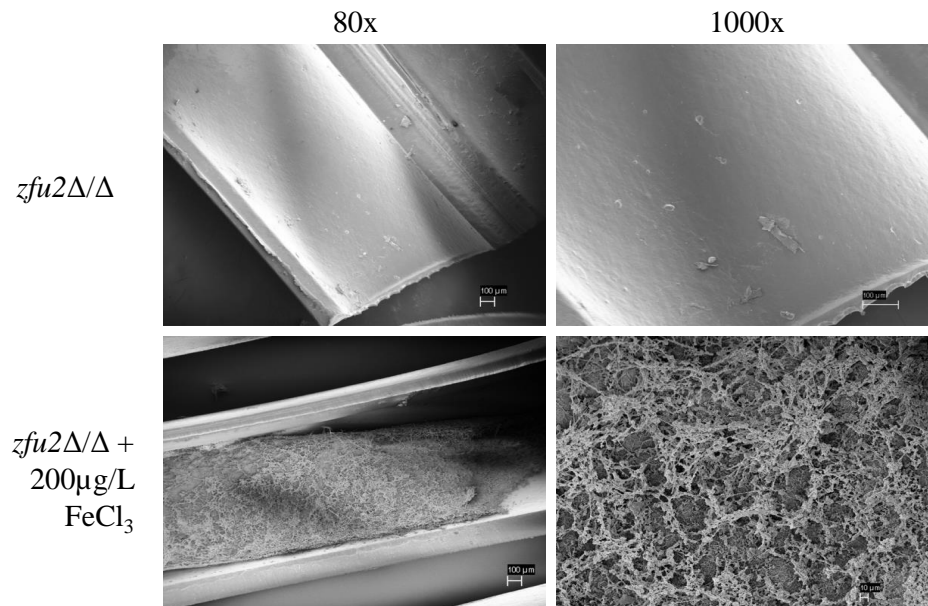


FIGURE 6.5: **Addition of FeCl_3 restores biofilm formation of the *zfu2* mutant**

Strain TA114 (*zfu2* Δ/Δ) and strain TA114 (*zfu2* Δ/Δ) plus a solution of 200 $\mu\text{g/L}$ FeCl_3 were inoculated in rat venous catheters for 24 hours. Catheters were removed and the luminal surfaces were visualized using scanning electron microscopy at 80x and 1000x magnification.

6.5 Zfu2 and Hap43 may be dispensable for virulence in an oral candidiasis model

Knowing that Zfu2 plays a role in biofilm formation *in vivo*, and a role in mouse GI tract colonization[31], we were curious as to whether it might play a role in oral candidiasis infections. The role that iron plays in nutritional immunity of the tongue is unclear. Therefore, we tested another mutant strain of the transcription factor, Hap43. Previous studies have shown that Hap43 is necessary for growth under low-iron conditions and is also required for virulence in a model of systemic candidiasis[99]. This mutant would add evidence as to whether an OPC infection is limited for iron. We challenged immunosuppressed wild-type BALB/c mice with wild-type, *zfu2* mutant, and *hap43* mutant strains of *C. albicans*. We found that the fungal burden of the tongue tissue after 5 days of infection was not significantly different between the *zfu2* or *hap43* mutant strains compared to the wild-type (See Fig. Fig6.6). However a *HAP43* complemented strain surprisingly showed significantly increased fungal burden compared to the wild-type strain. This

strain contains one copy of the *HAP43* gene integrated at the *IRO1* locus. Gene expression analysis would have to be performed to test whether expression of *HAP43* at the *IRO1* locus increases expression of *HAP43*. Also, multiple biological replicates of this assay would have to be performed in order to confirm the phenotype.

We performed nanoString profiling analysis on infected tissue from the *zfu2* mutant strain, and found that the CFEM protein genes were not differentially expressed in the mutant strain (Table 6.1). The transcripts for *CSA2* from the *in vivo* infection were too low to be analyzed, but in line with previous results[91][92] *PGA7* and *RBT5* were highly expressed and could be analyzed. Therefore, we conclude Zfu2 does not regulate the CFEM protein genes in this context of infection.

Often, the progression of an infection can vary dramatically in both response of the host and the pathogen [21]. To test if Hap43 plays a role in the early onset of an OPC infection, we repeated the experiment using wild-type, *hap43* mutant, and *rim101* mutant strains and quantified fungal burdens in the tongue tissue after 24 h. For this experiment, a *rim101* mutant was used as a positive control due to its known role in mucosal infections *in vivo* [141]. Mice infected with the *hap43* and *rim101* mutant strains did not show a statistically significant difference in fungal burdens compared to the wild-type control (6.7). However, the *rim101* mutant showed a trend towards a reduction in fungal burden, as the tongue tissue from two mice produced no CFUs resulting in a geometric mean of 85 CFUs/gram of tissue for the mutant strain compared to 15,846 CFUs/gram of tissue for the wild-type strain. Since only 5 mice were used for each strain of *C. albicans* and the experiment was only repeated for 1 biological replicate, the statistical power of the study was not sufficient to determine whether either mutant showed a significant difference in fungal burdens.

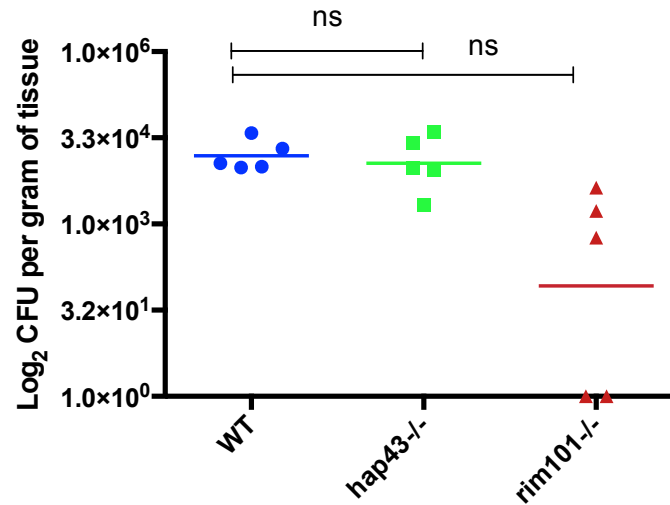


FIGURE 6.7: **Hap43 may be dispensable for virulence in a mouse model of a 24 h oral candidiasis infection**

Fungal burden was assessed by CFU counts from tongue homogenates after 1 day of infection. Bars show geometric mean of 5 total mice. One-way ANOVA was used to assess significance $p < 0.05$

	wild-type avg counts	zfu2 Δ/Δ avg counts	zfu2 Δ/Δ + pZFU2 avg counts	zfu2 Δ/Δ vs. wild-type	zfu2 Δ/Δ vs. zfu2 Δ/Δ +pZFU2	zfu2 Δ/Δ +pZFU2 vs. wild-type
ZFU2	41.93	1.00	26.05	0.02	0.04	0.62
CSA2	4.19	1.54	1.00	0.37	1.54	0.24
PGA7	127.84	139.98	64.47	1.09	2.17	0.50
RBT5	989.76	1306.24	609.55	1.32	2.14	0.62

TABLE 6.1: **NanoString gene expression results from *in vivo* OPC infection showing normalized counts and ratio comparisons between strains**

Left half of the table shows the normalized transcript levels of *ZFU2* and the three CFEM protein genes. The right half of the table shows ratios between the *zfu2* mutant strain compared to wild-type and the complemented strain.

6.6 Discussion

Our data show that the transcription factor *Zfu2* is required for *in vivo* biofilm formation in the rat venous catheter model, but *Zfu2* is not required for biofilm formation *in vitro*. From RNA-seq profiling of the *zfu2* mutant, we found that expression of the CFEM protein genes were downregulated in the mutant *in vitro*. We were able to show functional importance of expression of the CFEM protein genes in a rat venous catheter model of

in vivo biofilm formation. Subsequently, we were able to bypass the need for CFEM gene expression by exogenously adding FeCl₃ as an iron source. There are several possible explanations for the data shown. One possible explanation is that the only source of iron in the venous catheter is hemoglobin, and the addition of FeCl₃ allows the *zfu2* mutant strain to grow *in vivo* when it otherwise cannot grow. To confirm this hypothesis, the *CSA2* overexpression construct used to rescue the biofilm formation defect of the *zfu2* mutant could be mutated so that Csa2 cannot coordinate heme iron. Nasser et al. showed that the Asp80 residue of Csa2 coordinates Fe²⁺heme and mutation of that aspartic residue to a histidine residue abolishes its ability to exchange heme with other CFEM proteins *in vivo* [93]. Therefore, if the *zfu2* mutant strain overexpressing a *CSA2* construct that cannot exchange heme does not form a biofilm *in vivo*, then that would suggest that the *zfu2* mutant biofilm defect is due solely to its inability to acquire heme iron. If the mutated construct overexpressed in the *zfu2* mutant does form a biofilm, then that would suggest that Csa2 may play a different role in biofilm formation *in vivo* other than heme iron acquisition.

Another explanation could be that the addition of iron causes some other phenotypic change that influences the proteins that are expressed on the cell wall. Iron restriction has been shown to influence cell wall protein expression and morphogenesis in *C. albicans*[170][171]. Similarly, the CFEM proteins likely have molecular functions other than heme acquisition. Als3 is a prime example of this phenomenon. Als3 is a cell wall protein that functions not only as an adhesion and invasion, but also binds ferritin[172]. Further evidence that the CFEM proteins might employ multiple functions is highlighted by work using atomic force microscopy to examine the surface of yeast cells. Mutations in CFEM protein genes resulted in altered topography of the yeast cell surface[173]. The CFEM proteins also play a role in biofilm formation *in vitro*[174]. Therefore, although the role of Csa2, Pga7, and Rbt5 in the extraction of iron from hemoglobin is well understood[93][92], their role in biofilm formation is less well understood. Work by Xu et al. has highlighted the stark difference between *in vivo* and *in vitro* gene expression profiles[21]. For example, when profiles of an *efg1* mutant strain were compared between *in vivo* and *in vitro* conditions, only 4 out of 148 genes analyzed were similarly regulated[21]. Therefore, understanding the role of transcription factors and their gene regulatory networks in the context of infection is of the greatest necessity. Similarly, the gene expression profiles in different models of infection are important to understand

different types of infection.

The importance of testing different *in vivo* models of infection was highlighted in this work by the results from the *zfu2* and *hap43* mutant strains in an *in vivo* mouse model of a oropharyngeal candidiasis. An OPC infection is thought to be a type of biofilm due to the large fungal mass that invades the surface of the tongue tissue[175]. Mutation of another transcription factor gene, *BCR1* was shown to cause defects in both *in vivo* models of infection [44][123], giving some precedent to conservation of regulatory control of biofilm formation in both models. Since the *zfu2* mutant was defective in biofilm formation in the *in vivo* rat venous catheter model, we wanted to know whether the mutant would also be defective in a mouse model of OPC. Although only one biological replicate of the *zfu2* mutant was tested in the mouse model of OPC, the mutant strain was not significantly different from the wild-type strain. Based on the preliminary results from that replicate, the experiment was not repeated for further biological replicates. Furthermore, the nanoString profiling results show that Zfu2 does not regulate the CFEM protein genes in this *in vivo* model indicating that Zfu2 has divergent regulatory targets during *in vivo* biofilm infection and during an oral candidiasis infection. The leading hypothesis was that the *zfu2* mutant was defective in biofilm formation in the rat venous catheter due to the inability to acquire iron from heme. This hypothesis was supported by the fact that the addition of ferric chloride restored the ability of the *zfu2* mutant to form a biofilm. Therefore, we were interested in understanding how other transcriptional regulators of iron utilization affect the progression of an oral candidiasis infection. The *hap43* mutant was tested because it had been shown to be defective in virulence in a model of systemic candidiasis [99] and is required for responses to low iron. Therefore, if *HAP43* was required for virulence in an OPC infection, it would suggest that *C. albicans* is limited for iron. However, HAP43 appeared to be dispensable for virulence in a mouse model of OPC. Again, only one biological replicate was performed, but preliminary data was not promising, so further experiments were not performed. Since *ZFU2* and *HAP43* were both dispensable for virulence in a mouse model of OPC, it is possible that *C. albicans* is not limited for iron in this *in vivo* model. This result is surprising due to evidence that the regulation of iron acquisition and utilization is important for infection in systemic models of candidiasis [176][99] and in gut commensalism models [30].

Chapter 7

Supplement

TABLE 7.1: *zfu2* Strain List

Strain	Genotype	Reference
DAY185	ura3 Δ iro1 Δ :: λ imm434 ARG4:URA3:arg4::hisG HIS1::his1::hisG ura3 Δ iro1 Δ :: λ imm434 arg4::hisG his1::hisG	PMID:10992507
BWP17	ura3 Δ iro1 Δ :: λ imm434 arg4::hisG his1::hisG ura3 Δ iro1 Δ :: λ imm434 arg4::hisG his1::hisG	PMID:10074081
TA114	ura3 Δ iro1 Δ :: λ imm434 arg4::hisG his1::hisG::pHIS1 Δ zfu2::ARG4 ura3 Δ iro1 Δ :: λ imm434 arg4::hisG his1::hisG Δ zfu2::URA3	This study
KL124	ura3 Δ iro1 Δ :: λ imm434 arg4::hisG his1::hisG::pHIS1-ZFU2 Δ zfu2::ARG4 ura3 Δ iro1 Δ :: λ imm434 arg4::hisG his1::hisG Δ zfu2::URA3	This study
KL269	ura3 Δ iro1 Δ :: λ imm434 arg4::hisG his1::hisG::pHIS1 Δ zfu2::ARG4 CSA2::pAgTEF1-NAT1-AgTEF1UTR- TDH3-CSA2 ura3 Δ iro1 Δ :: λ imm434 arg4::hisG his1::hisG Δ zfu2::URA3 CSA2	This study
KL271	ura3 Δ iro1 Δ :: λ imm434 arg4::hisG his1::hisG::pHIS1 Δ zfu2::ARG4 PGA7::pAgTEF1-NAT1-AgTEF1UTR- TDH3-PGA7 ura3 Δ iro1 Δ :: λ imm434 arg4::hisG his1::hisG Δ zfu2::URA3 PGA7	This study
KL273	ura3 Δ iro1 Δ :: λ imm434 arg4::hisG his1::hisG::pHIS1 Δ zfu2::ARG4 RBT5::pAgTEF1-NAT1-AgTEF1UTR- TDH3-RBT5 ura3 Δ iro1 Δ :: λ imm434 arg4::hisG his1::hisG Δ zfu2::URA3 RBT5	This study

KL 1	Zfu2_Del_F	AAC TCC AAA AAA AAA TGG CAA CTT TAA ATT TCT GGA TAA ACT TGT AAA CAA ATT CAT TAT CAT TAA TAT CAT AAT CTT CAT TAT CAT TTT CAT TTT CGC ATT TCC CAG TCA CGA CGT T
KL2	Zfu2_Del_R	AAA CAA TAA CAA TTA ATT ATA TCA ATA GTG CAA CTT CCC CCT CTC CCC CCT CCC CCC CTA TTC CTC TCA TCT CAA TTT ATA CAT ATA GGT ATA CAC CTA TGT GGA ATT GTG AGC GGA TA
KL31	Zfu2_F_Comp PDDB78	TTC ACA CAG GAA ACA GCT ATG ACC ATG ATT ACG CCA AGC TAT TAA GCC ATG ATA TTG AAA GAT ATA GAC
KL 32	Zfu2_R_Comp PDDB78	TCG ACC ATA TGG GAG AGC TCC CAA CGC GTT GGA TGC ATA GGT ATG TGT GTA TAG GTT GAT GAA
KL188	Zfu2_DetF Up338	GAA TCA CCA ATA GAT CAA CAA CGA
KL189	Zfu2_DetR Int508	CTT TTT CAA CCG GCA GAG AA
KL83	CSA2-OE-F	ACC AGC ATA AAT CGG AAA CCG GAC GTA CAA TTA ATG GTT AGT GTT TCA CTT TTT CCA TTG TTT TAT AGT TGT ATA GCG TTA GAC AAT GTG TAC CAA AAC ATC AAG CTT GCC TCG TCC CC
KL84	CSA2-OE-R	TAT CAG CAG CAG GGG CTG GGG CAG CAG TAA CAG CAG GAG CAG CAG CAG CAT TGG CAA AGG CAA TTG CAA ATG GAA TGG CTA AAA TAG TAG AAA ATT TCA TTG TTA ATT AAT TTG ATT GTA AAG TTT GTT GAT G

KL85	Csa2-F-OECheck	CCA TTG ACA ATG GAA TAA GTG GAC
KL86	PGA7-F-OECheck	GCA ACC CTG TTA TTG ATG TCA A
KL87	PGA7-OE-R	CCC ATT AAT GGA AGC AGT TTT AGG GAC TTT TGG GTA TGT ACC AAA GTT ACC GTA ATC AGC AGC AGA TAC TAA AAG AAT CAA GTA GAA TAT GAA ATG CAT TGT TAA TTA ATT TGA TTG TAA AGT TTG TTG ATG
KL88	PGA7-F-OECheck	GCA ACC CTG TTA TTG ATG TCA A
KL89	RBT5-OE-F	GGC CAT TCG AGG TCA CCT ATG GTT GCT GCC ATG TGG ATG TTT ATG CAA GAA ACA TGC CTG GAA TAT CCA GAT TTG GTA ACT AAA GTT CTA CAA ACA GCA TCA AGC TTG CCT CGT CCC C
KL90	RBT5-OE-R	CTT GGG AAA ATA GTG TAT GGA TTA TCA CCT TCT GGG ATA GCA GTG ACA CCA GCA GCT GAA GCA ATG GAA ACG ATT GAC AAT AAG GAT AAG GCG AGC ATT GTT AAT TAA TTT GAT TGT AAA GTT TGT TGA TG
KL91	RBT5-F-OECheck	GCT TCA ATA ACA ATT GTA GTC AAC
KL106	CSA2-RT-F	CAGCTCTACTCCTTGTCAT
KL107	CSA2-RT-R	ACTTGAGACACTTGCTGGAA
KL108	RBT5-RT-F	ACCACTGCCGAATCTACTG
KL109	RBT5-RT-R	TCAACGGAAACAGAAGCAAC
KL110	PGA7-RT-F	GCTGGAGATGCTAAGGAAGT

KL111	PGA7-RT-R	AAGAGGAGGAGTCTGTGGAT
KL112	THD3-RT-F	ATCCCACAAGGCCTGGAGA
KL113	TDH3-RT-R	GCAGAAGCTTTAGCAACGTG
KL168	Hap43_DelF	GAA ATC AGC GAG TAA TCG GCC AGA CAA AAA AAA ACA ACA GAG TCC AAA AAA ATA CAT AAT AAT TAG AAT TTC AAT TTG AAC AAC TTT CCC AGT CAC GAC GTT
KL169	Hap43_DelR	GTA TAT TAT TAA TCA ATT CAA AAC GAA AAG AAA AGA AAA AAA AAA CTG AAG TGT CGG AAA TAC TTC ATA CTG TAA GTC AAA CGT GGA ATT GTG AGC GGA TA
KL170	Hap43_SgRNA/F	CTA TTG TGA TGG GAT GGA GAG TTT TAG AGC TAG AAA TAG CAA GTT AAA
KL171	Hap43_SNR52/R	TCT CCA TCC CAT CAC AAT AGC AAA TTA AAA ATA GTT TAC GCA AGT C
KL172	Hap43_DetF Up420	CAC AAA GCT CTC ATA GTT GGA GG
KL173	Hap43_DetR Int297	GGC TCT CTG TGC AGC TCT A
KL227	Hap43 pSG1Comp_F	AGC TAT GAC CAT GAT TAC GCC AAG CAG CTG ACA ATA CAT ACA GCT AAA AGT GTG TCG TAG
KL228	Hap43 pSG1Comp_R	CTT TAA ACC ATC TTC GAC CGT CAT GAA GCT CGT ATG AGT GTT GTC AAG ATT GTC TTG CAT

TABLE 7.2: *zfu2* Primer List

Chapter 8

Conclusion

This thesis has attempted to characterize and discover the gene functions of three transcription factors Zfu2, Mig1, and Mig2. Investigating transcription factors is of interest because the control of gene regulatory networks has been shown to be an important mechanism for evolution[177]. Through this work, it was shown that the structure and function of Mig1 and Mig2 display some conservation and some divergence throughout evolution between *Saccharomyces cerevisiae* and *Candida albicans*. On the other hand, Zfu2 has no known homolog in *Saccharomyces cerevisiae* and therefore represents the possibility of a new transcriptional regulatory network in *C. albicans*. Although it is convenient to investigate transcription factors of *C. albicans* in the context of evolution and in regards to the model yeast *Saccharomyces cerevisiae*, this work has focused primarily on the role of gene regulatory networks that affect *C. albicans* pathogenicity. Over 400,000 lives worldwide are threatened by invasive candidiasis infections each year[4], so understanding how Zfu2, Mig1, and Mig2 contribute to pathogenicity of *C. albicans* is the main goal of this work.

One theme that emerges from this work is the importance of investigating transcriptional networks in *C. albicans* in the *in vivo* condition. This work and the work of others has provided ample evidence that *in vitro* conditions are not always predictive of *in vivo* conditions [21][44]. Most researchers would not have chosen to investigate the role of the transcription factor Zfu2 in an *in vivo* model of biofilm formation based on its lack of altered phenotypes *in vitro*. However, this work was serendipitous in that the CFEM protein gene targets of Zfu2 were identified by gene expression profiling *in vitro*, and were

also critical targets of Zfu2 *in vivo*. Additionally, the investigation of Zfu2 in two different *in vivo* models illustrates that it has divergent roles as a transcriptional regulator of the CFEM protein genes. NanoString profiling results indicate that Zfu2 does not control expression of *PGA7* or *RBT5* in a mouse model of oropharyngeal candidiasis. Expression levels of *CSA2* were too low in the tongue tissue to conclude whether Zfu2 regulates its expression. Therefore, Zfu2 plays different roles as a transcriptional regulator *in vitro*, in an *in vivo* rat venous catheter model of biofilm formation, and in an *in vivo* model of an OPC infection. The divergent role of Zfu2 in these three contexts, highlights the transcriptional plasticity that *C. albicans* displays in response to diverse niches.

In this work, the function of the transcription factors Mig1 and Mig2 were only investigated *in vitro*. An *in vitro* endothelial cell damage assay and a murine macrophage cell damage assay were performed and showed that the *mig1 mig2* double mutant exhibited defects in damage in both assays. These assays have been shown to correlate with *in vivo* responses [159], but cells in a culture dish cannot account for the complexities of the *in vivo* condition. For the macrophage cell damage assay, J774 mouse macrophages were used to assess virulence of *C. albicans*. These cells were used due to the ease of culturability, and due to the fact that they have been well characterized in the fungal field [24][49]. However, mouse cells have been shown to have drastically different killing ability and immune responses to *C. albicans* compared to primary human macrophage cells [178]. To make a definitive claim that Mig1 and Mig2 control pathogenicity in regards to the innate immune system, primary human macrophage cells or other primary phagocytic cells such as polymorphonuclear neutrophils should be used in the future.

The role of Mig1 and Mig2 as transcriptional repressors of alternative carbon utilization genes is consistent with the gene expression profiling data presented in this thesis. Additional evidence was presented by the epistasis tests showing that a *mig1 mig2* double mutant in a *sak1* mutant background restores growth of the *sak1* mutant on alternative carbon sources and the reversal of the essentiality of *SNF1* in a *mig1 mig2* double mutant background. However, the role of Mig1 and Mig2 in the context of caspofungin responses is far less clear from the data presented here. It is interesting to note that the cell wall integrity response signaling downstream of Mig1 and Mig2 is likely independent of Sak1 and Snf1. This claim is based on the fact that a *sak1* mutant and a viable, non-phosphorylatable mutant strain of *snf1* are both sensitive to cell wall stress [32]. If Sak1 and Snf1 negatively regulate the function of Mig1 and Mig2 as transcriptional

repressors, then you might expect that a *mig1 mig2* double mutant would be resistant to cell wall stress. Additional data to support the hypothesis that Mig1 and Mig2 control cell wall integrity independent of Sak1 and Snf1 was shown in figure 3.9. The *mig1 mig2* double mutant was still sensitive to caspofungin in glycerol media, indicating that their function in cell wall integrity signaling may be independent of their function as transcriptional repressors in response to glucose. Additionally, the gene expression profiling of the double mutant in YPD containing caspofungin was not informative due to the lack of a unique gene expression response to the drug. Therefore, no concrete conclusions can be made about how Mig1 and Mig2 control cell wall integrity signaling from the work presented here.

Overall, this work has shown that gene expression profiling can successfully be used to characterize new genetic pathways and test functional hypotheses. It has also illustrated the power of genetic analyses and epistasis tests to elucidate redundancy between transcription factors and to elucidate relationships between kinases and transcription factors. Through these genetic and molecular analyses, this work has uncovered new genetic determinants for virulence in *Candida albicans* in regards to biofilm formation *in vivo* and interactions with host cells *in vitro*.

Bibliography

- [1] Erna M Kojic and Rabih O Darouiche. “Candida infections of medical devices”. In: *Clinical microbiology reviews* 17.2 (2004), pp. 255–267.
- [2] Peter G Pappas et al. “A prospective observational study of candidemia: epidemiology, therapy, and influences on mortality in hospitalized adult and pediatric patients”. In: *Clinical Infectious Diseases* 37.5 (2003), pp. 634–643.
- [3] Marek S Skrzypek et al. “The Candida Genome Database (CGD): incorporation of Assembly 22, systematic identifiers and visualization of high throughput sequencing data”. In: *Nucleic acids research* (2016), gkw924.
- [4] Gordon D Brown et al. “Hidden killers: human fungal infections”. In: *Science translational medicine* 4.165 (2012), 165rv13–165rv13.
- [5] Julia Oh et al. “The altered landscape of the human skin microbiome in patients with primary immunodeficiencies”. In: *Genome research* (2013).
- [6] Andrea K Nash et al. “The gut mycobiome of the Human Microbiome Project healthy cohort”. In: *Microbiome* 5.1 (2017), p. 153.
- [7] Slavena Vylkova. “Environmental pH modulation by pathogenic fungi as a strategy to conquer the host”. In: *PLoS pathogens* 13.2 (2017), e1006149.
- [8] Pedro Miramón and Michael C Lorenz. “A feast for Candida: Metabolic plasticity confers an edge for virulence”. In: *PLoS pathogens* 13.2 (2017), e1006144.
- [9] S Blair Hedges. “The origin and evolution of model organisms”. In: *Nature Reviews Genetics* 3.11 (2002), p. 838.
- [10] Jeffrey Sabina and Victoria Brown. “Glucose sensing network in *Candida albicans*: a sweet spot for fungal morphogenesis”. In: *Eukaryotic cell* 8.9 (2009), pp. 1314–1320.

- [11] Caroline J Barelle et al. “Niche-specific regulation of central metabolic pathways in a fungal pathogen”. In: *Cellular microbiology* 8.6 (2006), pp. 961–971.
- [12] CLYDE L Denis and ELTON T Young. “Isolation and characterization of the positive regulatory gene ADR1 from *Saccharomyces cerevisiae*.” In: *Molecular and cellular biology* 3.3 (1983), pp. 360–370.
- [13] M Ciriacy. “Genetics of alcohol dehydrogenase in *Saccharomyces cerevisiae*: I. Isolation and genetic analysis of *adh* mutants”. In: *Mutation Research/Fundamental and Molecular Mechanisms of Mutagenesis* 29.3 (1975), pp. 315–325.
- [14] Elton T Young et al. “Multiple pathways are co-regulated by the protein kinase Snf1 and the transcription factors Adr1 and Cat8”. In: *Journal of Biological Chemistry* 278.28 (2003), pp. 26146–26158.
- [15] Melissa A Ramirez and Michael C Lorenz. “The transcription factor homolog CTF1 regulates β -oxidation in *Candida albicans*”. In: *Eukaryotic cell* 8.10 (2009), pp. 1604–1614.
- [16] Melissa A Ramirez and Michael C Lorenz. “Mutations in alternative carbon utilization pathways in *Candida albicans* attenuate virulence and confer pleiotropic phenotypes”. In: *Eukaryotic cell* 6.2 (2007), pp. 280–290.
- [17] Doblin Sandai et al. “The evolutionary rewiring of ubiquitination targets has reprogrammed the regulation of carbon assimilation in the pathogenic yeast *Candida albicans*”. In: *MBio* 3.6 (2012), e00495–12.
- [18] Juana M Gancedo. “Yeast carbon catabolite repression”. In: *Microbiology and molecular biology reviews* 62.2 (1998), pp. 334–361.
- [19] Jochen Regelmann et al. “Catabolite degradation of fructose-1, 6-bisphosphatase in the yeast *Saccharomyces cerevisiae*: a genome-wide screen identifies eight novel GID genes and indicates the existence of two degradation pathways”. In: *Molecular biology of the cell* 14.4 (2003), pp. 1652–1663.
- [20] YS Lopez-Boado et al. “Catabolite inactivation of isocitrate lyase from *Saccharomyces cerevisiae*”. In: *Archives of microbiology* 147.3 (1987), pp. 231–234.
- [21] Wenjie Xu et al. “Activation and alliance of regulatory pathways in *C. albicans* during mammalian infection”. In: *PLoS biology* 13.2 (2015), e1002076.

- [22] Alistair JP Brown et al. “Metabolism impacts upon *Candida* immunogenicity and pathogenicity at multiple levels”. In: *Trends in microbiology* 22.11 (2014), pp. 614–622.
- [23] Timothy M Tucey et al. “Glucose Homeostasis Is Important for Immune Cell Viability during *Candida* Challenge and Host Survival of Systemic Fungal Infection”. In: *Cell metabolism* 27.5 (2018), pp. 988–1006.
- [24] Michael C Lorenz and Gerald R Fink. “The glyoxylate cycle is required for fungal virulence”. In: *Nature* 412.6842 (2001), p. 83.
- [25] Zain Kassam et al. “Fecal microbiota transplantation for *Clostridium difficile* infection: systematic review and meta-analysis”. In: *The American journal of gastroenterology* 108.4 (2013), p. 500.
- [26] Dina Kao et al. “Effect of oral capsule–vs colonoscopy–delivered fecal microbiota transplantation on recurrent *clostridium difficile* infection: a randomized clinical trial”. In: *Jama* 318.20 (2017), pp. 1985–1993.
- [27] Kearney TW Gunsalus et al. “Manipulation of host diet to reduce gastrointestinal colonization by the opportunistic pathogen *Candida albicans*”. In: *mSphere* 1.1 (2016), e00020–15.
- [28] Pascalis Vergidis et al. “Intra-abdominal candidiasis: the importance of early source control and antifungal treatment”. In: *PLoS One* 11.4 (2016), e0153247.
- [29] J Christian Pérez, Carol A Kumamoto, and Alexander D Johnson. “*Candida albicans* commensalism and pathogenicity are intertwined traits directed by a tightly knit transcriptional regulatory circuit”. In: *PLoS biology* 11.3 (2013), e1001510.
- [30] Changbin Chen et al. “An iron homeostasis regulatory circuit with reciprocal roles in *Candida albicans* commensalism and pathogenesis”. In: *Cell host & microbe* 10.2 (2011), pp. 118–135.
- [31] Lena Böhm et al. “The yeast form of the fungus *Candida albicans* promotes persistence in the gut of gnotobiotic mice”. In: *PLoS pathogens* 13.10 (2017), e1006699.
- [32] Bernardo Ramirez-Zavala et al. “The Snf1-activating kinase Sak1 is a key regulator of metabolic adaptation and in vivo fitness of *Candida albicans*”. In: *Molecular microbiology* 104.6 (2017), pp. 989–1007.
- [33] Prashant R Desai et al. “Hypoxia and temperature regulated morphogenesis in *Candida albicans*”. In: *PLoS genetics* 11.8 (2015), e1005447.

- [34] Andrew Y Koh. “Murine models of *Candida* gastrointestinal colonization and dissemination”. In: *Eukaryotic cell* (2013), EC–00196.
- [35] Natsu Yamaguchi et al. “Gastric colonization of *Candida albicans* differs in mice fed commercial and purified diets”. In: *The Journal of nutrition* 135.1 (2005), pp. 109–115.
- [36] Eduardo Lopez-Medina and Andrew Y Koh. “The complexities of bacterial-fungal interactions in the mammalian gastrointestinal tract”. In: *Microbial Cell* 3.5 (2016), p. 191.
- [37] Fabien Cottier et al. “MIG1 regulates resistance of *Candida albicans* against the fungistatic effect of weak organic acids”. In: *Eukaryotic cell* (2015), EC–00129.
- [38] Ara Koh et al. “From dietary fiber to host physiology: short-chain fatty acids as key bacterial metabolites”. In: *Cell* 165.6 (2016), pp. 1332–1345.
- [39] Iuliana V Ene et al. “Host carbon sources modulate cell wall architecture, drug resistance and virulence in a fungal pathogen”. In: *Cellular microbiology* 14.9 (2012), pp. 1319–1335.
- [40] Victoria Brown, Jessica A Sexton, and Mark Johnston. “A glucose sensor in *Candida albicans*”. In: *Eukaryotic Cell* 5.10 (2006), pp. 1726–1737.
- [41] Nora Grahl and Robert A Cramer Jr. “Regulation of hypoxia adaptation: an overlooked virulence attribute of pathogenic fungi?” In: *Medical mycology* 48.1 (2010), pp. 1–15.
- [42] Duncan Wilson et al. “Identifying infection-associated genes of *Candida albicans* in the postgenomic era”. In: *FEMS yeast research* 9.5 (2009), pp. 688–700.
- [43] Katherina Zakikhany et al. “In vivo transcript profiling of *Candida albicans* identifies a gene essential for interepithelial dissemination”. In: *Cellular microbiology* 9.12 (2007), pp. 2938–2954.
- [44] Saranna Fanning et al. “Divergent targets of *Candida albicans* biofilm regulator Bcr1 in vitro and in vivo”. In: *Eukaryotic cell* (2012), EC–00103.
- [45] Neide Vieira et al. “Functional specialization and differential regulation of short-chain carboxylic acid transporters in the pathogen *Candida albicans*”. In: *Molecular microbiology* 75.6 (2010), pp. 1337–1354.

- [46] Carlos Gancedo and Carmen-Lisset Flores. “Moonlighting proteins in yeasts”. In: *Microbiology and Molecular Biology Reviews* 72.1 (2008), pp. 197–210.
- [47] Ana Gil-Bona et al. “Candida albicans cell shaving uncovers new proteins involved in cell wall integrity, yeast to hypha transition, stress response and host–pathogen interaction”. In: *Journal of proteomics* 127 (2015), pp. 340–351.
- [48] Slavena Vylkova et al. “The fungal pathogen *Candida albicans* autoinduces hyphal morphogenesis by raising extracellular pH”. In: *MBio* 2.3 (2011), e00055–11.
- [49] Elisa M Vesely et al. “N-Acetylglucosamine Metabolism Promotes Survival of *Candida albicans* in the Phagosome”. In: *mSphere* 2.5 (2017), e00357–17.
- [50] Heather A Danhof and Michael C Lorenz. “The *Candida albicans* ATO gene family promotes neutralization of the macrophage phagolysosome”. In: *Infection and immunity* (2015), IAI-00984.
- [51] Nathalie Uwamahoro et al. “The pathogen *Candida albicans* hijacks pyroptosis for escape from macrophages”. In: *MBio* 5.2 (2014), e00003–14.
- [52] Anja Wartenberg et al. “Microevolution of *Candida albicans* in macrophages restores filamentation in a nonfilamentous mutant”. In: *PLoS genetics* 10.12 (2014), e1004824.
- [53] Alex J Freerman et al. “Metabolic reprogramming of macrophages: glucose transporter (GLUT1)-mediated glucose metabolism drives a pro-inflammatory phenotype”. In: *Journal of Biological Chemistry* (2014), jbc-M113.
- [54] Daniel Garcia and Reuben J Shaw. “AMPK: mechanisms of cellular energy sensing and restoration of metabolic balance”. In: *Molecular cell* 66.6 (2017), pp. 789–800.
- [55] Linda L Lutfiyya and Mark Johnston. “Two zinc-finger-containing repressors are responsible for glucose repression of SUC2 expression.” In: *Molecular and cellular biology* 16.9 (1996), pp. 4790–4797.
- [56] Michelle A Treitel, Sergei Kuchin, and Marian Carlson. “Snf1 protein kinase regulates phosphorylation of the Mig1 repressor in *Saccharomyces cerevisiae*”. In: *Molecular and cellular biology* 18.11 (1998), pp. 6273–6280.
- [57] Michael J De Vit, James A Waddle, and Mark Johnston. “Regulated nuclear translocation of the Mig1 glucose repressor.” In: *Molecular biology of the cell* 8.8 (1997), pp. 1603–1618.

- [58] R Petter, YC Chang, and KJ Kwon-Chung. “A gene homologous to *Saccharomyces cerevisiae* SNF1 appears to be essential for the viability of *Candida albicans*.” In: *Infection and immunity* 65.12 (1997), pp. 4909–4917.
- [59] Marianna Orlova, LaKisha Barrett, and Sergei Kuchin. “Detection of endogenous Snf1 and its activation state: application to *Saccharomyces* and *Candida* species”. In: *Yeast* 25.10 (2008), pp. 745–754.
- [60] Kristina Hedbacker and Marian Carlson. “SNF1/AMPK pathways in yeast”. In: *Frontiers in bioscience: a journal and virtual library* 13 (2008), p. 2408.
- [61] Gaowen Liu et al. “Gene essentiality is a quantitative property linked to cellular evolvability”. In: *Cell* 163.6 (2015), pp. 1388–1399.
- [62] Linda L Lutfiyya et al. “Characterization of three related glucose repressors and genes they regulate in *Saccharomyces cerevisiae*”. In: *Genetics* 150.4 (1998), pp. 1377–1391.
- [63] Nandita Nath, Rhonda R McCartney, and Martin C Schmidt. “Yeast Pak1 kinase associates with and activates Snf1”. In: *Molecular and Cellular Biology* 23.11 (2003), pp. 3909–3917.
- [64] Oscar Zaragoza, Cristina Rodriguez, and Carlos Gancedo. “Isolation of the MIG1 Gene from *Candida albicans* and Effects of Its Disruption on Catabolite Repression”. In: *Journal of bacteriology* 182.2 (2000), pp. 320–326.
- [65] A Munir A Murad et al. “Transcript profiling in *Candida albicans* reveals new cellular functions for the transcriptional repressors CaTup1, CaMig1 and CaNrg1”. In: *Molecular microbiology* 42.4 (2001), pp. 981–993.
- [66] Burkhard R Braun and Alexander D Johnson. “Control of filament formation in *Candida albicans* by the transcriptional repressor TUP1”. In: *Science* 277.5322 (1997), pp. 105–109.
- [67] A Munir A Murad et al. “NRG1 represses yeast–hypha morphogenesis and hypha-specific gene expression in *Candida albicans*”. In: *The EMBO journal* 20.17 (2001), pp. 4742–4752.
- [68] Jakub Orzechowski Westholm et al. “Combinatorial control of gene expression by the three yeast repressors Mig1, Mig2 and Mig3”. In: *BMC genomics* 9.1 (2008), p. 601.

- [69] Alejandra Fernández-Cid et al. “Glucose levels regulate the nucleo-mitochondrial distribution of Mig2”. In: *Mitochondrion* 12.3 (2012), pp. 370–380.
- [70] Dakshayini G Chandrashekarappa et al. “The β subunit of yeast AMP-activated protein kinase directs substrate specificity in response to alkaline stress”. In: *Cellular signalling* 28.12 (2016), pp. 1881–1893.
- [71] Suzanne M Noble et al. “Systematic screens of a *Candida albicans* homozygous deletion library decouple morphogenetic switching and pathogenicity”. In: *Nature genetics* 42.7 (2010), p. 590.
- [72] Oliver R Homann et al. “A phenotypic profile of the *Candida albicans* regulatory network”. In: *PLoS genetics* 5.12 (2009), e1000783.
- [73] Kevin P Byrne and Kenneth H Wolfe. “The Yeast Gene Order Browser: combining curated homology and syntenic context reveals gene fate in polyploid species”. In: *Genome research* 15.10 (2005), pp. 1456–1461.
- [74] Jonathan L Gordon, Kevin P Byrne, and Kenneth H Wolfe. “Additions, losses, and rearrangements on the evolutionary route from a reconstructed ancestor to the modern *Saccharomyces cerevisiae* genome”. In: *PLoS genetics* 5.5 (2009), e1000485.
- [75] Geraldine Butler et al. “Evolution of pathogenicity and sexual reproduction in eight *Candida* genomes”. In: *Nature* 459.7247 (2009), p. 657.
- [76] Louis D Saravolatz, Stanley C Deresinski, and David A Stevens. “Caspofungin”. In: *Clinical Infectious Diseases* 36.11 (2003), pp. 1445–1457.
- [77] CM Douglas et al. “Identification of the FKS1 gene of *Candida albicans* as the essential target of 1, 3-beta-D-glucan synthase inhibitors.” In: *Antimicrobial agents and chemotherapy* 41.11 (1997), pp. 2471–2479.
- [78] Marie Desnos-Ollivier et al. “Mutations in the *fkp1* gene in *Candida albicans*, *C. tropicalis*, and *C. krusei* correlate with elevated caspofungin MICs uncovered in AM3 medium using the method of the European Committee on Antibiotic Susceptibility Testing”. In: *Antimicrobial agents and chemotherapy* 52.9 (2008), pp. 3092–3098.
- [79] Vincent M Bruno et al. “Control of the *C. albicans* cell wall damage response by transcriptional regulator Cas5”. In: *PLoS pathogens* 2.3 (2006), e21.

- [80] JL Xie et al. *The Candida albicans transcription factor Cas5 couples stress responses, drug resistance and cell cycle regulation*. *Nat Commun* 8: 499. 2017.
- [81] Erin M Vasicek et al. “Disruption of the transcriptional regulator Cas5 results in enhanced killing of *Candida albicans* by Fluconazole”. In: *Antimicrobial agents and chemotherapy* (2014), AAC-00064.
- [82] Jill R Blankenship et al. “An extensive circuitry for cell wall regulation in *Candida albicans*”. In: *PLoS pathogens* 6.2 (2010), e1000752.
- [83] Jason M Rauceo et al. “Regulation of the *Candida albicans* cell wall damage response by transcription factor Sko1 and PAS kinase Psk1”. In: *Molecular biology of the cell* 19.7 (2008), pp. 2741–2751.
- [84] Susana Garcia-Sánchez et al. “Global roles of Ssn6 in Tup1-and Nrg1-dependent gene regulation in the fungal pathogen, *Candida albicans*”. In: *Molecular biology of the cell* 16.6 (2005), pp. 2913–2925.
- [85] Teresa T Liu et al. “Genome-wide expression profiling of the response to azole, polyene, echinocandin, and pyrimidine antifungal agents in *Candida albicans*”. In: *Antimicrobial agents and chemotherapy* 49.6 (2005), pp. 2226–2236.
- [86] James E Posey and Frank C Gherardini. “Lack of a role for iron in the Lyme disease pathogen”. In: *Science* 288.5471 (2000), pp. 1651–1653.
- [87] Suzanne M Noble. “*Candida albicans* specializations for iron homeostasis: from commensalism to virulence”. In: *Current opinion in microbiology* 16.6 (2013), pp. 708–715.
- [88] Ziva Weissman and Daniel Kornitzer. “A family of *Candida* cell surface haem-binding proteins involved in haemin and haemoglobin-iron utilization”. In: *Molecular microbiology* 53.4 (2004), pp. 1209–1220.
- [89] Dexter H Howard. “Acquisition, transport, and storage of iron by pathogenic fungi”. In: *Clinical Microbiology Reviews* 12.3 (1999), pp. 394–404.
- [90] James E Cassat and Eric P Skaar. “Iron in infection and immunity”. In: *Cell host & microbe* 13.5 (2013), pp. 509–519.
- [91] Ziva Weissman et al. “An endocytic mechanism for haemoglobin-iron acquisition in *Candida albicans*”. In: *Molecular microbiology* 69.1 (2008), pp. 201–217.

- [92] Galit Kuznets et al. “A relay network of extracellular heme-binding proteins drives *C. albicans* iron acquisition from hemoglobin”. In: *PLoS pathogens* 10.10 (2014), e1004407.
- [93] Lena Nasser et al. “Structural basis of haem-iron acquisition by fungal pathogens”. In: *Nature microbiology* 1.11 (2016), p. 16156.
- [94] Thyagarajan Srikantha et al. “Identification of genes upregulated by the transcription factor Bcr1 that are involved in impermeability, impenetrability and drug-resistance of *Candida albicans* a/ α biofilms”. In: *Eukaryotic cell* (2013), EC–00071.
- [95] Sophie Moreau-Marquis, George A O’Toole, and Bruce A Stanton. “Tobramycin and FDA-approved iron chelators eliminate *Pseudomonas aeruginosa* biofilms on cystic fibrosis cells”. In: *American journal of respiratory cell and molecular biology* 41.3 (2009), pp. 305–313.
- [96] Kimberley A Savage et al. “Iron restriction to clinical isolates of *Candida albicans* by the novel chelator DIBI inhibits growth and increases sensitivity to azoles in vitro and in vivo in a murine model of experimental vaginitis”. In: *Antimicrobial agents and chemotherapy* (2018), AAC–02576.
- [97] Markus Niewerth et al. “Ciclopirox olamine treatment affects the expression pattern of *Candida albicans* genes encoding virulence factors, iron metabolism proteins, and drug resistance factors”. In: *Antimicrobial agents and chemotherapy* 47.6 (2003), pp. 1805–1817.
- [98] Chung-Yu Lan et al. “Regulatory networks affected by iron availability in *Candida albicans*”. In: *Molecular microbiology* 53.5 (2004), pp. 1451–1469.
- [99] Po-Chen Hsu, Cheng-Yao Yang, and Chung-Yu Lan. “*Candida albicans* Hap43 is a repressor induced under low-iron conditions and is essential for iron-responsive transcriptional regulation and virulence”. In: *Eukaryotic Cell* 10.2 (2011), pp. 207–225.
- [100] Katherine Lagree and Aaron P Mitchell. “Fungal Biofilms: Inside Out”. In: *Microbiology spectrum* 5.2 (2017).
- [101] J William Costerton et al. “Microbial biofilms”. In: *Annual Reviews in Microbiology* 49.1 (1995), pp. 711–745.

- [102] Moselio Schaechter. “A brief history of bacterial growth physiology”. In: *Frontiers in microbiology* 6 (2015), p. 289.
- [103] Rodney M Donlan and J William Costerton. “Biofilms: survival mechanisms of clinically relevant microorganisms”. In: *Clinical microbiology reviews* 15.2 (2002), pp. 167–193.
- [104] Kevin J Verstrepen and Frans M Klis. “Flocculation, adhesion and biofilm formation in yeasts”. In: *Molecular microbiology* 60.1 (2006), pp. 5–15.
- [105] Susana Garcia-Sánchez et al. “Candida albicans biofilms: a developmental state associated with specific and stable gene expression patterns”. In: *Eukaryotic cell* 3.2 (2004), pp. 536–545.
- [106] Jigar V Desai et al. “Regulatory role of glycerol in Candida albicans biofilm formation”. In: *MBio* 4.2 (2013), e00637–12.
- [107] Luis A Murillo et al. “Genome-wide transcription profiling of the early phase of biofilm formation by Candida albicans”. In: *Eukaryotic cell* 4.9 (2005), pp. 1562–1573.
- [108] Clarissa J Nobile et al. “A recently evolved transcriptional network controls biofilm development in Candida albicans”. In: *Cell* 148.1 (2012), pp. 126–138.
- [109] Jyotsna Chandra and Pranab K Mukherjee. “Candida biofilms: development, architecture, and resistance”. In: *Microbiology spectrum* 3.4 (2015).
- [110] Emily P Fox et al. “An expanded regulatory network temporally controls Candida albicans biofilm formation”. In: *Molecular microbiology* 96.6 (2015), pp. 1226–1239.
- [111] KW Nickerson. “Quorum sensing in the dimorphic fungus”. In: *Candida albicans* (2001).
- [112] Gordon Ramage et al. “Inhibition of Candida albicans biofilm formation by farnesol, a quorum-sensing molecule”. In: *Applied and environmental microbiology* 68.11 (2002), pp. 5459–5463.
- [113] Jeniel E Nett et al. “Time course global gene expression analysis of an in vivo Candida biofilm”. In: *The Journal of infectious diseases* 200.2 (2009), pp. 307–313.
- [114] Tristan Rossignol et al. “Correlation between biofilm formation and the hypoxic response in Candida parapsilosis”. In: *Eukaryotic cell* 8.4 (2009), pp. 550–559.

- [115] Julie Bonhomme et al. “Contribution of the glycolytic flux and hypoxia adaptation to efficient biofilm formation by *Candida albicans*”. In: *Molecular microbiology* 80.4 (2011), pp. 995–1013.
- [116] Anup K Ghosh et al. “The GRF10 homeobox gene regulates filamentous growth in the human fungal pathogen *Candida albicans*”. In: *FEMS yeast research* 15.8 (2015), fov093.
- [117] Jamie A Greig et al. “Cell cycle-independent phospho-regulation of Fkh2 during hyphal growth regulates *Candida albicans* pathogenesis”. In: *PLoS pathogens* 11.1 (2015), e1004630.
- [118] Karla J Daniels et al. “The impact of environmental conditions on the form and function of *Candida albicans* biofilms”. In: *Eukaryotic cell* (2013), EC–00127.
- [119] David R Soll and Karla J Daniels. “Plasticity of *Candida albicans* biofilms”. In: *Microbiology and Molecular Biology Reviews* 80.3 (2016), pp. 565–595.
- [120] D Andes et al. “Development and characterization of an in vivo central venous catheter *Candida albicans* biofilm model”. In: *Infection and immunity* 72.10 (2004), pp. 6023–6031.
- [121] Jonathan S Finkel et al. “Portrait of *Candida albicans* adherence regulators”. In: *PLoS pathogens* 8.2 (2012), e1002525.
- [122] Jeniel E Nett et al. “Role of Fks1p and matrix glucan in *Candida albicans* biofilm resistance to an echinocandin, pyrimidine, and polyene”. In: *Antimicrobial agents and chemotherapy* 54.8 (2010), pp. 3505–3508.
- [123] Clarissa J Nobile et al. “Critical role of Bcr1-dependent adhesins in *C. albicans* biofilm formation in vitro and in vivo”. In: *PLoS pathogens* 2.7 (2006), e63.
- [124] Clarissa J Nobile et al. “Biofilm matrix regulation by *Candida albicans* Zap1”. In: *PLoS biology* 7.6 (2009), e1000133.
- [125] Nicole Robbins et al. “Hsp90 governs dispersion and drug resistance of fungal biofilms”. In: *PLoS pathogens* 7.9 (2011), e1002257.
- [126] Ira Herskowitz. “A regulatory hierarchy for cell specialization in yeast”. In: *Nature* 342.6251 (1989), p. 749.
- [127] AARON P Mitchell. “Control of meiotic gene expression in *Saccharomyces cerevisiae*.” In: *Microbiological reviews* 58.1 (1994), pp. 56–70.

- [128] Gordon Ramage et al. “The filamentation pathway controlled by the Efg1 regulator protein is required for normal biofilm formation and development in *Candida albicans*”. In: *FEMS microbiology letters* 214.1 (2002), pp. 95–100.
- [129] Clarissa J Nobile and Aaron P Mitchell. “Regulation of cell-surface genes and biofilm formation by the *C. albicans* transcription factor Bcr1p”. In: *Current Biology* 15.12 (2005), pp. 1150–1155.
- [130] Clarissa J Nobile and Alexander D Johnson. “*Candida albicans* biofilms and human disease”. In: *Annual review of microbiology* 69 (2015), pp. 71–92.
- [131] Binghua Hao et al. “*Candida albicans* RFX2 encodes a DNA binding protein involved in DNA damage responses, morphogenesis, and virulence”. In: *Eukaryotic cell* 8.4 (2009), pp. 627–639.
- [132] Xiaomin Zhao et al. “*Candida albicans* Als3p is required for wild-type biofilm formation on silicone elastomer surfaces”. In: *Microbiology* 152.8 (2006), pp. 2287–2299.
- [133] Jeniel E Nett et al. “Interface of *Candida albicans* biofilm matrix-associated drug resistance and cell wall integrity regulation”. In: *Eukaryotic cell* (2011), EC–05126.
- [134] K Lagree et al. “Microscopy of fungal biofilms.” In: *Current opinion in microbiology* 43 (2018), pp. 100–107.
- [135] Andrea Walther and Jürgen Wendland. “An improved transformation protocol for the human fungal pathogen *Candida albicans*”. In: *Current genetics* 42.6 (2003), pp. 339–343.
- [136] Kyunghun Min et al. “*Candida albicans* gene deletion with a transient CRISPR-Cas9 system”. In: *mSphere* 1.3 (2016), e00130–16.
- [137] Abdul Munir Abdul Murad et al. “Cip10, an efficient and convenient integrating vector for *Candida albicans*”. In: *Yeast* 16.4 (2000), pp. 325–327.
- [138] Carol A Woolford et al. “Bypass of *Candida albicans* filamentation/biofilm regulators through diminished expression of protein kinase Cak1”. In: *PLoS genetics* 12.12 (2016), e1006487.
- [139] R Bryce Wilson, Dana Davis, and Aaron P Mitchell. “Rapid hypothesis testing with *Candida albicans* through gene disruption with short homology regions”. In: *Journal of bacteriology* 181.6 (1999), pp. 1868–1874.

- [140] Elisabetta Spreghini et al. “Roles of *Candida albicans* Dfg5p and Dcw1p cell surface proteins in growth and hypha formation”. In: *Eukaryotic cell* 2.4 (2003), pp. 746–755.
- [141] Clarissa J Nobile et al. “*Candida albicans* transcription factor Rim101 mediates pathogenic interactions through cell wall functions”. In: *Cellular microbiology* 10.11 (2008), pp. 2180–2196.
- [142] Dana A Davis et al. “*Candida albicans* Mds3p, a conserved regulator of pH responses and virulence identified through insertional mutagenesis”. In: *Genetics* 162.4 (2002), pp. 1573–1581.
- [143] Rutilio A Fratti et al. “Endothelial cell injury caused by *Candida albicans* is dependent on iron”. In: *Infection and immunity* 66.1 (1998), pp. 191–196.
- [144] Scott G Filler et al. “Penetration and damage of endothelial cells by *Candida albicans*.” In: *Infection and Immunity* 63.3 (1995), pp. 976–983.
- [145] Thomas D Schmittgen and Kenneth J Livak. “Analyzing real-time PCR data by the comparative C T method”. In: *Nature protocols* 3.6 (2008), p. 1101.
- [146] Norma V Solis and Scott G Filler. “Mouse model of oropharyngeal candidiasis”. In: *Nature protocols* 7.4 (2012), p. 637.
- [147] Fabian Sievers et al. “Fast, scalable generation of high-quality protein multiple sequence alignments using Clustal Omega”. In: *Molecular systems biology* 7.1 (2011), p. 539.
- [148] David E Levin. “Cell wall integrity signaling in *Saccharomyces cerevisiae*”. In: *Microbiology and molecular biology reviews* 69.2 (2005), pp. 262–291.
- [149] Fabien Cottier et al. “The Transcriptional Response of *Candida albicans* to Weak Organic Acids, Carbon Source and MIG1 Inactivation Unveils a Role for HGT16 in Mediating the Fungistatic Effect of Acetic Acid”. In: *G3: Genes, Genomes, Genetics* (2017), g3-300238.
- [150] Frank C Odds et al. *Candida and candidosis: a review and bibliography*. Bailliere Tindall, 1988.
- [151] Alistair JP Brown and Neil AR Gow. “Regulatory networks controlling *Candida albicans* morphogenesis”. In: *Trends in microbiology* 7.8 (1999), pp. 333–338.

- [152] Ilse D Jacobsen and Bernhard Hube. *Candida albicans morphology: still in focus*. 2017.
- [153] Ning-Ning Liu et al. “Phosphate is the third nutrient monitored by TOR in *Candida albicans* and provides a target for fungal-specific indirect TOR inhibition”. In: *Proceedings of the National Academy of Sciences* 114.24 (2017), pp. 6346–6351.
- [154] Robert J Bastidas, Joseph Heitman, and Maria E Cardenas. “The protein kinase Tor1 regulates adhesin gene expression in *Candida albicans*”. In: *PLoS pathogens* 5.2 (2009), e1000294.
- [155] Sviatlana Shashkova, Niek Welkenhuysen, and Stefan Hohmann. “Molecular communication: crosstalk between the Snf1 and other signaling pathways”. In: *FEMS yeast research* 15.4 (2015).
- [156] Joseph Heitman, N Rao Movva, and Michael N Hall. “Targets for cell cycle arrest by the immunosuppressant rapamycin in yeast”. In: *Science* 253.5022 (1991), pp. 905–909.
- [157] John Rohde, Joseph Heitman, and Maria E Cardenas. “The TOR kinases link nutrient sensing to cell growth”. In: *Journal of Biological Chemistry* 276.13 (2001), pp. 9583–9586.
- [158] R Bryce Wilson et al. “A recyclable *Candida albicans* URA3 cassette for PCR product-directed gene disruptions”. In: *Yeast* 16.1 (2000), pp. 65–70.
- [159] Scott G Filler. “In vitro models of hematogenously disseminated candidiasis”. In: *Virulence* 5.2 (2014), pp. 240–242.
- [160] Slavena Vylkova and Michael C Lorenz. “Modulation of phagosomal pH by *Candida albicans* promotes hyphal morphogenesis and requires Stp2p, a regulator of amino acid transport”. In: *PLoS pathogens* 10.3 (2014), e1003995.
- [161] Paula G Bertram et al. “Convergence of TOR-nitrogen and Snf1-glucose signaling pathways onto Gln3”. In: *Molecular and cellular biology* 22.4 (2002), pp. 1246–1252.
- [162] Mélissa Caza et al. “The zinc finger protein Mig1 regulates mitochondrial function and azole drug susceptibility in the pathogenic fungus *Cryptococcus neoformans*”. In: *mSphere* 1.1 (2016), e00080–15.

- [163] Lucia F Zacchi, Jonatan Gomez-Raja, and Dana A Davis. “Mds3 regulates morphogenesis in *Candida albicans* through the TOR pathway”. In: *Molecular and cellular biology* 30.14 (2010), pp. 3695–3710.
- [164] Robbie Loewith and Michael N Hall. “Target of rapamycin (TOR) in nutrient signaling and growth control”. In: *Genetics* 189.4 (2011), pp. 1177–1201.
- [165] Tahmeena Chowdhury and Julia R Köhler. “Ribosomal protein S 6 phosphorylation is controlled by TOR and modulated by PKA in *Candida albicans*”. In: *Molecular microbiology* 98.2 (2015), pp. 384–402.
- [166] H Baker et al. “Rapamycin (AY-22, 989), a new antifungal antibiotic”. In: *The Journal of antibiotics* 31.6 (1978), pp. 539–545.
- [167] Francis J Dumont and Qingxiang Su. “Mechanism of action of the immunosuppressant rapamycin”. In: *Life sciences* 58.5 (1995), pp. 373–395.
- [168] Steffen Priebe et al. “FungiFun2: a comprehensive online resource for systematic analysis of gene lists from fungal species”. In: *Bioinformatics* 31.3 (2014), pp. 445–446.
- [169] Resham D Kulkarni, Hemant S Kelkar, and Ralph A Dean. “An eight-cysteine-containing CFEM domain unique to a group of fungal membrane proteins”. In: *Trends in biochemical sciences* 28.3 (2003), pp. 118–121.
- [170] Elizabeth J Polvi et al. “Metal chelation as a powerful strategy to probe cellular circuitry governing fungal drug resistance and morphogenesis”. In: *PLoS genetics* 12.10 (2016), e1006350.
- [171] Grazyna J Sosinska et al. “Hypoxic conditions and iron restriction affect the cell-wall proteome of *Candida albicans* grown under vagina-simulative conditions”. In: *Microbiology* 154.2 (2008), pp. 510–520.
- [172] Ricardo S Almeida et al. “The hyphal-associated adhesin and invasin Als3 of *Candida albicans* mediates iron acquisition from host ferritin”. In: *PLoS pathogens* 4.11 (2008), e1000217.
- [173] Ana Pérez et al. “Some biological features of *Candida albicans* mutants for genes coding fungal proteins containing the CFEM domain”. In: *FEMS yeast research* 11.3 (2011), pp. 273–284.

- [174] Ana Pérez et al. “Biofilm formation by *Candida albicans* mutants for genes coding fungal proteins exhibiting the eight-cysteine-containing CFEM domain”. In: *FEMS yeast research* 6.7 (2006), pp. 1074–1084.
- [175] Shantanu Ganguly and Aaron P Mitchell. “Mucosal biofilms of *Candida albicans*”. In: *Current opinion in microbiology* 14.4 (2011), pp. 380–385.
- [176] Narendrakumar Ramanan and Yue Wang. “A high-affinity iron permease essential for *Candida albicans* virulence”. In: *Science* 288.5468 (2000), pp. 1062–1064.
- [177] Jian Ming Khor and Charles A Ettensohn. “Functional divergence of paralogous transcription factors supported the evolution of biomineralization in echinoderms”. In: *eLife* 6 (2017), e32728.
- [178] Javier Mestas and Christopher CW Hughes. “Of mice and not men: differences between mouse and human immunology”. In: *The Journal of Immunology* 172.5 (2004), pp. 2731–2738.